UNIVERSITY OF CALIFORNIA, SAN DIEGO

Sorted Patterned Ground:
Numerical Models Exhibiting Self-Organization

A dissertation submitted in partial satisfaction of the
requirements for the degree Doctor of Philosophy in
Earth Sciences

by

Mark A. Kessler

Committee in charge:

Brad Werner, Chair
J. Freeman Gilbert
Joe D. Goddard
William R. Young
Mark A. Zumberge

2002

The dissertation of Mark A. Kessler is approved, and it is acceptable in quality and form for publication on microfilm:

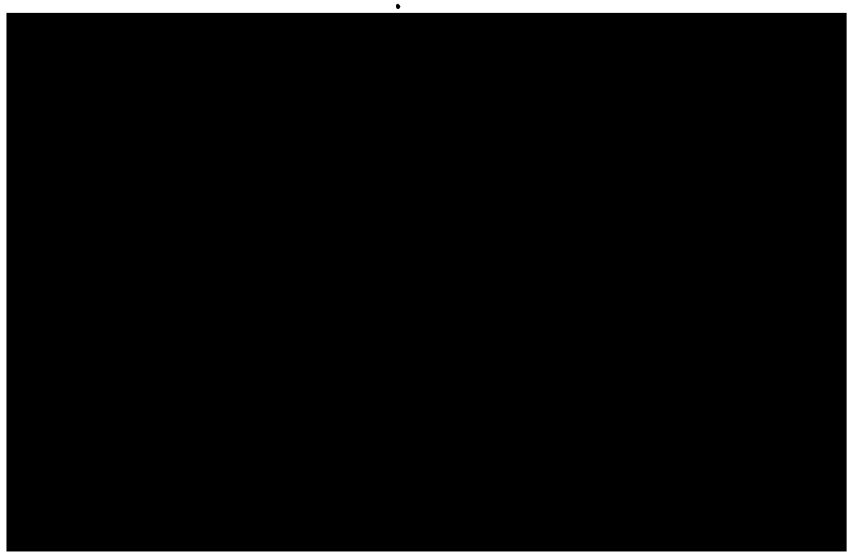

University of California, San Diego

2002

To my wife Nancy, who slept soundly in my office by my side.

Contents

List of Tables

List of Figures

ACKNOWLEDGEMENTS

First, I would like to thank my advisor and friend Brad Werner, who continually inspired me with new ideas and direction, and who always encouraged me to seek and follow my own path and way of doing science.

I would also like to thank the members, spouses and children of the Complex Systems Laboratory who were both colleagues and family throughout my years in San Diego. Thank you Brad Murray for your guidance during my initial thinking about sorted patterned ground, for keeping me alive in the arctic and for the innumerable discussions of these odd patterns. Thank you Lawrence Plug for the many engaging conversations and for sharing your vast arctic knowledge. Thank you Linden Clarke for the countless times you helped me with projects both in and outside the lab, and for keeping me from falling. Thank you Michele Okihiro for your invaluable counsel over early morning coffee. Thank you Jon O'Brien for injecting realism into an often esoteric pastime. Thank you Karen Scott for taking care of all the things that made life here so much easier. Thank you Giovanni Coco and Dylan McNamara for rejuvenating my scientific spirit later in my Ph.D. career with your new ideas and opinions on science, and for the wacky conversations that so typified the Complex Systems Lab.

Thank you Bernard Hallet for inviting me to your field sites, for sharing your invaluable observations of sorted circles, and for posing challenges that pushed me to better understand sorted patterned ground.

I am greatly indebted to Glenn Ierley, who was a tremendous help in bringing together some of the more analytical portions of this dissertation, and who made me think harder (and longer) than I wanted to but more effectively than I formerly

could.

To my parents, both old and new, thank you. Your parental vision of my ability has always pushed me along and given me something to shoot for.

Lastly, thank you Nancy for always standing by my side even when it means being thousands of miles apart, for encouraging me to make the right decisions and supporting any decision I make. Your unwavering confidence in me, in spite of reading early drafts, has pulled me through when my confidence was lacking. Remembering that I already have the greatest thing I could ever want makes all the other challenges, disappointments and successes insignificant.

The text of Chapter 2, in full, is a reformatted version of the material as it appears in Kessler, M. A., A. B. Murray, B. T. Werner, and B. Hallet, A Model for Sorted Circles as Self-Organized Patterns, *Journal of Geophysical Research,* **106**, 13,287–13,306, July 10^{th}, 2001. I was the primary researcher and author. The original paper is copyrighted by the American Geophysical Union, and the material is included here by permission of AGU.

This thesis was supported by the National Science Foundation, Arctic Natural Sciences Program [OPP-9530860], the Andrew W. Mellon Foundation, A National Defense Science and Engineering Graduate Fellowship and a Whole Earth Society Student Research Grant.

VITA

November 28^{th}, 1971	Born: Rochester, New York
1991–1992	Research Assistant, Eastman Kodak Company
1994–1996	Undergraduate Researcher, Solid State Physics State University of New York at Stony Brook
1996	Bachelor of Science, Physics and Anthropology State University of New York at Stony Brook
1996–2002	Graduate Research Assistant Scripps Institution of Oceanography University of California, San Diego
1999, 2001	Teaching Assistant University of California, San Diego
2002	Doctor of Philosophy, Earth Sciences University of California, San Diego

PUBLICATIONS

Kessler, M. A., Murray, A. B., Werner, B. T., and B. Hallet, A model for sorted circles as self-organized patterns, *J. Geophys. Res.*, **106(B7)**, 13,287–13,306, 2001.

ABSTRACTS AND PRESENTATIONS

Kessler, M. A., and B. T. Werner, An intermediate-scale model for karst terrain, *EOS, Trans. Am. Geophys. Un.*, **81(48)**, F579, 2000.

Kessler, M. A., A model for sorted patterned ground planforms, including: circles, islands, mazes and polygons, *EOS, Trans. Am. Geophys. Un.*, **80(46)**, F384, 1999.

Kessler, M. A., Murray, A. B., and B. Hallet, A model for sorted circle formation and evolution, contributed paper at *The Seventh International Conference on Permafrost*, held in Yellowknife, Canada, 1998.

Kessler, M. A., Murray, A. B., Werner, B. T., and B. Hallet, A dynamical feedback model for sorted circles, *EOS, Trans. Am. Geophys. Un.*, **78(46)**, F270, 1997.

ABSTRACT OF THE DISSERTATION

Sorted Patterned Ground:
Numerical Models Exhibiting Self-Organization

by

Mark A. Kessler
Doctor of Philosophy in Earth Sciences
University of California, San Diego, 2002
Professor Brad Werner, Chair

Sorted patterned ground, decimeter- to meter-scale patterns of circular, polygonal, striped and labyrinthine stone and soil domains, form in Arctic, sub-Arctic and high alpine environments where the surface ground layer, the active layer, experiences cyclic freezing and thawing that drives transport by frost heave, which is soil expansion via ice lens formation. In numerical models encapsulating observed and inferred active layer processes, all forms of sorted patterned ground emerge from an interplay between two mechanisms: (i) lateral sorting occurs by frost heave transporting soil toward soil rich regions, and (ii) stone domain extension and thinning occurs by lateral frost heave squeezing elongate stone domains, thereby driving stone transport along the axis of stone domains.

Sorted circles self-organize in a three-dimensional, cellular model of the active layer in which the first feedback is implemented by cyclic freezing and thawing driving transport of stone and soil particles via processes related to frost heave, gravity and water migration in soils. Modeled sorted circle size ($\sim 3\ m$), spacing

($\sim$4 m), and circulation time ($\sim$750 yr) are consistent with measurements from western Spitsbergen. The initial wavelength of perturbations on the stone/soil interface is accurately predicted using a linear stability analysis, but increase in wavelength through time reflects nonlinearities that control the spacing of soil plugs and sorted circles, namely, interactions and mergers between neighboring forms.

In a two-dimensional numerical model abstracting both feedbacks, circles, labyrinths, and islands emerge when lateral sorting dominates (with increasing volumetric fraction of soil); polygons emerge when along-axis transport dominates. The first class of patterns transitions to the second as soil compressibility is decreased and freezing rate in stone domains is increased. Islands transition to stripes on hillslopes.

The observed range of patterns also can be generated when the larger-scale properties of enhanced squeezing and rapid freezing of air cooled stone domains are included in the three-dimensional model. An increase in the volumetric fraction of soil, V_s, causes transitions between circles ($V_s < 0.47$), labyrinths ($0.47 < V_s < 0.66$), and islands ($V_s > 0.66$). Polygons transition to labyrinths as the magnitude of squeezing decreases relative to processes associated with lateral sorting. Islands and polygons grade into stripes on hillslopes greater than 2^o and 4^o, respectively.

Chapter 1

Introduction

1.1 Background

Circular, labyrinthine, linear and polygonal patterns of distinct stone and soil domains (sorted patterned ground) form in ground layers experiencing cyclic freezing and thawing (active layers). Over twenty hypotheses for mechanisms underlying various aspects of sorted patterned ground have been proposed, but no general consensus, even on the fundamental physical processes, exists. The diversity of patterns and their behaviors and the broad range of locations where they occur have caused the development of a multiplicity of pattern formation mechanisms [*Washburn,* 1956, 1997]. However, the common underlying process of freezing and thawing and the common result of patterned coarse and fine domains suggests the possibility that parameter variation within a single set of physical processes is responsible for the initiation and development of all forms of sorted patterned ground. The dissipative, nonlinear nature of active layer processes as

well as the collective behavior and decrease in the number of operative variables evidenced by these regular patterns suggests self-organization might be a general mechanism underlying the formation of sorted patterned ground and the transitions between patterns [*Hallet,* 1990; *Werner and Hallet,* 1993]. The hypothesis I will investigate here is that all forms of sorted patterned ground self-organize owing to robust feedbacks between transport of stones and soil and the pattern of stone and soil domains; all patterns are produced by the same set of physical processes, with transitions between patterns resulting from changes in environmental conditions and material properties.

1.1.1 Environment

Patterned ground forms in Arctic, sub-Arctic and high alpine surface soil layers that undergo cyclic freezing and thawing: active layers. Periglacial environments, nonglaciated terrain where processes related to freezing, thawing and permafrost are the dominant processes affecting the ground surface, cover 35% of Earth's land surface [*Williams and Smith,* 1989, p. 2]; 10% to 20% of the periglacial land surface exhibits features related to sorting by particle size [*Goldthwait,* 1976]. Active layers are complicated systems in which coupled nonlinear processes act on heterogeneous materials within the context of time-dependent energy and water exchange with the environment. Numerous active layer transport processes are driven by a seasonal or sometimes diurnal temperature variation, which results in freezing and thawing fronts that descend from the surface to depths up to 3 m [*Williams and Smith,* 1989, p. 15]. During freezing, water is drawn to the freezing front in fine-grained soils, where it forms discrete lenses

of ice that increase the soil volume (frost heave) and force the surface to rise and the underlying unfrozen soil, desiccated by water migration, to consolidate [*Taber,* 1929; *O'Neill and Miller,* 1985]. Thawing of frozen soils leads to consolidation as the water from melted ice lenses, in excess of the soil pore space, is expelled [*Williams and Smith,* 1989, p. 138]. Desiccated, consolidated soil expands when water either is drawn into soil pores [*Steche,* 1933, as cited by *Washburn,* 1956; *Lambe and Whitman,* 1969] or migrates to ice lenses forming lower in the active layer, where the temperature is below $0°C$ [*Parmuzina,* 1978, as cited in *Mackay,* 1980]. Contraction cracks result from moisture migration owing to freezing and thawing, as well as wetting and drying within the active layer [*Ballantyne and Matthews,* 1983]. On the surface, gravity, in conjunction with freezing and thawing, drives soil creep on gradients as small as $2°$ [*Norikazu,* 2001]. Fine particles are transported by the flow of water from melting ice lenses downward through pores between larger grains [*Huxley and Odell,* 1924; *Washburn,* 1997].

1.1.2 Pattern Descriptions

Sorted patterned ground is a category of active layer patterns for which lateral sorting by size produces circular, linear, polygonal and labyrinthine patterns of stone and soil domains with length scales ranging from 0.1 to 10 m.

Sorted circles (Figure 1) are a form of sorted patterned ground found most prominently in Spitsbergen [*Huxley and Odell,* 1924; *Elton,* 1927; *Jahn,* 1963; *Hallet and Prestrud,* 1986], the Canadian Arctic [*Washburn,* 1997] and Greenland [*Schmertmann and Taylor,* 1965; *Washburn,* 1969]. Sorted circles are char-

acterized by a 1-3 m wide soil cylinder, which extends to the depth of the active layer, surrounded by a 0.5-1 m wide annulus of stones devoid of soil. The peak of the stone domain is up to 0.5 m above the contact between the stone and soil domains, and up to 0.5 m above the surrounding surface. The center of the soil domain typically lies $\sim$0.1 m above the contact with the stone domain, with most of this height difference occurring near the stone/soil contact [*Sharp,* 1942; *Hallet and Prestrud,* 1986]; however, considerable variation in surface morphology exists. Sorted circles have been studied extensively, including measurements of surface and subsurface displacements, and temperature profiles from field sites in, for example, Spitsbergen [*Jahn,* 1963; *Hallet and Prestrud,* 1986], Thule, Greenland [*Schmertmann and Taylor,* 1965], and Cornwallis Island, Arctic Canada [*Washburn,* 1997]. Coherent surface soil motion directed toward the stone/soil contact, with velocity $\sim$0.01 m/yr, has been measured in soil domains in Thule, Greenland [*Schmertmann and Taylor,* 1965] and in both stone and soil domains on Kvadehuksletta, Spitsbergen [*Hallet and Prestrud,* 1986]. Measurements of subsurface tilt indicate that soil domains might be circulating [*Hallet,* 1998]. Temperature measurements during freezing have recorded cooling rates within stone domains that are two to three times the cooling rates in soil domains [*Cook,* 1955; *Schmertmann and Taylor,* 1965]. The active layer is commonly observed to be vertically sorted into a layer of stones overlying a layer of soil near sorted circles [*Elton,* 1927; *Washburn,* 1997], a configuration resulting from layered deposition, for example, in a prograding beach deposit, or from sorting processes. This layered configuration often is assumed to constitute an initial condition for sorted patterned ground formation [*Elton,* 1927; *Van Vliet-Lanoe,* 1991; *Washburn,* 1997]. Soil plugs, cylindrical soil features upwelling from an underlying soil layer, sometimes

are found at depth in the neighborhood of sorted circles; it has been suggested that they are a precursor to sorted circles [*Elton,* 1927; *Washburn,* 1997]. Stone islands and labyrinthine stone and soil domains (Figure 2) occur in areas where sorted circles are coalescing, as seen on Kvadehuksletta, Spitsbergen [*Hallet and Prestrud,* 1986]. Stone islands, sometimes referred to as stone pits, also occur as isolated features (Figure 3) or in association with sorted polygons (Figure 4). This pattern generally has been classified as being related to sorted circles [*Washburn,* 1956], but also has been termed "negative stone polygons" [*Beskow,* 1930, as cited in *Washburn,* 1956].

Sorted polygons are the most widespread form of sorted patterned ground, found, for example, in western Spitsbergen (Figure 4)[*Huxley and Odell,* 1924; *Elton,* 1927], Northeast Greenland [*Washburn,* 1969], Norway [*Ballantyne and Matthews,* 1983], the White Mountains of California [*Wilkerson,* 1995], the High Drakensberg Escarpment of Southern Africa [*Grab,* 1997], the Kjolur plateau, Iceland [*Schunke,* 1975], Interior Alaska (Figures 5, 6) and the St. Elias Range, Canada [*Sharp,* 1942]. Unlike sorted circles, which can be isolated features, sorted polygons are 0.1 to 10 m wide polygonal soil domains separated by a connected network of 0.01 to 0.5 m wide stone domains (Figures 5, 6) [*Huxley and Odell,* 1924; *Washburn,* 1956]. In summer, the surface of stone domains can be lower than, level with or raised above the stone/soil contact [*Huxley and Odell,* 1924; *Washburn,* 1969; *Schunke,* 1975], the last often by single large stones projecting out of the stone domain [*Huxley and Odell,* 1924; *Sharp,* 1942; *Washburn,* 1969]. Also during summer, soil domains can be convex, flat or concave [*Huxley and Odell,* 1924; *Washburn,* 1969]; however, concave and flat soil domains might be indicative of inactive patterns [*Huxley and Odell,* 1924; *Elton,* 1927]. The soil

domains of sorted polygons probably circulate in a manner similar to those of sorted circles, as indicated by folds in algal mats covering soil domains that are oriented parallel to the stone/soil contact [*Huxley and Odell,* 1924]. The primary characteristic distinguishing sorted polygons from other patterns with similar volumetric fractions of stones (stone islands and labyrinths) is the connectedness of stone domains, which tend to enclose equidimensional soil domains. Although sorted circles and sorted polygons have similar, well-defined equidimensional soil domains, the hypothesis that sorted polygons form from expanding sorted circles [*Elton,* 1927; *George et al.,* 1989] is rendered unlikely by three observations: (i) sorted circles grade into labyrinths, indicating that densely packed sorted circles coalesce; (ii) stone domains in polygons are narrow relative to adjacent soil domains [*Huxley and Odell,* 1924; *Washburn,* 1969], whereas stone domains in sorted circles and labyrinths are of similar width to their soil domains [*Jahn,* 1963; *Hallet and Prestrud,* 1986; *Washburn,* 1997]; and (iii) stone domains in some sorted polygons, such as on the Kjolur plateau in southwest Iceland [*Schunke,* 1975] are straight, unlike the curved stone domains of sorted circles. The uniform width and narrow character of sorted polygon stone domains, as well as their occurrence as networks and not isolated polygons, probably indicate that the interactions between neighboring soil domains are stronger than in sorted circles.

Sorted stripes (Figure 7) are characterized by decimeter- to meter-scale, gradient-parallel alternating bands of stones and soil on hillslopes of 3^o [*Goldthwait,* 1976] to 30^o [*Sharp,* 1942]. Single stripes can extend downslope many times the spacing between stripes (Figure 7); in some cases single stripes have been observed to extend continuously for $\sim$100 m [*Sharp,* 1942]. Sorted stripes form in polar and high alpine environments, including: Spitsbergen [*Huxley and Odell,*

1924], St. Elias Range, Canada [*Sharp,* 1942], the Lake District, North England [*Caine,* 1963], East Greenland [*Washburn,* 1969] and Mauna Kea, Hawaii [*Werner and Hallet,* 1993], and have often been observed in association with other forms of patterned ground on smaller gradient slopes [*Washburn,* 1956]. Gradations from sorted polygons into sorted stripes as the gradient increases have been reported [*Goldthwait,* 1976].

1.1.3 Proposed Origins of Sorted Patterned Ground

In a thorough review of sorted patterned ground [*Washburn,* 1956], nineteen processes were cited as contributing to active layer dynamics; these have been assembled into more than twenty hypotheses for sorted patterned ground [*Elton,* 1927; *Washburn,* 1956, 1997]. Most hypotheses have been based on four basic processes: frost heave [*Hogbom,* 1914, as cited in *Huxley and Odell,* 1924; *Elton,* 1927; *Corte,* 1962; *Nicholson,* 1976; *McKay,* 1980; *Van Vliet-Lanoe,* 1991; *Lewis et al.,* 1993], differential rock weathering [*Nansen,* 1921, as cited in *Huxley and Odell,* 1924; *Huxley and Odell,* 1924], soil and water density gradients (buoyancy-driven convection) [*Low,* 1925; *Ray et al.,* 1983; *Hallet and Waddington,* 1991], and contraction cracking of soil [*Longwell,* 1928, as cited in *Washburn,* 1956; *Pissart,* 1977; *Ballantyne and Mathews,* 1983]. Soil expansion by water absorption, differential settling during thaw, vibration, artesian pressures and solifluction, among others, also have been suggested (reviewed in [*Washburn,* 1956]).

Frost heave, soil expansion owing to water migration toward the freezing front during freezing, constitutes the principal physical process in many hypotheses for the formation of sorted patterned ground [e.g., *Hogbom,* 1914, as cited in

Elton, 1927; *Elton,* 1927; *Corte,* 1962; *Nicholson,* 1976; *Mackay,* 1980; *Van Vliet-Lanoe,* 1991]. As soil freezes, water is drawn to the freezing front, creating thin layers of ice, ice lenses [*Taber,* 1929]. Ice lens formation considerably slows the descent of the freezing front in water-laden soils because latent heat is released when water freezes. Frost heave sets up states within the active layer that thawing, water migration and gravity act upon to produce stone uplift [*Corte,* 1961; *Anderson,* 1988], downslope creep [*Norikazu,* 2001] and soil illuviation [*Forman and Miller,* 1984].

It is plausible that frost heave is the primary physical process responsible for sorted patterned ground because: (i) frost heave drives transport in the active layer, with free surface displacements that can exceed 20% of the active layer depth [*Williams and Smith,* 1989, p. 3]; vertical heave in soil domains as high at 0.4 m have been observed [*Jahn,* 1963]; (ii) frost heave can be spatially non-uniform because it depends on active layer properties, such as particle size, overburden weight, soil compressibility and water availability, that are time varying and spatially heterogeneous [*Taber,* 1929; *Corte,* 1961, 1962; *O'Neill and Miller,* 1985]; (iii) transport by frost heave can increase the spatial heterogeneity of soil properties (sorting), thereby changing the freezing front inclination and the horizontal location at which maximum frost heave occurs [*Corte,* 1962; *Nicholson,* 1976]; and (iv) differences in frost heave susceptibility have been shown in laboratory experiments to transport soil [*Taber,* 1929]. The interplay between differential frost heave and soil transport has been suggested as a mechanism behind sorted circles [*Taber,* 1929; *Nicholson,* 1976; *Mackay,* 1980; *Van Vliet-Lanoe,* 1991; *Lewis et al.,* 1993]. It also has been suggested that gradients in thermal properties, resulting in non-horizontal freezing fronts and lateral frost heave, lead

to circulation in soil domains [*Nicholson,* 1976]. The effect of freezing upward from a bowl-shaped active layer/permafrost interface has been invoked in a model for earth hummocks [*Mackay,* 1980] and was suggested to be applicable to other forms of patterned ground. Upwelling of soil, either owing to frost heave, overburden stress or density gradients, has been advanced as a mechanism for the initiation of sorted circles. A full range of forms, from small soil plugs at depth to fully developed sorted circles, have been reported at single field sites [*Washburn,* 1997].

One hypothesis for sorted polygon initiation is that a network of soil contraction cracks, owing to desiccation, initiates the network of stone domains by trapping and retaining stones moving on the surface [*Hogbom,* 1914, as cited in *Washburn,* 1956; *Pissart,* 1977]. Contraction cracks and stone domains have been reported in association at some locations (the French Alps [*Pissart,* 1977] and Jotunheimen, Norway [*Ballantyne and Matthews,* 1983]). The generality of this mechanism is questionable because many locations where sorted polygons are well formed are waterlogged for the entire period of thawing [*Elton,* 1927; *Sharp,* 1942; *Washburn,* 1969], precluding fracture by desiccation. However, contraction cracks could result from water withdrawal by frost heave during freezing [*Taber,* 1943; *Ballantyne and Matthews,* 1983].

An inverted soil density gradient causing buoyancy driven convection has been invoked in a range of mechanisms proposed for the circulation of sorted circle soil domains [*Nordenskjold,* 1907, as cited in *Washburn,* 1997; *Low,* 1925; *Hallet and Prestrud,* 1986]. The buoyancy force initially was hypothesized to arise during thawing of the active layer from the slight increase in water density from 0^oC to 4^oC [*Nordenskjold,* 1907, as cited in *Washburn,* 1997]; however, field

evidence suggests the forces generated are of insufficient magnitude to drive soil convection (reviewed in [*Washburn,* 1997]). More recently, soil density gradients caused by compaction of soil during thawing have been investigated as a possible source of density inversion [*Hallet and Prestrud,* 1986]. Because thaw and compaction proceed from the surface downward, and the density of soil is about twice the density of ice, soil near the surface will be more compacted and denser than soil at depth. However, field measurements have shown very little density variation with depth and the Rayleigh number is below the critical value by almost six orders of magnitude [*Hallet and Waddington,* 1991].

A related process, buoyancy-driven convection of water through pores in the active layer, has been proposed as a mechanism for the initiation of patterned ground [*Ray et al.,* 1983; *Gleason et al.,* 1986; *George et al.,* 1989]. As the active layer thaws, the surface temperature rises and the 0^oC isotherm descends. The water density increase from 0^oC to 4^oC results in a water density inversion with depth. Resulting convection cells of water through soil pores transfer heat from the ground surface to the top of the permafrost, thereby forming a permafrost surface with isolated peaks where water is rising and a hexagonal network of depressions where water is descending. Freezing upward from this surface drives stones outward from the peaks toward the ground surface, forming sorted polygons [*George et al.,* 1989]. The predicted aspect ratio, of about 3, is in good agreement with sorted circles in western Spitsbergen and elsewhere [*Ray et al.,* 1983; *Gleason et al.,* 1986]. Predictions for the change in aspect ratio with slope and for sub-aqueous patterns have been made and also are consistent with measurements [*Gleason et al.,* 1986]. The general assumption underlying this model for pattern initiation is that the mechanisms determining where circles

form, their size and their shape, and the mechanisms leading to sorting and soil motions of individual circles are different. Difficulties with this model include: (i) once patterned ground forms the pre-existing pattern is no longer detectable and its properties can not be probed directly, (ii) owing to its focus on pattern initiation, only a small number of predictions are possible, (iii) laterally homogeneous soil properties are assumed, an assumption that does not hold in the active layer [*George et al.,* 1989]; inhomogeneous soil might have significant effects on the pattern of convection, and (iv) convection of water through pores in an active layer has not been reported.

Many hypothesized models for the formation of sorted patterned ground have not been presented with sufficient quantitative detail to enable predictions that can distinguish between competing models. In addition, most models pertain only to isolated aspects of a single pattern. The relationships between different patterns and between the developmental stages of a single pattern generally have not been treated. Therefore, a self-consistent model for the full range of patterns, or even the range of behaviors of a single pattern, has not been developed. Because only a limited range of behaviors have been modeled, predictions that would permit discriminating between models are limited.

1.1.4 Self-Organization and Modeling

Recent investigations of patterning in natural systems, including beach cusps [*Werner and Fink,* 1993], braided rivers [*Murray and Paola,* 1994] and sand dunes [*Werner,* 1995], employed numerical simulations in which patterns self-organize as a result of robust feedbacks between transport, sorting and/or morphology.

In these simulations, patterns are long time-scale, large-spatial scale emergent features that slave the short time-scale, small-spatial scale processes such that the pattern of transport resulting from those processes sustains or enhances the pattern of sorting or morphology.

Numerical simulation models for sorted patterned ground that address various patterns and aspects of pattern development have been developed. Stone chains and clusters form in a two-dimensional model for patterning in granular media based upon transport variations resulting from stones impeding the otherwise random motion of neighboring stones [*Ahnert,* 1981].

In a model for sorted stripes [*Werner and Hallet,* 1993], gradient-parallel alternating bands of stones and soil develop from stochastic transport of stones on a two-dimensional plan view lattice according to processes associated with the diurnal uplift of stones by columns of needle ice and their redistribution as the columns melt and topple. Toppling is biased downhill and toward stone domains, because the surfaces of the intervening soil domains are elevated by frost heave. The fundamental contribution of this model is that it exhibits self-organization of sorted patterned ground from an initially non-patterned state.

1.2 Summary of Thesis

Here, I present three models for sorted patterned ground that were developed by adopting the viewpoint that the formation of sorted patterned ground results from self-organization. In these models, a reduced set of physical processes and material properties interact to produce features and behaviors resembling the

natural patterns. With this viewpoint, I have generated models that predict both the formation and behavior of sorted patterned ground, and therefore are amenable to testing. Additionally, with these models I have investigated how feedback mechanisms can give rise to the observed range of sorted patterned ground in a self-consistent manner.

First, a three-dimensional cellular model for sorted circles was developed that incorporates feedback mechanisms sufficient to produce sorted circles. In this model, stone, soil, ice and void particles (a discrete representation of compressibility) reside within a ground layer acted upon by cyclic freezing and thawing. The primary processes driving transport are frost heave, surface creep, compaction of ice rich soil during thawing, expansion of desiccated soil by water absorption and soil illuviation. Given an active layer configuration in which a layer of stones overlies a layer of soil, the freezing front descends rapidly in the stone domain and more slowly in the soil domain, (in which latent heat is released as water is converted to ice), thus conforming to the stone/soil interface. Frost heave at the stone/soil interface uplifts the overburden and compacts the underlying soil. Perturbations on the stone/soil interface are unstable because frost heave transports soil uniformly from the stone/soil interface, but preferentially toward existing soil concentrations owing to their greater capacity for compaction. This positive feedback causes soil plugs to rise toward the surface, pushing stones to the side. Negative feedbacks arising from differences between the stone/soil interface and the freezing front increase the wavelength of initial perturbations on the stone/soil interface. This model simulates the three-dimensional development of sorted circles and is quantitatively consistent with field measurements of pattern size, spacing, circulation rates and formation times of sorted circles.

Second, a two-dimensional model for initiation and pattern-scale dynamics for the observed range of sorted patterned ground was developed. The basis of this model is a new transport process that is instrumental in the transition between the isolated stone domains of stone islands and the connected networks of sorted polygons. In this model, stone particles move on a two-dimensional lattice driven by two abstracted transport processes: (i) stones move downslope on a surface (calculated from the current configuration of stones) that dips toward stone domains, abstracting the processes responsible for the lateral sorting feedback of the three-dimensional model; and (ii) stones move along the axis of elongate stone domains in response to surface uplift from squeezing and lateral confinement by frost heave perpendicular to highly inclined freezing fronts near the stone/soil interface. These processes diffuse perturbations in depth and width, and extend elongate stone domains, resulting in stable networks of narrow, straight stone domains. The relative magnitude of transport by these two mechanisms effects the transition between polygons and islands. When the lateral sorting mechanism dominates, increase in stone abundance causes transitions from islands to labyrinths and from labyrinths to circles, and increase in hillslope gradient causes the transition from islands to stripes.

Third, the three-dimensional model for sorted circles was modified to include the lateral squeezing mechanism hypothesized in the two-dimensional model. When transport fluxes owing to squeezing are sufficiently large, sorted polygons result. Additionally, transitions between islands, labyrinths and circles result in the three-dimensional sorted circle model as the volumetric fraction of soil is decreased, and stripes result as the hillslope gradient is increased. Patterns forming principally from lateral sorting (islands, labyrinths and circles) are simu-

lated robustly, whereas the formation of sorted polygons, which results from the interplay of two transport mechanisms, is sensitive to the specific parameters and model implementation. The difficulty with which sorted polygons form in this model contrasts with their preponderance in natural sorted patterned ground. This sensitivity might indicate a failure of the discrete, stochastic approach to accurately simulate the continuous process of squeezing or that the current physical picture is incomplete; this is an area where further research is needed.

In these models, the same processes act throughout all stages of pattern evolution, modified only by the emergent properties of stone and soil domains. The larger-scale patterns that emerge are those that slave the short-time, small-spatial scale transport processes such that they reinforce the current configuration. Although sorted patterned ground could be influenced, in principle, by external forcing and spatial variation in material properties, these models suggest that patterns can emerge from an initially random configuration without a template in environmental forcing or material properties. The long-time-scale geometry, dynamics and stability, which result from feedbacks between transport and the pattern, are not addressed by models for initiation.

According to the picture presented here, the occurrence of patterned ground reflects the dominant active layer processes, most notably frost heave. Variation in patterns at a location indicates variation in a controlling parameter (e.g., volumetric fraction of soil, hillslope gradient, relative soil compressibility and cooling rate in stone domains) and can be used to test the models. Lastly, the introduction of the previously unrecognized role of lateral squeezing in the formation of sorted polygons has enabled the formation of all forms of sorted patterned ground to be modeled by a single set of physical processes.

Figure 1.1: Sorted circles, Kvadehuksletta, Spitsbergen. Dark soil domains are $\sim$1.5 m across.

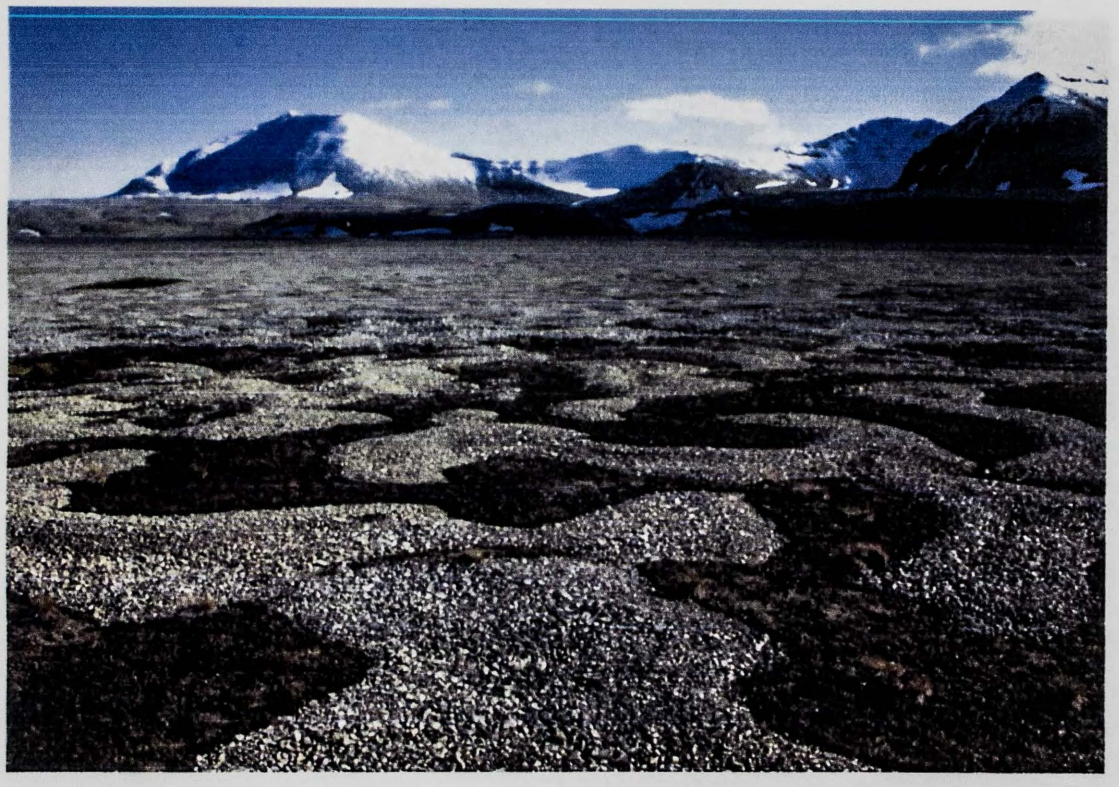

Figure 1.2: Labyrinthine stone and soil patterns, Kvadehuksletta, Spitsbergen. Dark soil domains vary from $\sim$1 m to $\sim$2 m across.

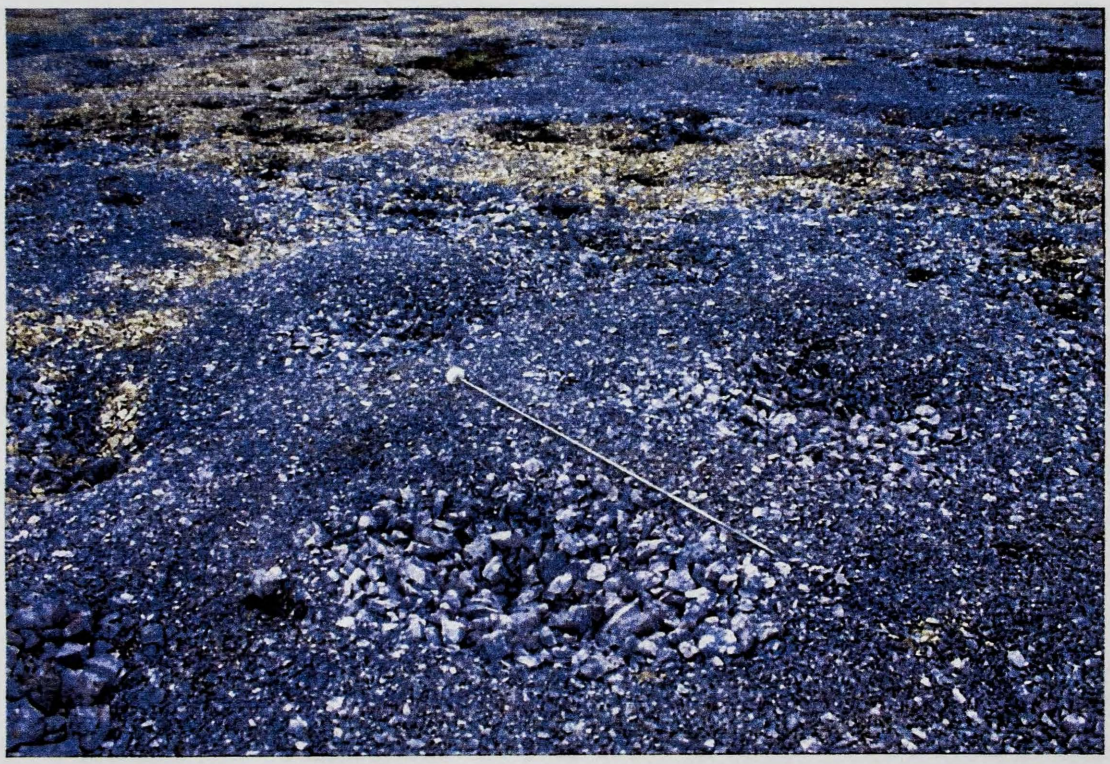

Figure 1.3: Stone islands, or stone pits, with meter-scale spacing, Kvadehuksletta, Spitsbergen.

Figure 1.4: Sorted polygons, Broggerhalvoya, Spitsbergen. Dark soil domains are $\sim$1 m across.

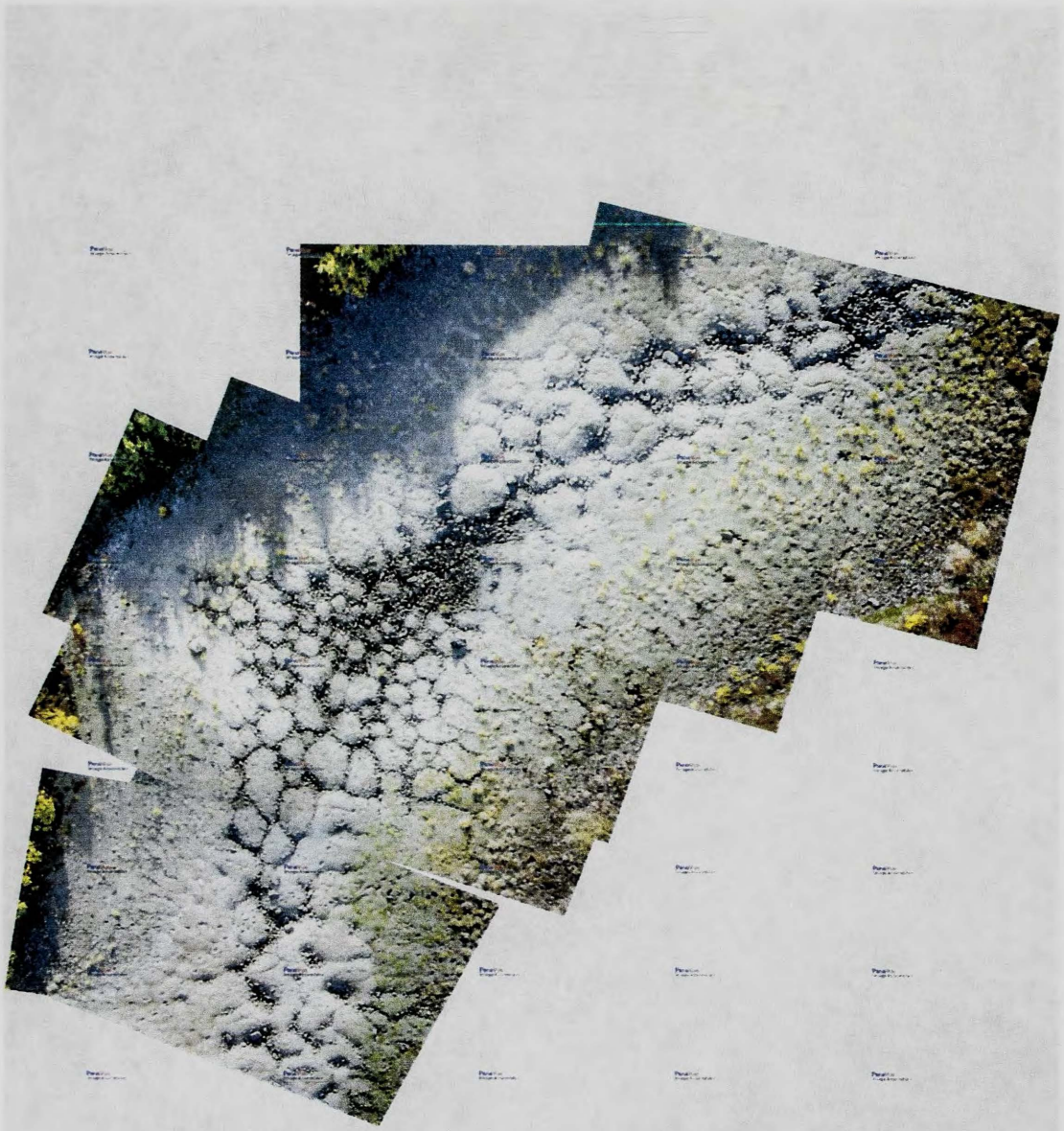

Figure 1.5: Sorted polygons within a desiccated pond $\sim$200 m south of Denali highway, $\sim$112 km east from Cantwell, Alaska. Composite of nine images taken from $\sim$20 m elevation by a 35mm camera suspended from a kite. Darker areas (lines) are stones, lighter areas are soil. The largest polygons are $\sim$2 m across. Pronounced pattern variability is exhibited along the axis of the pond.

Figure 1.6: Sorted polygons within a desiccated pond 100 m north of Denali highway, approximately 115 km east from Cantwell, Alaska. Aerial photograph taken at $\sim$100 m elevation from a slow flying plane. Darker areas (lines) are stones, lighter areas are soil. The largest polygons are $\sim$2 m across.

Figure 1.7: Sorted stripes with decimeter-scale spacing, Mauna Kea, Hawaii. Soil domains raised $\sim$5 *cm* above stone domains by frost heave. (Photo: B.T. Werner)

1.3 References

Ahnert, F., Stone rings from random walks, *Transactions, Japanese Geomorphological Union*, **2**, 301–312, 1981.

Anderson, S. P., The upfreezing process: Experiments with a single clast, *Geological Society of America Bulletin*, **100**, 609–621, 1988.

Ballantyne, C. K. and J. A. Mathews, Desiccation cracking and sorted polygon development, Jotunheimen, Norway, *Arctic and Alpine Research*, **15(3)**, 339–349, 1983.

Beskow, G., Erdfliessen und strukturboden der Hochgebirge im Licht der Frosthebung, *Geol. Foren. Stockholm, Forh*, **52**, 622–638, 1988.

Caine, T. N., The origin of sorted stripes in the Lake District, Northern England, *Geografiska Annaler*, **45**, 172–179, 1963.

Corte, A. E., The frost behavior of soils: Laboratory and field data for a new concept. Part I: Vertical sorting, *Tech. rep.*, U. S. Army Cold Regions and Engineering Laboratory, 1961.

Corte, A. E., The frost behavior of soils: Laboratory and field data for a new concept. Part II: Horizontal sorting, *Tech. rep.*, U. S. Army Cold Regions and Engineering Laboratory, 1962.

Elton, C., The nature and origin of soil polygons in Spitsbergen, *Geological Society of London Quarterly Journal*, **83**, 163–194, 1927.

Forman, S. L. and G. H. Miller, Time-dependent soil morphologies and pedogenic processes, *Arctic and Alpine Research*, **16(4)**, 381–394, 1984.

George, J. H., R. D. Gunn, and B. Straughan, Patterned ground formation and penetrative convection in porous media, *Geophys. Astrophys. Fluid Dynamics*, **46**, 135–158, 1989.

Gleason, K. J., W. B. Krantz, N. Caine, J. H. George, and R. D. Gunn, Geometrical aspects of sorted patterned ground in recurrently frozen soil, *Science*, **232**, 216–220, 1986.

Goldthwait, R. P., Frost sorted patterned ground: A review, *Quaternary Research*, **6**, 27–35, 1976.

Grab, S. W., Annually re-forming miniature sorted patterned ground in the High Drakensberg, Southern Africa, *Earth Surface Processes and Landforms*, **22**, 733–745, 1997.

Hallet, B., Self-organization in freezing soils: from microscopic ice lenses to patterned ground, *Can. J. Phys.*, **68**, 842–852, 1990.

Hallet, B., Measurement of soil motion in sorted circles, Western Spitsbergen, in *Proceedings of the Seventh International Conference on Permafrost*, edited by A. G. Lewkowicz, vol. 57, pp. 415–420, Centre d'Etudes Nordiques, Universite Laval, Quebec, PQ, 1998.

Hallet, B. and S. Prestrud, Dynamics of periglacial sorted circles in Western Spitsbergen, *Quaternary Research*, **26**, 81–99, 1986.

Hallet, B. and E. D. Waddington, Buoyancy forces induced by freeze-thaw in the active layer: Implications for diapirism and soil circulation, in *Periglacial Geomorphology*, vol. 22, pp. 251–279, 1992.

Hogbom, B., Uber die geologische bedeutung des frostes, *Upsala Univ. Geol. Inst. Bull.*, **12**, 257–389, 1986.

Huxley, J. S. and N. E. Odell, Notes on the surface markings in Spitsbergen, *Geographical Journal*, **63**, 207–229, 1924.

Jahn, A., Origin and development of patterned ground in Spitsbergen, *Proceedings of the First International Conference on Permafrost*, pp. 140–145, 1963.

Lambe, T. W. and R. V. Whitman, *Soil Mechanics*, John Wiley & Sons, Inc., New York, New York, 1969.

Longwell, C. R., Three common types of desert mud-cracks, *Am. Jour. Sci., 5th ser.*, **15**, 136–145, 1928.

Low, A. R., Instability of viscous fluid motion, *Nature*, **115**, 299–300, 1925.

Mackay, J. R., The origin of hummocks, Western Arctic coast, Canada, *Canadian Journal of Earth Sciences*, **17**, 996–1006, 1980.

Murray, A. B. and C. Paola, A cellular model of braided rivers, *Nature(London)*, **371(6492)**, 54–57, 1994.

Nansen, F., *Spitzbergen*, Leipzig, F. A. Brockhaus, 1922.

Nicholson, F. H., Patterned ground formation and description as suggested by low Arctic and sub-Arctic examples, *Arctic and Alpine Research*, **8**, 329–34, 1976.

Nordenskjold, O., Uber die natur der polarlander. 2: Spitzbergen un die umliegenden inseln, *Geographische Zeitschrift*, **13**, 557–568, 1907.

Norikazu, M., Solifluction rates, processes and landforms: a global review, *Earth-Science Reviews*, **55**, 107–134, 2001.

O'Neill, K. and R. D. Miller, Exploration of a rigid ice model of frost heave, *Water Resource Research*, **21**, 281–296, 1985.

Parmuzina, O. Y., *The cryogenic structure and certain ice features of ice seperation in a seasonally thawed layer (in Russian)*, pp. 141–164, Moscow University Press, Moscow, 1978.

Pissart, A., Apparition et evolution des sols structuraux periglaciires de haute montagne. experiences de terrain au chanbeyron (Alpes, France), *Abhandlungen der Akademie der Wissenschaften in Gottingen, Mathematisch-Physikalische Klasse*, **3(31)**, 142–156, 1977.

Prestrud, S., *The upfreezing process and its role in sorted circles*, Masters thesis, University of Washington, 1987.

Ray, R. J., W. B. Krantz, T. N. Caine, and R. D. Gunn, A model for sorted patterned-ground regularity, *Journal of Glaciology*, **29(102)**, 317–337, 1983.

Schmertmann, J. and R. S. Taylor, Quantitative data from a patterned ground site over permafrost, *Tech. rep.*, U.S. Army Cold Regions and Engineering Laboratory, 1965.

Schunke, E., Die periglazialerscheinungen islands in Abhangigkeit von klima und substrat, *Abhandlungen der Akademie der Wissenschaften in Gottingen, Mathematisch-Physikalische Klasse*, **30**, 1–273, 1975.

Sharp, R. P., Soil structures in the St. Elias Range, Yukon Territory, *Journal of Geomorphology*, **5**, 274–301, 1942.

Steche, H., Beitrage zur frage der strukturboden, *Sachs. Akad. Wiss., Math.-phys. Kl., Ber.*, **85**, 193–272, 1933.

Taber, S., Frost heaving, *J. Geology*, **37**, 428–461, 1929.

Taber, S., Perennially frozen ground in Alaska: its origin and history, *Geological Society of America Bulletin*, **54**, 1433–1548, 1943.

Van Vliet-Lanoe, B., Differential frost heave, loadcasting and convection, converging mechanisms, a discussion of the origin of cryoturbations, *Permafrost and Periglacial Processes*, **2**, 123–139, 1991.

Washburn, A. L., Classification of patterned ground and review of suggested origins, *Geological Society of America Bulletin*, **67**, 823–865, 1956.

Washburn, A. L., Weathering, frost action, and patterned ground in the Mesters Vig District, Northeast Greenland, *Meddelelser om Gronland*, **176**, 1969.

Washburn, A. L., *Plugs and Plug Circles: A Basic Form of Patterned Ground, Cornwallis Island, Arctic Canada-Origin and Implications*, The Geological Society of America, Inc., Boulder, Colorado, 1997, Memoir 190.

Werner, B. T., Eolian dunes; computer simulations and attractor interpretation, *Geology*, **23(12)**, 1107–1110, 1995.

Werner, B. T. and T. M. Fink, Beach cusps as self-organized patterns, *American Association for the Advancement of Science*, **260(5110)**, 968–971, 1993.

Werner, B. T. and B. Hallet, Numerical simulation of self-organized stone stripes, *Nature*, **361**, 142–145, 1993.

Wilkerson, F. D., Rates of heave and surface rotation of periglacial frost boils in the White Mountains, California, *Geology*, **25(9)**, 771–774, 1997.

Williams, P. J. and M. W. Smith, *The Frozen Earth: Fundamentals of Geocryology*, Cambridge University Press, New York, New York, 1989.

Chapter 2

A Model for Sorted Circles as Self-Organized Patterns

2.1 Abstract

Sorted circles emerge as self-organized patterns from a laterally uniform active layer that becomes laterally sorted as frost heave deforms the interface between a stone layer and an underlying soil layer. In a three-dimensional, cellular model of the active layer, cyclic freezing and thawing drives transport of stone and soil particles by (1) addition of ice particles representing soil expansion by frost heave, (2) removal of ice particles representing soil consolidation during thawing, (3) addition of void particles (a discrete abstraction of soil compressibility) representing soil expansion by water absorption, (4) removal of void particles representing compaction and desiccation of underlying soil by frost heave, (5) relaxation of surface morphology by soil creep and stone avalanche, and (6)

vertical sorting of stones and soil by illuviation. These transport processes give rise to sorted circles, which are characterized by a mean spacing of 3.6 m, a 2.4 m wide soil domain surrounded by a 1.0 m wide, 0.3 m high annulus of stones, and a 750 year period of circulation in the soil domain, all consistent with measured characteristics of sorted circles in western Spitsbergen. In the model, instabilities on the stone-soil interface grow upward as soil plugs by drawing in soil from the surrounding subsurface soil layer; soil plugs develop into sorted circles as they contact the ground surface, simultaneously elevating an encircling annulus of stones. Sorted circles are dynamically maintained by circulation within the stone and soil domains. Initiation of soil plugs is driven by a positive feedback in which frost heave near the stone-soil interface pushes soil toward more compressible soil regions, where the soil layer is thicker. The lateral component of these frost-heave-induced displacements is not reversed during thaw because soil consolidation (as ice-rich soil melts and drains) and soil expansion (as desiccated and compacted soil hydrates) displace soil vertically. Further development of soil plugs and sorted circles is determined by an interplay between this positive feedback and amplitude dependent negative feedbacks that result from decoupling of the freezing front from the stone-soil interface. Parameters outside the range in which sorted circles form can result, for example, in stone islands and labyrinthine patterns. The initial wavelength of perturbations on the stone-soil interface is accurately predicted using a linear stability analysis, but increase in this wavelength through time reflects the nonlinearities that control the spacing of soil plugs and sorted circles, namely, interactions and mergers between neighboring forms.

2.2 Introduction

Freezing and thawing of Arctic surface soil results in sorted patterns of soil and stones, the most striking of which assume circular, polygonal, linear, and labyrinthine shapes. Although a range of mechanisms have been proposed for the origin of sorted patterned ground *Washburn* [1980, 1997], few of these hypotheses can be excluded, either because the proposed mechanisms have been only qualitatively described or because of a lack of discriminating measurements. Numerical models can be used to explore the consequences and consistency of these mechanisms. Here, a numerical model for one form of sorted patterned ground, sorted circles, is presented and investigated.

2.2.1 Sorted Circles

A model for sorted circles should reproduce observed features and behaviors of the archetypical sorted circles found in western Spitsbergen [*Hallet and Prestrud*, 1986], the Canadian Arctic [*Washburn*, 1997], and Greenland [*Schmertmann and Taylor*, 1965]. In western Spitsbergen, sorted circles (Figure 1) typically consist of a 2-3 m wide cylinder of soil, the axis of which extends 1-1.5 m downward to the base of the active layer, the near-surface zone that freezes and thaws annually. The soil surface is domed upward as much as 0.1 m and is surrounded by a 0.5-1 m wide annulus of gravel, devoid of soil, that rises as much as 0.5 m above the soil domain [*Hallet and Prestrud*, 1986; *Hallet et al.*, 1988]. Well-developed sorted circles in western Spitsbergen did not detectably change form over a decade of measurements [*Hallet*, 1998]. Coherent surface soil motion of $\sim$0.01 m/yr outward from the center of the soil domain has been

recorded in Greenland [*Schmertmann and Taylor*, 1965] and in western Spitsbergen [*Hallet and Prestrud*, 1986], as has stone motion of comparable velocity down the inner slope of the gravel annulus [*Hallet and Prestrud*, 1986]. Subsurface soil transport toward the center of the soil domain has been inferred from surface morphology, surface soil motion, and the assumption that soil volume is conserved [*Hallet and Prestrud*, 1986], but no direct measurements are available. This inference is supported by tilt measurements from within a sorted circle soil domain that record substantial yearly subsurface rotational motion [*Hallet*, 1998]. A soil domain circulation period of 500 years has been estimated for a sorted circle in western Spitsbergen with a 3 m wide, 1 m thick soil domain [*Hallet et al.*, 1988].

Cyclic freezing and thawing drives processes that transport stones, soil, and water in the active layer, resulting in the development of sorted circles. During winter, a freezing front descends from the ground surface with a velocity dependent on the thermal properties and configuration of stones and soil in the active layer. Measurements of temperature within a sorted circle during freezing indicate faster freezing front propagation in the stone domain than in the soil domain [*Schmertmann and Taylor*, 1965]. Freezing of fine-grained soils impels moisture migration to the freezing front, resulting in expansion where water freezes, termed frost heave, and contraction where soils are desiccated by water withdrawal [*Taber*, 1929]. During thaw, ice-rich soils compact by expelling excess water and desiccated soils expand by absorbing water. Soil expansion is also caused by frost heave in still frozen underlying soils as water released by melting percolates downward [*Mackay*, 1980]. Percolating water entrains soil particles and transports them downward through pores between stones to the base of stone

regions with unfilled pores, a process termed soil illuviation [*Corte*, 1966; *Forman and Miller*, 1984; *Washburn*, 1997]. Surface gradients generated by the subsurface redistribution of stones and soil by freezing and thawing cause downslope soil creep [*Hallet and Prestrud*, 1986; *Hallet et al.*, 1988]. Sorting in the active layer arises from the dependence of these transport processes on the thermal and hydrological differences between stones and soil, resulting in laterally and vertically nonuniform stone and soil displacements [*Taber*, 1929; *Corte*, 1961; *Anderson*, 1988].

Several environmental conditions are common to locations where sorted circles are found. First, the surface layer experiences cycles of annual freezing and thawing. Second, soil with volumetric fractions of frost-susceptible fine material in the range 12-42% is present in the active layer for all types of sorted patterned ground [*Goldthwait*, 1976]. Third, water remains near the ground surface during freezing because underlying permafrost inhibits drainage and the high-fine-content soils retain water. Fourth, air temperatures only moderately below 0°C during freezing cause the active layer to freeze slowly (over a period of several weeks to months), resulting in substantial frost heave [*Hallet and Prestrud*, 1986; *Hallet*, 1998].

2.2.2 Current Problem State

Dozens of hypotheses, relying on 19 basic mechanisms [*Washburn*, 1956, 1997], have been proposed for specific types and aspects of sorted patterned ground. Proposed mechanisms for sorted circles have primarily addressed three stages in their development: pattern initiation, accumulation of soil into a central

soil domain, and the dynamics of well-developed forms.

In one model for pattern initiation, inversion in the density of interstitial water from the base of the active layer (at 0°C) to the ground surface (at 4°C) during thawing results in a cellular pattern of thermal convection. Down welling warm water melts the upper surface of the permafrost, modifying the interface between the active layer and the underlying permafrost. The resulting undulating interface biases active layer transport processes to produce sorted circles with the same pattern as the convection cells. The ratio of sorted circle width to active layer depth predicted from a linear stability analysis is consistent with measurements [*Ray et al.*, 1983; *Gleason et al.*, 1986; *Krantz*, 1990]. However, this model relies on coherent convection of water through soil pores, which has been documented in aquifers and snow layers [*Combarnous and Bories*, 1975] but not within the highly heterogeneous soil of the active layer.

Because a layer of soil commonly underlies a layer of stones in areas where sorted circles are forming [*Elton*, 1927; *Corte*, 1961; *Washburn*, 1956, 1969, 1997], a layered configuration often is hypothesized to constitute an initial condition for sorted circle formation. Layering can arise directly from sorting inherent in the depositional processes that produced the soil (e.g., beach deposits and differential weathering) or from active layer processes, such as illuviation and frost-heave-driven stone uplift, operating on an initially mixed soil [*Washburn*, 1997]. Mechanisms proposed for the accumulation of the soil layer into a central soil domain include spatially varying frost heave [*Washburn*, 1956; *Nicholson*, 1976; *Van Vliet-Lanoe*, 1991; *Washburn*, 1997] and a density-driven instability of the stone-soil interface [*Van Vliet-Lanoe*, 1991; *Washburn*, 1997]. These mechanisms are related to sorted circle formation with the assumption that diapiric soil plugs

are a precursor to well-developed sorted circles.

One mechanism proposed for the maintenance of fully developed sorted circles is convection of soil owing to decreasing soil density with depth. This density inversion is hypothesized to be caused by compaction during thaw that starts at the ground surface and descends through the active layer (*Mortensen* [1932] referenced by *Washburn* [1956] [see also *Hallet and Prestrud*, 1986]). However, measured soil density gradients are below the predicted value necessary to initiate soil convection [*Hallet and Waddington*, 1991]. In a second mechanism, frost heave at inclined freezing fronts maintains sorted circles because stones move upward toward a descending freezing front but fine-grained particles are expelled downward away from the freezing front [*Nicholson*, 1976]. In a third mechanism, first proposed for earth hummocks [*Mackay*, 1979, 1980] and later extended to sorted circles [*Washburn*, 1997], frost heave at a descending freezing front desiccates and compacts the soil domain, followed by vertical soil expansion during thaw and inward soil transport along a concave upward thaw front. The second and third mechanisms are incomplete in that they postulate but do not produce an initial freezing front or thawing front inclination [*Washburn*, 1997].

Many of the proposed mechanisms have not been modeled physically, analytically, or numerically. None of the models or mechanisms treat sorted circles from inception to fully developed forms. The predictive capacity of individual models is limited because of the small range of behavior to which they are applicable and because the consistency between models for different aspects of sorted circles has not been explored.

2.2.3 New Approach

Here we present a numerical model for sorted circle initiation, formation, and maintenance based on a set of hypothesized simplifications of the interactions between lateral sorting, freezing front inclination, and transport of stones and soil in an active layer undergoing repeated freezing and thawing. The approach underlying this model relies on two key assumptions. First, sorted circles emerge owing to self-organization, the development of global order from local interactions [*Nicolis and Prigogine*, 1977], implying that mechanisms in the model need not reflect the form or scale of the patterns, which emerge spontaneously. The initiation and stabilization of self-organized patterns are dependent only on the general nature of positive and negative feedbacks acting locally. Second, it is assumed that many of the details of heat flow and stone, soil and water transport processes need not be included in a model for sorted circles. This insensitivity to detail stems from a robust property of nonlinear, dissipative systems: the loss of information associated with dissipation results in only some aspects of fast, small-scale processes contributing to the dynamics of slower-evolving, larger-scale patterns that emerge [*Werner*, 1995, 1999].

2.3 Conceptual Model

In our conceptual model, sorted circles evolve within an active layer that is forced by an annual cycle of freezing and thawing. The ground surface and the surface of the underlying permafrost constitute the boundaries of the active layer. Heat flow through the ground surface and flow of water into or out of

the active layer are the primary interactions between the active layer system and the external environment. Active layer processes act on stones and soil differently because of their differing thermal and hydrological properties. Soil retains water, releases latent heat during freezing, enables frost heave, compacts when desiccated or compressed, creeps down low slopes, sifts downward through the pores between stones, and expands upon absorption of water. Stones exhibit none of these behaviors. Sorted circles emerge because of feedbacks between the configuration of stones and soil in the active layer and the transport resulting from active layer processes acting on that configuration.

2.3.1 Processes

Frost heave is the primary transport process in our conceptual model for sorted circle formation. Soil expansion at the freezing front, by ice growth, and contraction of the underlying unfrozen soil, by compaction and desiccation, result in subsurface transport away from the freezing front. The freezing front moves downward from the ground surface at a rate determined by heat conduction and the release of latent heat when water freezes. Where stones and soil form distinct domains separated by a well-defined interface, with stones overlying soil, the morphology of the freezing front approximates the stone-soil interface because the freezing front moves rapidly through dry stones but more slowly through wet soil. Frost heave pushes upward, displacing stones and soil, and deforming the ground surface. In addition, frost heave and frost-heave-induced desiccation displace soil downward, compacting soil well below the stone-soil interface. Frost heave primarily induces soil expansion near the top of the soil layer because of the

limited supply of water available for ice formation, limited soil compressibility, and increasing overburden with depth.

Gravity drives three relaxation phenomena: compaction during thaw, soil illuviation, and downslope surface transport. Thawing, ice-rich soils expel water and compact vertically under the overburden. A distinct interface between stone and soil domains is maintained by illuviation, soil sifting downward through the pores between stones. On the ground surface, soil creeps downslope, and gradients within the stone domain relax (stone particles avalanche) when the surface slope exceeds the angle of repose.

During thawing, compressed and desiccated soil expands by absorption of downward percolating water. The direction of expansion is vertical because stresses caused by lateral confinement are assumed to exceed those from the overburden. Expansion of soil by water absorption during thaw reverses (in magnitude, not direction) the compaction of soil by frost heave during freezing because the soil is assumed to have undergone many loading and unloading (freeze-thaw) cycles with similar maximum stresses, which bring a soil into a steady state with equal magnitudes of compression and expansion [*Lambe and Whitman*, 1969, p. 321].

2.3.2 Positive Feedback Mechanism

In the conceptual model, the initial configuration of the active layer is a uniform layer of mixed stones and soil underlying a uniform layer of stones devoid of soil. Sorted circles initiate as an instability in the interface between the stone and soil layers. Small positive perturbations in the stone-soil inter-

face are more compressible because of the greater volume of soil beneath them. After compressing soil locally, frost heave near the stone-soil interface transports soil into nearby perturbations where unfrozen compressible soil remains. The net effect of soil transport by frost heave is to increase the amount of soil within those positive soil perturbations (Figure 2). Through repeated freezing and thawing, perturbations in the interface grow upward because of the asymmetry between soil compaction during freezing (Figure 2a), which has a lateral component, and vertical soil relaxation and expansion during thawing (Figures 2b and 2c). This positive feedback initiates the pattern and leads to the accumulation of soil and the formation of soil plugs. We hypothesize that these same processes underlying pattern initiation, combined with surface relaxation, can lead to the development and maintenance of sorted circles. Investigation of this hypothesis requires a numerical model implementing these processes.

2.4 Numerical Model

This conceptual model for sorted circles is encoded into a three-dimensional cellular computer model that simulates the annual freeze-thaw cycle of an active layer. The simulated active layer is bounded by a rigid plane lower surface, a mechanically free upper surface, and periodic lateral boundaries.

Four types of particles occupy the cells representing the active layer: stone, soil, ice, and void. These particles move as indivisible units. Ice particles and void particles occupy an entire cell. Stone and soil particles each fill 50% of the volume of a cell. Because small grain-size soil particles can fit in the pore space of cells containing large grain-size stone particles, a cell can contain either one

stone particle, one stone particle and one soil particle, or two soil particles, but not two stone particles. Stone particles represent either one or many stones that move as a unit. Void particles do not represent pores in soil; rather, void particles are a discrete representation of soil compressibility (given stresses from a typical freeze-thaw cycle). Cells containing one stone particle and one soil particle will be termed soil cells because in the simulations presented here (excepting section 4.4), all cells containing a soil particle also contain a stone particle (i.e., no cells contain two soil particles). The corresponding volumetric fraction of stones in soil domains, 0.5, is comparable to the value measured from a sorted circle in western Spitsbergen, 0.31 [*Prestrud*, 1987]. The numbers of stone and soil particles are conserved. Cells are half as high as they are wide to enhance vertical resolution while maintaining computational performance.

The thermal and hydrological properties of soil particles differ from those of stone particles. During freezing, the water content of soil particles, which determines the latent heat but does not constrain ice particle formation, is assumed to be a fraction w of the soil particle volume. Stone particles do not contain water. During freezing, ice particles can form in soil cells but not stone cells. Soil particles sift through the pore space of stone cells and creep downslope at the ground surface. Stone particles at the ground surface avalanche only when gradients exceed a specified angle of repose.

Void particles and ice particles are created and destroyed during the yearly freeze-thaw cycle. Void particles form within soil domains and render the simulated active layer compressible. The volume of void particles divided by the volume of soil particles (the volume of a soil particle is half the volume of a cell) is equivalent to the soil compressibility C. The formation of ice particles

simulates the expansion of soil by frost heave.

2.4.1 Freeze-Thaw Cycle

In the numerical model, a freeze-thaw cycle is represented by a sequence of steps corresponding to the physical processes of the conceptual model.

2.4.1.1 Freezing and frost heave

As the active layer freezes, the time-dependent temperature in each cell, the descent of the freezing front ($\equiv 0^{o}$C isotherm), the formation of ice particles, and the resulting stone and soil displacements are simulated (Figure 3a). An initial temperature profile, representative of late summer, is imposed, increasing linearly from T_b at the base of the active layer up to T_g at the ground surface. The temperature of unoccupied cells above cells representing the ground surface is held at T_a for the freezing step, representative of the average air temperature during freezing. The temperature within each cell in the active layer evolves because of heat diffusion and release of latent heat. The temperature change is calculated by time stepping the DuFort-Frankel finite difference approximation of the three-dimensional heat diffusion equation [*DuFort and Frankel*, 1953; *Nogotov*, 1978], with a correction for latent heat release after each time step; the change in temperature of a cell at 0^{o}C is converted to an equivalent release of latent heat and reduction in the unfrozen water content. When the unfrozen water reservoir of a cell at the freezing front is exhausted, the local freezing front descends to the cell below.

When the freezing front exits a cell containing a soil particle ("t" in Figure 3a), a test for formation of an ice particle in that cell is conducted. An ice particle displaces the particles from the cell in which it forms either toward a void cell in the unfrozen soil or toward the ground surface. The probability of an ice particle forming is the greater of two probabilities: that of displacing particles toward the nearest void cell or that of displacing particles toward the ground surface. These probabilities are assumed to decrease linearly with distance:

$$P_{\text{surf}} = \max(0, 1 - d_{\text{surf}}/d_s) \tag{2.1}$$

$$P_{\text{void}} = \max(0, 1 - d_{\text{void}}/d_v), \tag{2.2}$$

where d_{surf} is the distance to the ground surface, d_{void} is the distance to the void cell, parameters d_s and d_v are the distances at which P_{surf} and P_{void} are zero, and $\max(A, B)$ is the greater of A and B. Displacements toward the ground surface follow a path that is a weighted average of the unit vector normal to the freezing front at the ice particle and the unit vector pointing from each displaced cell in the path to the nearest empty cell above the ground surface. The weights are proportional to the inverse distances from the displaced cell to the ice particle and from the displaced cell to the ground surface, respectively. This path of displacements starts out perpendicular to the freezing front, then bends toward the ground surface. Displacements toward a void particle follow a straight line from the ice particle to the void particle. This algorithm for ice formation and particle displacement abstracts the complicated processes of frost heave, compaction, desiccation, granular shear, viscoelastic deformation, and water migration in partially frozen soils.

2.4.1.2 Surface morphology relaxation

During thawing, downslope surface motion relaxes surface morphology (Figure 3b). Two-dimensional diffusion of elevation, a continuum approximation that models surface soil flux proportional to slope [e.g., *Jyotsna and Haff*, 1997], is incorporated in the model by moving particles at the ground surface to the lowest of the eight surrounding cells with a probability $\Delta V/V_o$, where V_o is the volume of a cell and ΔV is the volume that would diffuse during a time interval Δt given a difference in elevation between the two cells of Δh:

$$\Delta V = K_{\text{surf}} \frac{\Delta h}{\Delta x} \Delta t, \tag{2.3}$$

where K_{surf} is a diffusion constant and Δx is the distance between cell centers. The time step Δt is chosen such that at most one particle per column is displaced in a single time step. Stone particles resting on stone particles move downslope only if the surface elevation difference exceeds two cells, which is equivalent to an angle of repose of 45^o.

2.4.1.3 Compaction during thaw and soil illuviation

During thaw, ice-rich soil compacts, and soil particles sift downward through the pore space of underlying stone cells (Figure 3c). First, ice particles are removed and the overlying column of particles is lowered one cell. Second, soil particles located above cells containing only a stone particle move downward to fill the lowest stone cell, thereby transforming it into a soil cell.

2.4.1.4 Soil expansion

During thaw, desiccated soil hydrates and expands (Figure 3d). Soil expansion is simulated by adding void particles to the soil domains until a prespecified soil compressibility (total volume of void particles divided by total volume of soil particles), C, is achieved. The probability of inserting a void particle in a cell is C times the volumetric fraction of soil particles in a $3 \times 3 \times 3$ cell neighborhood. To make room for a void particle, the column of particles above the cell in which it will be inserted is shifted up one cell. At the conclusion of the thaw stage, cells are assigned an unfrozen water content equal to the water fraction w times the volume of soil in that cell (half the volume of a cell for soil cells and zero for stone cells).

2.4.2 Reference Model

A set of parameters characterizing a reference model was chosen, in part, based on measurements from sorted circles in western Spitsbergen (Table 1). The active layer is 1 m thick [*Hallet and Prestrud*, 1986], with an initial configuration of a 0.6 m thick layer of stone cells, $h_{\text{stone}} = 0.6$ m, overlying a 0.4 m thick layer of soil cells, $h_{\text{soil}} = 0.4$ m. This ratio of stone to soil volume approximately corresponds to that of a 3 m wide soil cylinder surrounded by a 1 m wide stone annulus, within the observed range of sorted circles in western Spitsbergen [*Hallet and Prestrud*, 1986]. Before freezing, the soil compressibility C is 0.05, consistent with expansion measured in high clay content soils [*Lambe and Whitman*, 1969, p. 323]. The volumetric fraction of water in soil particles w is 0.1. This value, which is lower than observed in natural soils of this type, was chosen because higher

values of w have little effect on model results (e.g., Figure 12e) but result in significantly increased simulation time. The linear temperature profile before freezing is bounded by $T_b = 0^o$C at the base of the active layer and $T_g = 5^o$C at the ground surface (mean summer air temperature) [*Putkonen*, 1998]. The air temperature during freezing is assumed to be the annual mean, $T_a = -5^o$C [*Putkonen*, 1998]. Assuming the large difference in latent heat capacity between stones and soil overwhelms small differences in heat conductivity, a typical thermal diffusivity of $k_{\text{heat}} = 10^{-6}$ m^2/s is used for all cells [*Williams and Smith*, 1989]. The proportionality factor between surface slope and soil flux for surface creep is $K_{\text{surf}} = 5 \times 10^{-3}$ m^2/yr, yielding a surface velocity comparable to the measured value ~0.01 m/yr on a ~1 m radius sorted circle with a maximum elevation difference of ~0.1 m [*Hallet et al.*, 1988], assuming this velocity decreases linearly to zero at roughly the same depth as the maximum elevation difference, 0.1 m. Little information regarding the length scales characterizing subsurface displacement in the active layer is available. In the reference model, the distances at which the probabilities for displacing particles to the ground surface or to a void cell fall to zero are set to $d_s = d_v = 0.6$ m, a significant fraction of the active layer depth. Cells measure 0.1 m × 0.1 m × 0.05 m. A reference model simulation is 200 × 200 cells or 20 m × 20 m in size.

2.5 Results

2.5.1 Reference Model

In the reference model, patterns of stones and soil resembling sorted circles form and evolve over ~500-2000 freeze-thaw cycles (Figure 4; the simulation shown is 10 m × 10 m for illustrative purposes). The stages of sorted circle development, including initiation, soil accumulation, and maintenance, are steps in a continuous process that can be followed for any sorted circle in the reference model; however, the timing varies between individual sorted circles.

From an initially horizontal stone-soil interface (Figure 4a), coherent distortions of the interface much larger than the cell size develop in the first few freeze-thaw cycles. Between 1 and 200 freeze-thaw cycles, the peak wavelength in these perturbations, measured from a radial power spectrum (a two-dimensional power spectrum that has been averaged over angle for each radial wavenumber), increases from ~0.7 to ~3 m (Figure 5). Between 200 and 600 freeze-thaw cycles, discrete soil plugs emerge and expand toward the surface by collecting soil from the surrounding soil layer and through mergers with neighboring soil plugs (Figures 4b and 6). Between 500 and 700 freeze-thaw cycles, sorted circles emerge (Figures 4b and 4c). After soil domains contact the ground surface, they continue to expand rapidly over ~500 freeze-thaw cycles (Figures 4b-4e and 7) until the underlying soil layer is depleted (Figure 4e). In well-developed forms a 2.4 ± 0.5 m diameter circular soil domain extends to the base of the active layer and is surrounded by a 1 ± 0.2 m wide annulus of stones elevated ~0.3 m above the soil domain (Figure 4f). Sorted circles are spaced 3.6 ± 0.6 m apart in the

reference model.

Mean surface motion is outward from the center of the soil domain to its intersection with the stone domain (zone 1, Figure 8) and inward from the crest of the stone annulus to its intersection with the soil domain (zone 2, Figure 8). The small outward velocity beyond the crest of the stone annulus (zone 3, Figure 8) indicates continued radial growth. A 12 year record of the position of surface markers on a sorted circle in western Spitsbergen shows a similar pattern of surface motion. Subsurface recirculation of soil from the periphery of the soil domain inward (Figure 9) maintains the convex surface despite the high outward velocity in zone 1. The strong velocity gradients near the stone-soil interface and roughly uniform upward motion in the central region of the soil domain are similar to inferred sorted circle circulation patterns [*Pissart*, 1990]. Although the streamlines of circulation in the soil domain are irregular (Figure 9), the mean period of circulation can be approximated assuming a circular path with a radius half the active layer depth, 0.5 ± 0.2 m, and a mean soil velocity of 0.0042 ± 0.001 m/yr, which is averaged over 10 freeze-thaw cycles starting with cycle 1500 (the velocity field is calculated from 200 simulations starting with the same configuration of stones and soil but using different sequences of random numbers). The mean period of circulation, 750 ± 350 years, is comparable to the 500 year period inferred for sorted circles in western Spitsbergen [*Hallet and Prestrud*, 1986].

2.5.2 Sensitivity to Parameters

Qualitatively, whether sorted circles form does not depend on most of the model parameters. However, quantitative characteristics of sorted circles, including spacing, size, and formation time, are sensitive to some parameters. The effects of varying simulation parameters one at a time from their reference model values on the following characteristics of sorted circles are discussed: (1) initial spacing between soil plugs and between sorted circles, (2) time for sorted circles to form, (3) mean circulation velocity of the soil domain, and (4) sorted circle formation criteria.

2.5.2.1 Initial spacing

In the reference model, soil plugs form as isolated features in a manner that depends primarily on the initial thicknesses of the stone and soil layers, h_{stone} and h_{soil}, and on the distance at which the probability of an ice particle displacing soil to a void cell falls to zero, d_v. If the soil layer thickness is less than ~40% of the active layer thickness, the initial spacing between sorted circles equals the spacing between soil plugs. If the thickness of the soil layer is greater then ~40% of active layer thickness, soil plugs form faster and closer together, evolving into circular, elongate, and labyrinthine patterns (Figure 10), primarily through mergers between neighboring soil domains. In this case, spacing depends in a complicated manner on parameters.

The initial spacing between soil plugs, estimated from the peak of the radial power spectrum of the stone-soil interface height, increases as d_v increases (Figure 11a). Spacing also varies weakly with the inverse of the water content of soil

w, decreasing from 3.3 m to 2.5 m as w increases from 0.02 to 0.3. A similar dependence holds for T_a, with spacing decreasing as T_a increases. As the thickness of the initial soil layer h_{soil} increases, the spacing between soil plugs decreases (Figure 11b) because the minimum volume of soil required for soil plugs to rise to the surface can be acquired from a smaller area. Spacing does not fall below ~2 m because soil plugs separated by < 2 m readily merge.

2.5.2.2 Formation time

The time required for sorted circles to form, taken here to be the number of freeze-thaw cycles before a soil plug contacts the ground surface, depends on the rate at which soil accumulates into plugs and the volume of soil required for a soil plug to reach the ground surface.

The primary parameters determining soil accumulation rate are the compressibility C and h_{soil} (Figures 12a and 12b). As soil compressibility increases, the rate of soil accumulation is amplified by increasing the number of subsurface transport events per freeze-thaw cycle. An increase in h_{soil} also results in an increase in the number of subsurface transport events per freeze-thaw cycle and a consequent decrease in the time required to form sorted circles.

The volume of soil plugs contacting the surface is determined by the parameters d_v, h_{stone}, w, and T_a. The mean distance that soil is transported in a freeze-thaw cycle increases with d_v, thereby increasing the soil collection rate and tending to decrease sorted circle formation time. However, if $d_v < \sim 0.8$ m, the spacing between soil plugs (Figure 11a) and the initial soil plug volume both increase with increasing d_v sufficiently fast to overwhelm the increasing soil collec-

tion rate, resulting in increasing formation time (Figure 12c). If $d_v > \sim 0.8$ m, the spacing between developing soil plugs is determined by interactions and mergers that are less strongly correlated with d_v; in this case, the increasing mean soil displacement distance per freeze-thaw cycle with increasing d_v decreases formation time. Sorted circle formation time increases with increasing h_{stone} (Figure 12d) because soil plugs require more time to penetrate a thicker stone layer.

Formation time is sensitive to w and T_a through their effects on the amount of ice in soil plugs relative to surrounding regions. Greater ice formation in soil plugs displaces soil into the surrounding regions, suppressing soil plug growth and selecting for larger spacing and volume of soil plugs contacting the ground surface. Increasing w increases the stabilizing effect of latent heat (coupling the freezing front to the stone-soil interface), resulting in a more uniform distribution of ice on the stone-soil interface, less suppression of soil plug growth, smaller initial volumes, and shorter formation times for $w > \sim 0.05$ (Figure 12e). However, for $w < \sim 0.05$, negative perturbations in the stone-soil interface are unstable (increasingly unstable with decreasing w), driving soil away from soil-depleted regions, increasing the rate of soil accumulation, and decreasing the formation time (Figure 12e). Soil plug spacing and volume decrease with increasing surface temperature (closer to 0^oC) during freezing because the freezing front more closely conforms to the stone-soil interface when latent heat is removed more slowly. The resulting more uniform distribution of ice particles on the stone-soil interface suppresses soil plug growth less, thereby decreasing formation time, spacing, and volume (Figure 12f).

2.5.2.3 Mean soil domain velocity

The mean particle velocity in the soil domain of a well-developed sorted circle is primarily dependent on the soil compressibility C (Figure 13a). Particle velocities increase with increasing C because the overall number of displacements by frost heave scales with the number of void particles and because displacement directions become less random as the density of void particles increases, thereby increasing the net circulation velocity.

Mean soil domain particle velocity decreases with time (Figure 13b) because as the stone-soil interface steepens and the diameter of the soil domain increases, inward displacements originating at the stone-soil interface, which underlie circulation, become a smaller fraction of the total number of frost-heave-induced displacements. Variations in circulation velocity with C and time overwhelm variations in velocity with other parameters.

2.5.2.4 Formation criteria

In the model, the parameters determining whether sorted circles form and are maintained are d_s, d_v, h_{soil}, h_{stone}, C and w. Variation in these parameters from the reference model values, one at a time, can result in several alternatives to sorted circle formation and maintenance, including a persistent unpatterned state, formation of sorted circles as a transient state in the development of other patterns, or the direct emergence of patterns other than sorted circles.

Sorted circles form if $d_s < \sim 0.8$ m. If $d_s > \sim 0.8$ m, soil accumulates into subsurface plugs that cannot penetrate the stone layer because frost-heave-

induced displacements toward the surface that disperse soil overwhelm inward displacements that accumulate soil into soil plugs.

Sorted circles form if $d_v > 0.4$ m because positive perturbations in the stone-soil interface are unstable and develop into soil plugs. If $d_v < 0.4$ m, negative perturbations in the stone-soil interface are unstable, resulting in penetration of stone plugs to the base of the active layer rather than soil plugs to the ground surface. In this case, sorted circles do not form.

Stable sorted circles form if ~ 0.1 m $< h_{\text{soil}} < \sim 0.6$ m. If $h_{\text{soil}} < \sim 0.1$ m, an insufficient supply of soil exists for soil plugs to rise to the surface. If $h_{\text{soil}} > \sim 0.6$ m, sorted circles are a transient pattern, with mergers between sorted circles leading to the development of labyrinthine sorted features (Figure 10).

Sorted circles form if $h_{\text{stone}} > 0.4$ m. If $h_{\text{stone}} < 0.4$ m, small-amplitude soil plugs can form, but they do not rise to the surface because displacements toward the surface caused by frost heave, which disperse soil, overwhelm inward displacements, which accumulate soil (as for $d_s > 0.8$ m). Sorted circles form if h_{stone} is comparable to or greater than d_s ($\equiv 0.6$ m for the reference model).

Sorted circles form if $C > \sim 0.01$. If $C < \sim 0.01$, frost-heave-induced displacements toward the surface transporting soil away from the soil plugs dominate over soil accumulation through rare downward displacements toward sparsely distributed void cells.

Stable sorted circles form if $w > \sim 0.02$. If $w < 0.02$, sorted circles repeatedly form, expand radially, and collapse. This transient behavior reflects the interplay between fast soil accumulation and processes that disperse soil after surface morphology relaxes. For small w (minimal latent heat release), the freezing front

travels at nearly the same speed in the stone and soil domains; the morphology of the freezing front reflects the ground surface morphology instead of the stone-soil interface morphology (as for larger w). Initially, the freezing front morphology is coupled to the stone-soil interface morphology because perturbations in the stone-soil interface distort the ground surface. As the surface expression of the soil plug relaxes, the freezing front morphology decouples from the stone-soil interface morphology, and the soil plug freezes earlier and with greater frost heave than the surrounding region. As a result, the soil is displaced away from the soil plug, leading to its collapse.

2.5.3 Permafrost–Active Layer Interface

The emergence of features resembling sorted circles in the model, starting from an unpatterned state, indicates that the mechanisms included in this model are sufficient to produce the pattern without prior establishment of a template through additional mechanisms. To investigate the hypothesized influence of a morphological template pattern in the base of the active layer on sorted circle formation [*Ray et al.*, 1983; *Gleason et al.*, 1986; *Krantz*, 1990], two-dimensional sinusoidal perturbations, with an amplitude of 0.2 m and wavelength λ = 1-20 m, were applied to the lower boundary of the reference model. The effect of this template on sorted circle characteristics depends on the imposed wavelength relative to spacing between sorted circles in the reference model ($\sim$3.6 m). For all wavelengths, soil plugs first initiate at locations where the soil layer is thickest. If $\lambda < \sim$1.5 m, sorted circles develop as in the reference model. If $\sim$1.5 m $< \lambda <$ $\sim$2.5 m, sorted circles develop at the wavelength of the imposed perturbation,

but then they interact and merge to form sorted circles at the reference model spacing of ~3.6 m. If ~2.5 m $< \lambda <$ ~10 m, sorted circle spacing and location reflects the template. If $\lambda >$ ~10 m, sorted circle spacing and location initially reflects the template, but additional sorted circles later appear between these initial forms.

Frost heave at an upward propagating freezing front has been suggested as an operative process in patterned ground [*Mackay*, 1980; *Van Vliet-Lanoe*, 1991; *Washburn*, 1997]. Temperature gradients of 2°-4°C/m have been measured at the top of the permafrost near patterned ground on Cornwallis Island [*Cook*, 1955] and beneath a sorted circle in Thule, Greenland [*Schmertmann and Taylor*, 1965]; both locations have recorded annual mean temperatures of $-10°$ to $-15°$C. A series of simulations have been conducted using the processes and parameters of the reference model plus an upward propagating freezing front driven by a temperature gradient, ranging from 0.01° to 10°C/m, imposed at the base of the active layer. For temperature gradients $<$ 4°C/m, less then 1% of the soil compression results from the upward propagating freezing front, implying that an upward propagating freezing front has negligible impact on the initiation of soil plugs or the formation of sorted circles. For large temperature gradients ($>$ 5°C/m), the upward propagating freezing front has a significant impact on soil compression and can induce a change from sorted circle formation to stone island formation.

2.5.4 Upfreezing

Under repeated freezing and thawing, isolated stones migrate upward through the soil column and perpendicular to the freezing front a distance proportional to the strain induced in the surrounding soil by frost heave [*Anderson*, 1988]. Upfreezing of stones has been hypothesized to be a contributing mechanism to the formation of sorted circles [*Washburn*, 1956, 1997], but the rate of upfreezing and the depth to which it operates, as measured in laboratory experiments, might be insufficient to produce the initial conditions of a substantial soil-free stone layer overlying a soil layer and to maintain the well-defined stone-soil interface found in sorted circles [*Prestrud*, 1987]. In the model, the initial condition of stones overlying soil and the well-defined stone-soil interface result from soil illuviation, which is assumed to operate efficiently to the base of the active layer. To test the influence of upfreezing, in lieu of illuviation, the model was modified so that (in place of the illuviation step) the contents of a cell containing a stone particle is exchanged with the contents of the cell above with a probability that is proportional to the volumetric fraction of ice in the surrounding $3 \times 3 \times 3$ cell neighborhood (equivalent to the strain induced by frost heave). All other processes and parameters were left as in the reference model, except that the initial configuration was a 1 m thick layer of randomly mixed stone and soil cells in the same ratio as the reference model. In the model, probabilities of upfreezing as low as 10% of the volumetric fraction of ice (compared to values from upfreezing experiments as high as 50% of the frost heave strain [*Anderson*, 1988]) were sufficient to produce ill-formed sorted circles. Upfreezing probabilities as high as 100% of the volumetric fraction of ice lead to patterns lacking a coherent elevated stone annulus and a well-defined stone-soil interface (Figure

14).

In this upfreezing model, sorted-circle-like patterns emerge from an initial configuration with a randomly mixed layer of stones and soil; however, sorted circles form only after substantial vertical sorting has been achieved. In all simulations presented here (including either illuviation or upfreezing), soil plugs emerge from an underlying soil layer as the precursor to sorted circles, as hypothesized in numerous discussions of sorted patterned ground [e.g., *Washburn*, 1956; *Nicholson*, 1976; *Van Vliet-Lanoe*, 1991; *Washburn*, 1997].

2.6 Discussion

Employing only mechanisms documented in natural active layers, forms resembling sorted circles emerge in the reference model. Sorted circles in the model and those in natural settings have many characteristics and behaviors in common, including (1) a central, circular soil plug domed upward, with diameter ~3 m, (2) a surrounding annulus of stones, ~0.5-1 m across, elevated ~0-0.5 m above the intersection with the soil domain, (3) coherent circulation in the soil domain that is upward in the center, outward at the surface, downward at the interface between stone and soil domains, and toward the center at depth, with similar circulation periods (750 ± 350 years, ~500 years), (4) circulation within the stone domain in the opposite sense, and (5) environmental conditions consisting of annual freezing and thawing of the near-surface layer, saturated or near-saturated frost susceptible soil, and an initial mixture of stones and fine-grained soil, separated into distinct stone and soil layers.

In the model, sorted circles form by self-organization in which local and stochastic transport processes become globally coherent as the pattern develops. The formation and development of the pattern depend, in a complicated manner, on the parameters characterizing the fundamental processes of the model. However, sorted circle development is insensitive to most details of these processes because of self-organization, depending robustly on only a few critical feedbacks.

2.6.1 Sorted Circle Development

In the model, the same transport processes operate throughout all stages of sorted circle development. During freezing, frost heave pushes soil from the freezing front toward void cells in the unfrozen soil without regard to direction (Figure 15a). During thaw, soil compressibility is recovered by creation of void particles, resulting in vertical expansion (Figure 15b). Our interpretation of how this directional asymmetry acts to destabilize the initial stone-soil interface, form soil plugs, drive soil plugs to the surface to form sorted circles, and maintain the steady state form and behavior of sorted circles is described below.

2.6.1.1 Pattern initiation

In the model, sorted circles initiate through an instability in the stone-soil interface caused by frost heave. Positive perturbations in the interface grow because more soil is transported into a soil column below a perturbation by ice formation in adjacent regions than is transported to adjacent regions from ice formation within the soil column. This imbalance depends on two robust properties of the model: (1) the number of ice particles formed in a soil column (i.e., the

number of transport events away from that column) is roughly uniform, irrespective of stone-soil interface morphology (Figure 15a), because the freezing front mimics this interface for small-amplitude perturbations, and (2) the number of void particles in a soil column below a perturbation (i.e., the number of transport events into that column) is greater than the number of void particles in adjacent columns (Figure 15b) because the number of void particles emplaced in a column is proportional to the soil column height (i.e., uniform distribution of void particles). This positive feedback, in which frost heave transports soil laterally toward soil-rich regions, is not reversed during thaw because consolidation of soil by removal of ice particles and expansion of soil by addition of void particles both displace soil vertically (owing to lateral confinement). Consequently, the amplitude of perturbations on the stone-soil interface increases with time.

The origin of a prominent peak in the angle-averaged, radial power spectrum of the stone-soil interface height can be explored with a linear stability analysis. For small-amplitude perturbations the change in height of the interface at location $\boldsymbol{x_0}$ is approximately proportional to the difference between the height at $\boldsymbol{x_0}$, $\mathrm{H}(\boldsymbol{x_0})$, and a weighted average of the interface height over a distance d_v from $\boldsymbol{x_0}$. This relationship stems from mass conservation: change in height is proportional to the difference between the number of transport events bringing soil into the soil column below $\boldsymbol{x_0}$ and the number of transport events originating in and removing soil from the soil column below $\boldsymbol{x_0}$. The former is equal to the number of void particles in the column (proportional to $\mathrm{H}(\boldsymbol{x_0})$), and the latter is a weighted average of the number of void particles in the soil columns within a distance d_v, which is the average height weighted by the linearly decreasing probability of

forming an ice particle with increasing distance to a void particle:

$$\frac{dH(x_0,y_0)}{dt} = C\left(H(x_0,y_0) - \frac{\int_0^{d_v}\int_0^{2\pi} H_{r\theta}\left(1-\frac{r}{d_v}\right) r\,d\theta\,dr}{\int_0^{d_v}\int_0^{2\pi}\left(1-\frac{r}{d_v}\right) r\,d\theta\,dr}\right) \quad (2.4)$$

$$H_{r\theta} = H(r\cos\theta + x_0, r\sin\theta + y_0). \quad (2.5)$$

Assuming a solution of the form $H = H_0 e^{\omega t + i(k_x x + k_y y)}$ in (4,5), with wave numbers k_x and k_y, yields a growth rate ω of

$$\omega = C\left(1 - \frac{6}{d_v\sqrt{k_x^2+k_y^2}}\left(J_1 d_v\sqrt{k_x^2+k_y^2} + 2\sum_{l=0}^{\infty}\frac{J_{2l+1}d_v\sqrt{k_x^2+k_y^2}}{(2l+3)(2l-1)}\right)\right), \quad (2.6)$$

where J_m is the Bessel function of order m. The dependence on d_v of the wavelength of the peak of this dispersion relation, approximately linear with d_v, is consistent with the dependence on d_v of the initial wavelength of the peak of the radial power spectrum of the stone-soil interface height in the model (Figure 16). However, this analysis does not address the increase in peak wavelength with time in the model (Figures 5, 11a, and 16).

2.6.1.2 Soil plug formation

In the model, perturbations in the stone-soil interface initiate through a positive feedback, which favors wavelengths roughly equal to d_v. The development of this instability, as described in section 5.1.1, requires that ice particles form uniformly on the stone-soil interface, a circumstance achieved only if the freezing front mimics the stone-soil interface. If the freezing front velocity in the soil domain is not negligible compared with its velocity in the stone domain, the shape of the freezing front diverges from the shape of the stone-soil interface as

perturbations grow. The descending freezing front then penetrates a positive soil perturbation before reaching the stone-soil interface in surrounding regions; ice particles form first in the perturbation, pushing soil toward void cells in unfrozen soil surrounding the perturbation. This finite amplitude effect, which drives soil away from positive perturbations, is an amplitude-dependent negative feedback that favors long-wavelength features. As a result, the peak wavelength of perturbations on the stone-soil interface increases with time (Figures 5 and 16).

The increase in wavelength of perturbations on the stone-soil interface, driven by increasing negative feedback with increasing amplitude, is accomplished through mergers between initial forms. The wavelength stabilizes with further increases in amplitude because the redistribution of soil required to transition to the increasing favored wavelength cannot keep pace with the amplitude growth rate at the existing wavelength. As frost heave continues to displace soil into the core of these stabilized features, they rise toward the ground surface and develop a radially symmetric form (Figure 6) resembling soil plugs [*Washburn*, 1997]. This amplitude dependence of the length scale, indicative of nonlinearity, precludes application of a linear stability analysis to determine the spacing of either soil plugs or sorted circles.

2.6.1.3 Sorted circle formation and growth

As a rising soil plug approaches the ground surface, outward and upward transport by frost heave results in radial expansion of the soil domain, relaxation of the mound of stones elevated by the rising soil plug, and creation of an elevated stone annulus around the soil domain. After a soil plug contacts the ground

surface, its radial expansion is accelerated by outward soil creep on the convex soil domain surface formed through frost-heave-induced displacement of soil from the flanks of the soil domain to its center. Relatively rapid radial expansion of soil domains continues until all soil from the underlying soil layer has been depleted (Figures 4 and 7).

An additional mechanism by which sorted circle soil domains expand or contract involves exchanges of soil through a network of soil conduits connecting adjacent sorted circles at the base of the active layer (Figure 17). The order in which soil domains and soil conduits freeze determines which features grow at the expense of their neighbors. Those that freeze first expel soil into unfrozen adjacent features. A small sorted circle connected by a conduit to a larger sorted circle freezes more rapidly, displacing soil through the conduit to the larger soil domain and ultimately giving rise to a single, large sorted circle. Sorted circles of approximately the same size connected by a soil conduit expel soil into the conduit if they freeze first or receive soil from the conduit if the conduit freezes first. The length of the soil conduit (the distance between soil domain edges) is the primary factor determining the order of freezing. If the sorted circle soil domains freeze first (generally characterized by shorter conduits), an oblate sorted circle develops centered on the conduit. If the conduit freezes first (generally characterized by longer conduits), the conduit is severed, and the two isolated sorted circles evolve independently.

The long-term spacing between sorted circles depends, in a complicated manner, on the initial spacing of soil plugs and interactions between neighboring soil domains. However, a model that predicts the soil domain radius and the minimum distance between noninteracting sorted circles can be constructed from

geometrical arguments (Figure 18). Assuming that the soil domain of a sorted circle is a cylinder of soil with radius r_1 and height equal to the active layer depth ($h_{\text{soil}} + h_{\text{stone}}$), a soil domain expands by depleting the underlying soil layer to a distance d_v from the edge of the soil domain ($r_2 = r_1 + d_v$), and soil volume is conserved ($\pi {r_1}^2 (h_{\text{soil}} + h_{\text{stone}}) = \pi {r_2}^2 h_{\text{soil}}$), the resulting soil domain radius is

$$r_1 = \frac{d_v}{\sqrt{\frac{h_{\text{soil}}+h_{\text{stone}}}{h_{\text{soil}}}} - 1}. \tag{2.7}$$

For reference model parameters the predicted soil domain radius is 1.03 m, which is consistent with the 1.2 ± 0.3 m mean soil domain radius in the reference model. The minimum center-to-center spacing between noninteracting soil domains ($2(r_1 + d_v)$) is 3.3 m, consistent with the 3.6 ± 0.6 m mean spacing in the reference model. This simple model is limited in that it only applies when the volumetric fraction of soil is large enough that sorted circles abut but not so large that interactions between soil plugs or sorted circles lead to labyrinthine sorted patterns. With a thinner soil layer, soil accumulates more slowly, and soil plugs remain at depth as long-wavelength, low-amplitude features. The gradation in soil column height on the flanks of a soil plug results in a flux of soil toward the soil plug over distances much greater than d_v. To predict the length scale of soil plugs and sorted circles in this case, a model for the interplay between the negative feedback driving soil away from soil plugs and the positive feedback accumulating soil will be required.

2.6.1.4 Maintenance and dynamics of well-developed sorted circles

In the model, sorted circles in an approximate steady state are characterized by a convex circular soil domain surrounded by an elevated stone annulus with a distinct crestline and slopes at the angle of repose. The well-defined interface between stone and soil domains is maintained by soil illuviation. The surface morphology is maintained dynamically, with both stone and soil domains circulating upward in their centers and downward at their peripheries (Figures 9 and 19).

In the soil domain, frost heave forces soil from the stone-soil interface toward the center of the soil domain (Figure 19a), expansion by addition of void particles during thaw displaces soil upward (Figure 19c), soil relaxes outward on the convex soil domain surface by soil creep (Figure 19b), and soil on the flanks of the soil domain relaxes downward by removal of ice near the stone-soil interface and by soil illuviation in the stone domain (Figure 19b), completing the loop. Frost heave originating near the stone-soil interface in the upper part of the soil domain pushes outward and upward, elevating and steepening the surface of the stone annulus primarily inside its crestline and leading to inward transport of stones on slopes in excess of the angle of repose. This results in a pattern of circulation in the stone annulus opposite in sense to the circulation in the soil domain. Rare displacements by frost heave (lower in the soil domain) to the outer slope of the stone annulus displace its crestline outward.

2.6.2 Further Research

A number of problems and questions requiring further research are suggested by the results of the model and the interpretations we have presented, including how the abstracted rules and parameters in the model correspond to physical processes and measurable quantities in the natural system. For example, water is not treated explicitly in the model. The volumetric fraction of water in a soil cell w determines the velocity of the freezing front in soil; however, the soil compressibility C determines the number of ice particles that form (frost heave). The two parameters are not coupled, leading to the possibility of unrealistic behavior, such as frost heave and consequent pattern formation when $w = 0$. In natural active layers, frost heave might be limited by water availability, soil compressibility, or some combination of the two. Because of the prominent role frost heave plays in sorted circle formation a more complete treatment of water and soil compressibility would significantly improve the delineation of the physical parameters controlling the occurrence and properties of sorted circles. Similarly, the physical process underlying soil expansion during thaw could be treated more accurately with regard to the spatial distribution and the numerical value of C if the relative roles of water absorption and frost heave could be ascertained. Finally, vertical sorting between stone and soil domains is a critical process in sorted circle formation. In the model, illuviation transports soil to the base of the stone layer within one freeze-thaw cycle. Determining the contributions of soil illuviation and upfreezing to sorting and testing the assumption of rapid soil illuviation, through further modeling and measurements, could help to constrain the predicted conditions under which and the speed with which sorted circles form.

In the model, sorted circle formation, size, and spacing are strongly dependent on the parameter d_v. However, this parameter does not correspond clearly with an identified property of soils, nor has the functional dependence of ice formation on d_v been modeled or measured. In the model, soil displacements in sorted circles are coherent over a distance d_v, which is typically 25-50% of the soil domain diameter. Further progress on modeling sorted circles will require determining how ice lenses forming within a freezing front coherently displace soil over this range, perhaps using a model for stresses and strains within a partially frozen, partially saturated heterogeneous soil.

Because displacement paths of neighboring ice particles are determined sequentially and individually, the model introduces small-scale randomness and mixing that are not expected to be present in natural active layers, where frost-heave-induced displacements should be more coherent. Consequently, comparison between particle velocities in the model and measurements from natural sorted circles has required averaging over many simulations with different sequences of random numbers. Further and better comparisons might be facilitated by a model in which correlation of displacements is enforced.

In addition to exploring the range of conditions under which sorted circles form and are stable, variation of model parameters has indicated that a broader range of sorted patterns (i.e, labyrinthine sorted features, stone islands, and downward stone plugs) might be formed by these processes under different conditions, such as high volumetric fractions of soil, small d_v, low volumetric water fractions w, or an upward propagating freezing front. Moreover, a range of sorted patterns found in natural active layers do not occur in the model, including sorted polygons. Progress and insights into which mechanisms and parameters underlie the

transition between patterns could be gained from further exploration of this model and by developing models with additional or differing active layer processes.

2.7 Conclusions

Numerous hypotheses for the initiation, development, and long-term maintenance of sorted circles have been proposed; however, most of these hypotheses have not been modeled in sufficient detail that differing mechanisms can be compared. We have presented a numerical model for all stages of sorted circle development, in which freezing front propagation, frost heave, soil illuviation, surface creep, compaction during thawing, and soil expansion by water absorption act to transport stones and soil in a simulated active layer during an annual freeze-thaw cycle.

Many of the qualitative and quantitative characteristics of sorted circles are reproduced: (1) ~3 m wide convex circular soil domains, which emerge from a laterally uniform active layer after several hundred freeze-thaw cycles, (2) an encircling 0.5-1.0 m raised annulus of stones, and (3) coherent circulation in both stone and soil domains, with period ~750 years in the soil domain.

A robust positive feedback operates throughout all stages of sorted circle development. Expansion by frost heave at the interface between stone and soil domains transports soil toward the soil domain and stones toward the stone domain. Acted upon by this mechanism, a uniform layer of stones devoid of soil overlying a uniform layer of soil is unstable, leading to the development of soil plugs. A negative feedback, related to the decoupling of the freezing front from

the stone-soil interface as finite amplitude features emerge, causes soil plugs to grow radially and merge, while the positive feedback drives them to the surface, pushes up stone rings around the emerging soil plugs, and maintains long-term circulation within the stone and soil domains. The finite amplitude, nonlinear effects of the negative feedback render a linear stability analysis of the patterns inapplicable. The robust feedbacks that give rise to the self-organized pattern of sorted circles have been treated here. The formation of other types of sorted patterned ground will be explored in future work.

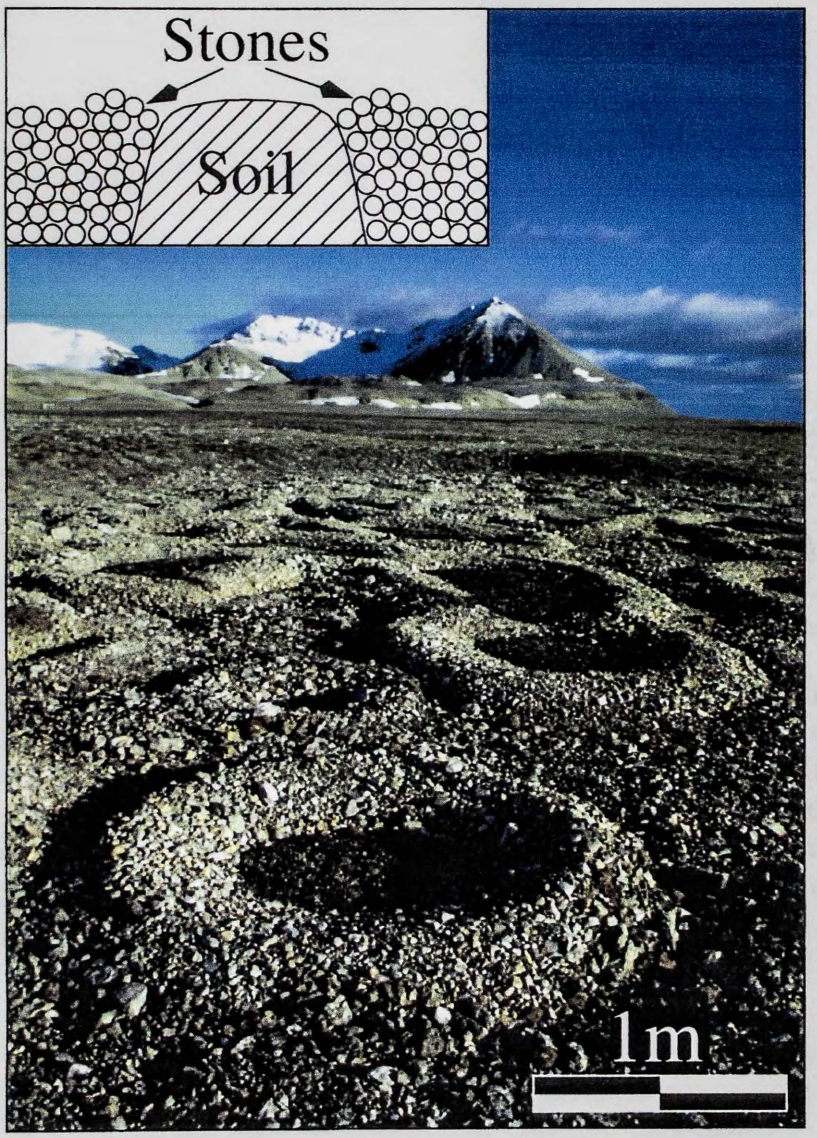

Figure 2.1: Sorted circles from the Kvadehuke Peninsula in western Spitsbergen. Inset shows schematic cross section of a sorted circle (after Prestrud, 1987).

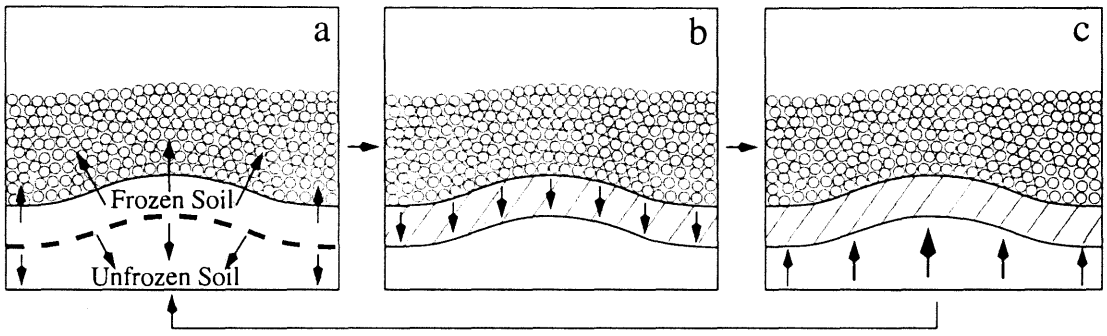

Figure 2.2: Conceptual model: cross sections indicating transport during a freeze-thaw cycle resulting in positive feedback mechanism for soil accumulation and destabilization of stone-soil interface. During freezing, (a) frost heave drives material away from the freezing front (dashed line), outward toward the ground surface and inward toward unfrozen soil. During thawing, (b) ice-rich soil near the stone-soil interface expels water and compacts vertically, while (c) desiccated and compacted soil expands vertically by absorbing water.

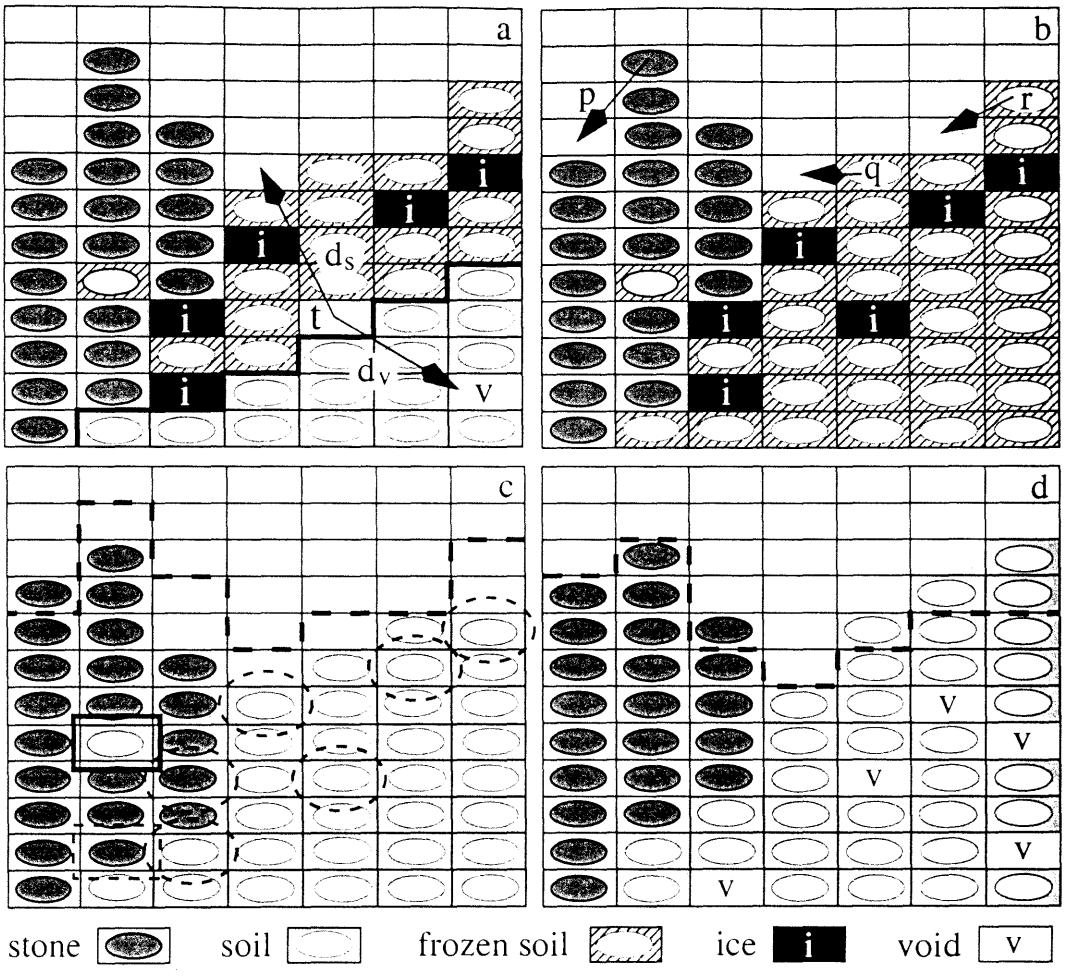

Figure 2.3: Cross sections through a schematic of the numerical model for several stages in the simulated freeze-thaw cycle. Stone, unfrozen soil, frozen soil, ice, and void particles are as indicated. (a) Freezing and frost heave stage. The freezing front (thick solid line) migrates from the surface downward by heat diffusion modulated by release of latent heat from soil particles. An ice particle can be inserted at the location labeled "t" on the freezing front, depending on the probability of displacing the particles at t toward the ground surface or toward a void cell, equations (1,2). (b) Surface morphology relaxation stage. Stone particle, labeled "p", moves down a slope exceeding the angle of repose. Soil particles, labeled "q" and "r", move downslope with probabilities proportional to slope. (c) Compaction during thaw and soil illuviation stage. Ice particles are removed (dashed ovals), and the columns of stone and soil particles above the vacated cells are shifted downward. Dashed line indicates the surface after freezing but before surface motion. Soil particle in the stone domain (solid rectangle) moves downward to the lowest stone cell in the column (dashed rectangle). (d) Soil expansion stage. Void particles are added with a probability equal to the local volume fraction of soil until a specified compressibility C' is reached. Dashed line indicates the surface before adding void particles.

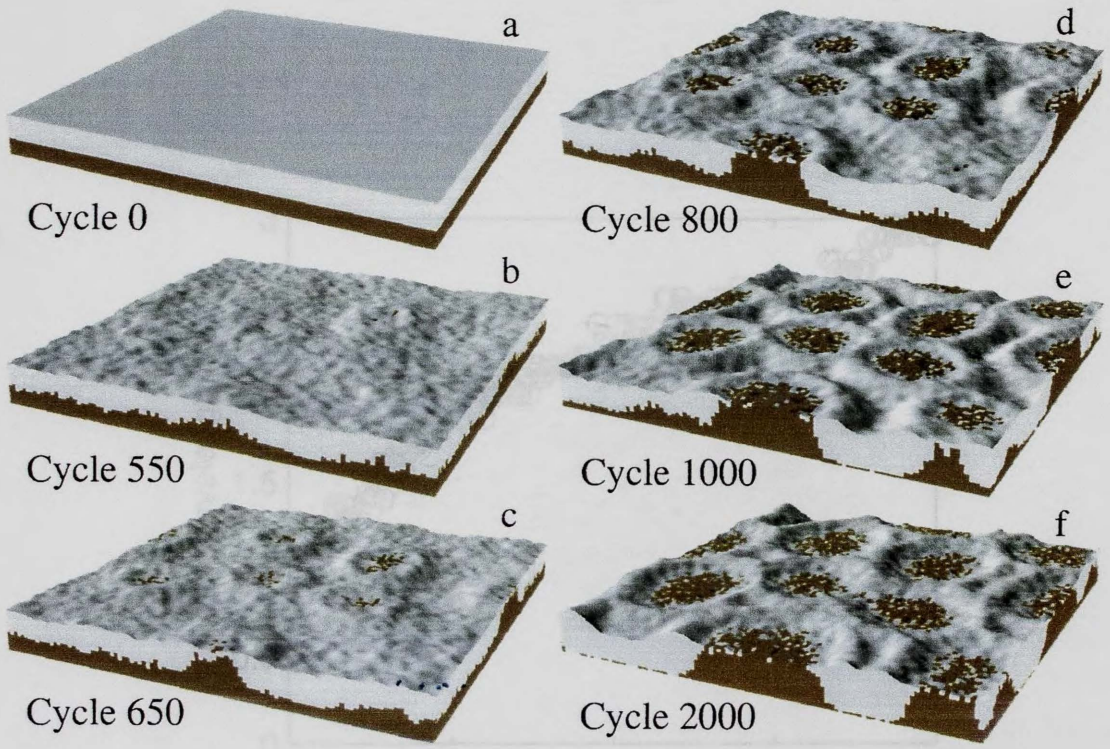

Figure 2.4: Sorted circle formation and development in a 10 m × 10 m simulation with reference model parameters. (a) Initial configuration has a 0.6 m thick stone layer (light shading) overlying a 0.4 m thick soil layer (dark shading). (b) Perturbations in the stone-soil interface first reach the surface at ~550 freeze-thaw cycles. (c) Frost heave at the stone-soil interface elevates a surrounding annulus of stones. (d) Frost heave drives relatively rapid radial expansion. (e) The underlying soil layer has been largely depleted. (f) Over long time scales relatively slow radial expansion, interaction between adjacent forms, and maintenance of fully developed forms continues.

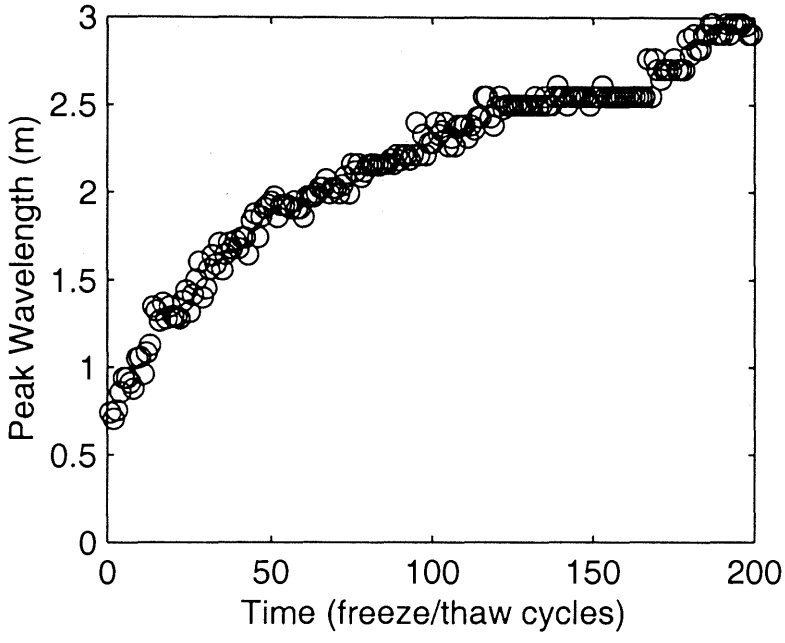

Figure 2.5: Peak wavelength (from angle-averaged, radial power spectrum) of perturbations on the stone-soil interface versus number of freeze-thaw cycles.

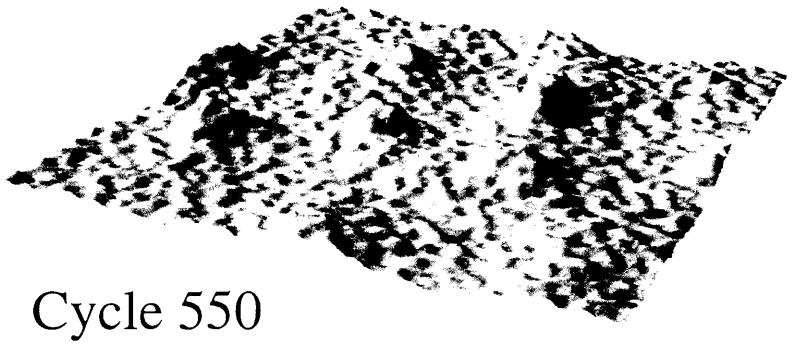

Figure 2.6: The stone-soil interface in the reference model after 550 freeze-thaw cycles, illustrating soil plugs. Overlying stone layer in Figure 4b has been removed.

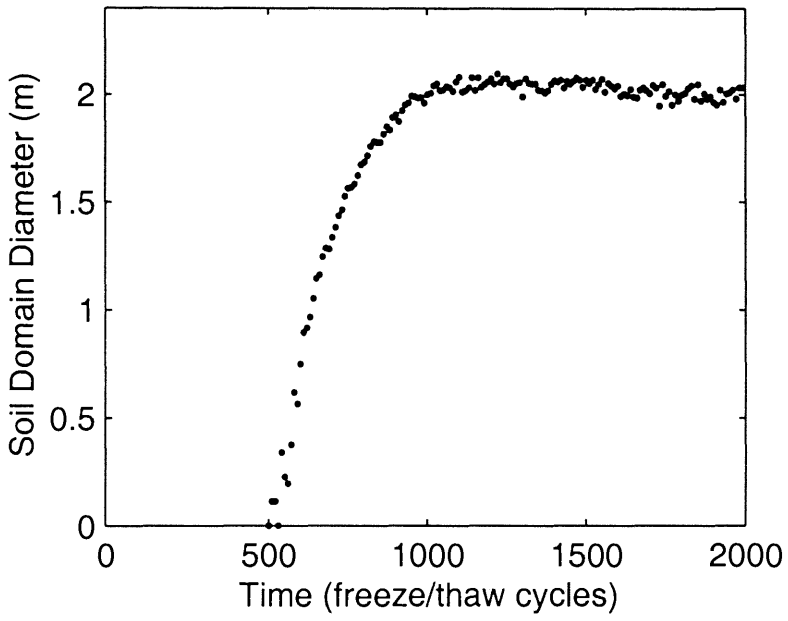

Figure 2.7: Soil domain diameter for a single sorted circle in the reference model versus number of freeze-thaw cycles. Diameter is calculated from the number of soil cells at the surface, assuming a circular soil domain.

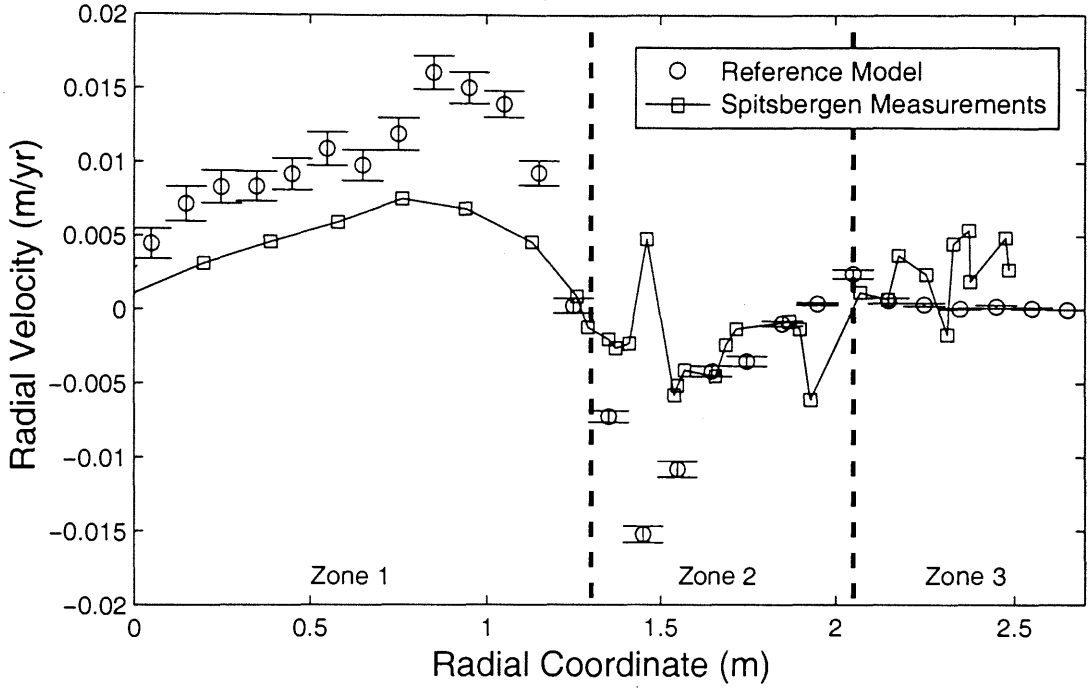

Figure 2.8: Mean surface velocity on a well-developed sorted circle in the reference model and mean surface velocity on a well-developed sorted circle in western Spitsbergen based on sequential measurements during a 12 year period starting in 1985. Markers, consisting of both marked stones and pegs vertically implanted within the upper decimeter of soil, were measured manually (see *Hallet and Prestrud* [1986] for discussion of the measurement technique and analysis of errors ($\sim$2 mm)). Reference model velocity field is an average of 200 simulations, with different sequences of random numbers, of a single sorted circle during the 10 year period from cycle 1501 to cycle 1510; 1σ error bars reflect the variation in these simulations. Positive velocities indicate motion away from the soil domain center. In the model, surface motion in zone 1 (soil domain) is away from the center of the sorted circle and decreases to zero at the stone-soil intersection. In zone 2 (inner slope of stone domain), surface motion is toward the center of the sorted circle. In zone 3 (outer slope of stone domain), surface motion is away from the center of the sorted circle, indicating radial growth. A similar pattern of displacements was measured in western Spitsbergen.

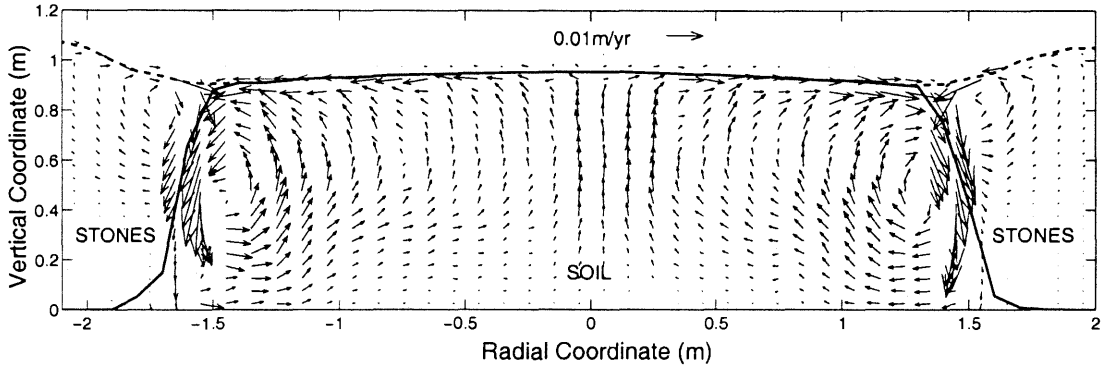

Figure 2.9: Velocity vectors in a cross section of a well-developed sorted circle from the reference model, as in Figure 8. Solid line is the soil surface; dashed line is the ground surface.

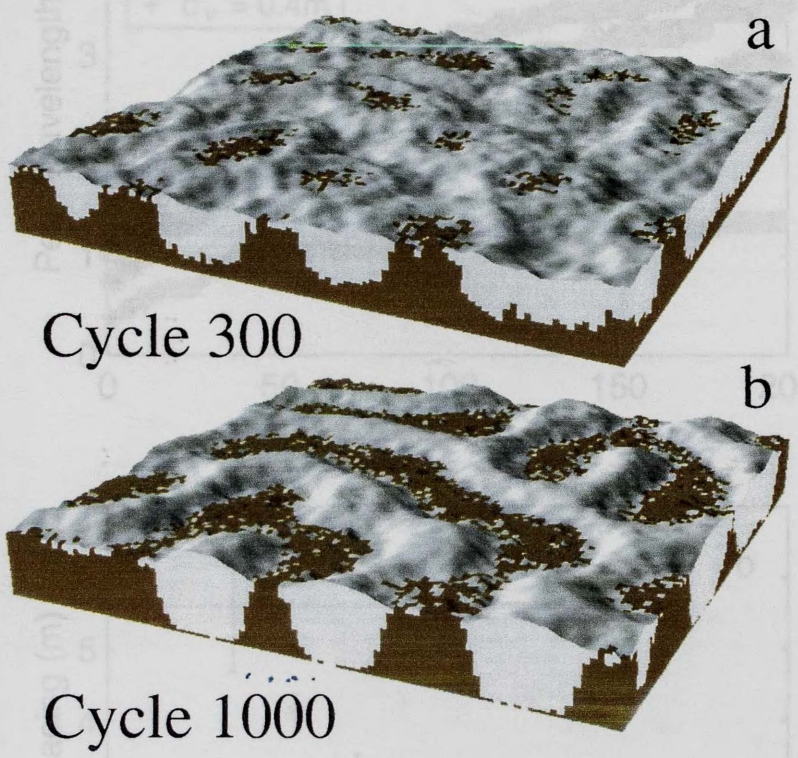

Figure 2.10: Sorted circles evolve to more geometrically complicated forms for volumetric fractions of soil in the active layer greater than ~0.4. Shown is a 10 m × 10 m simulation with reference model parameters, except the initial configuration is a 0.6 m thick stone layer (light shading) overlying a 0.6 m thick soil layer (dark shading), in contrast to $h_{\text{soil}} = 0.4$ m in the reference model. (a) After 300 freeze-thaw cycles circular soil plugs have risen to the surface. (b) After 1000 freeze-thaw cycles soil domains have coalesced, forming a labyrinthine pattern.

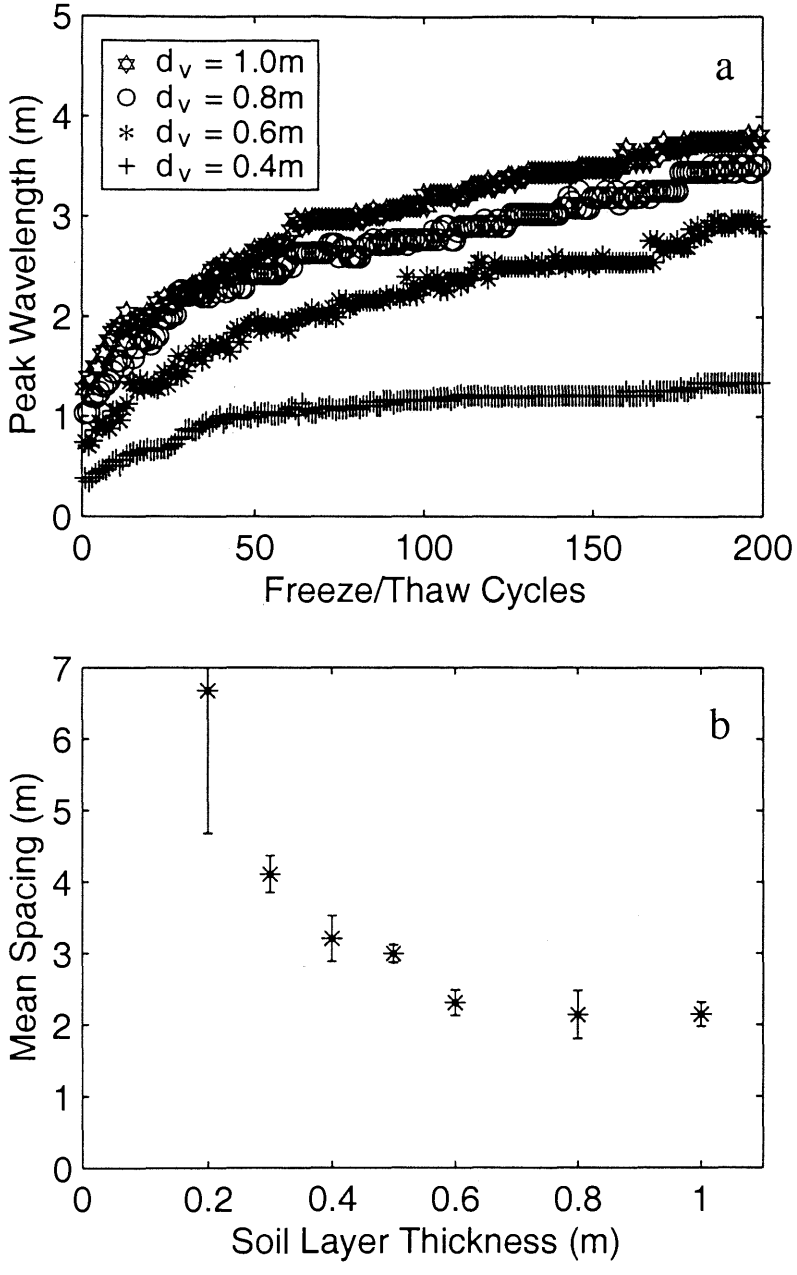

Figure 2.11: Dependence of spacing on d_v, time, and h_{soil}. (a) Peak wavelength of perturbations on the stone-soil interface versus time for d_v = 0.4-1.0 m. Increase in peak wavelength with time indicates nonlinearity. (b) Mean spacing of sorted circles versus soil layer thickness h_{soil}.

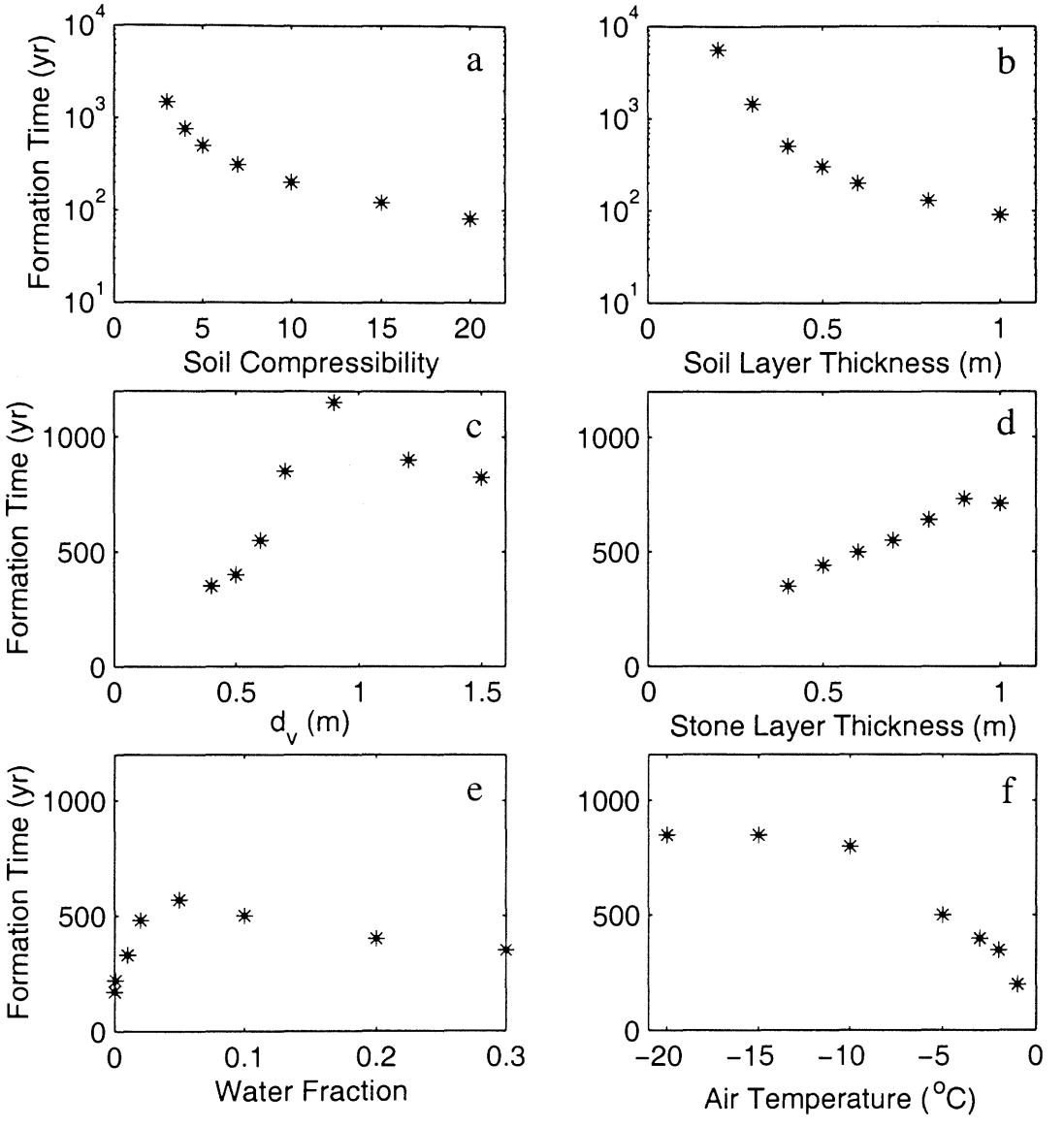

Figure 2.12: Dependence of formation time (number of freeze-thaw cycles until the soil domain first contacts the ground surface) on (a) soil compressibility C, (b) soil layer thickness h_{soil}, (c) maximum distance an ice particle can displace particles to a void cell d_v, (d) stone layer thickness h_{stone}, (e) volumetric fraction of water w, and (f) air temperature T_a.

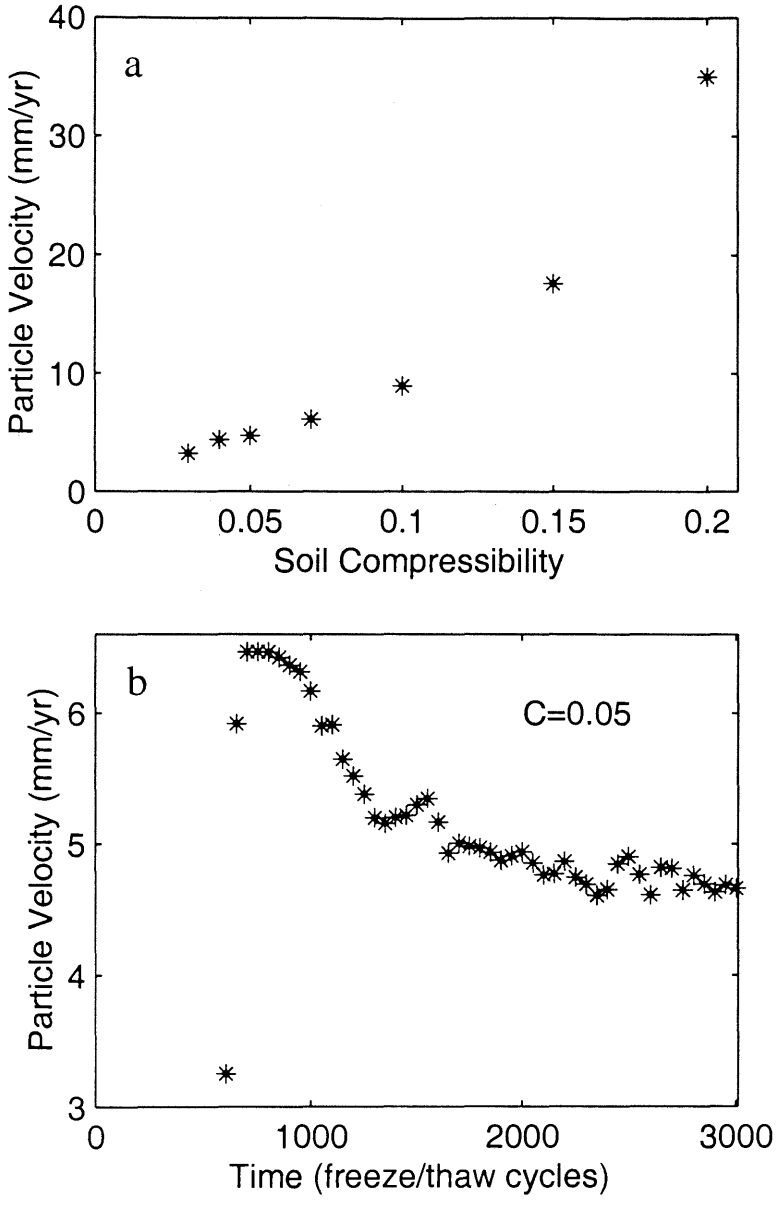

Figure 2.13: Dependence of mean particle velocity within soil domains on soil compressibility C and time. (a) Mean particle velocity versus C for well-developed sorted circles. (b) Mean particle velocity versus time for a developing sorted circle. Dependence of particle velocity on C and time overwhelms dependence on other parameters.

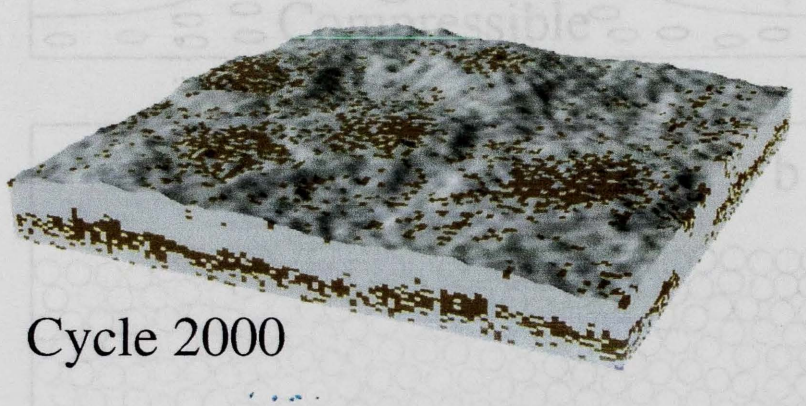

Figure 2.14: Reference model (10 m × 10 m) after 2000 freeze-thaw cycles with upfreezing instead of soil illuviation. Sorted circles with poorly defined stone annuli and incomplete lateral sorting develop.

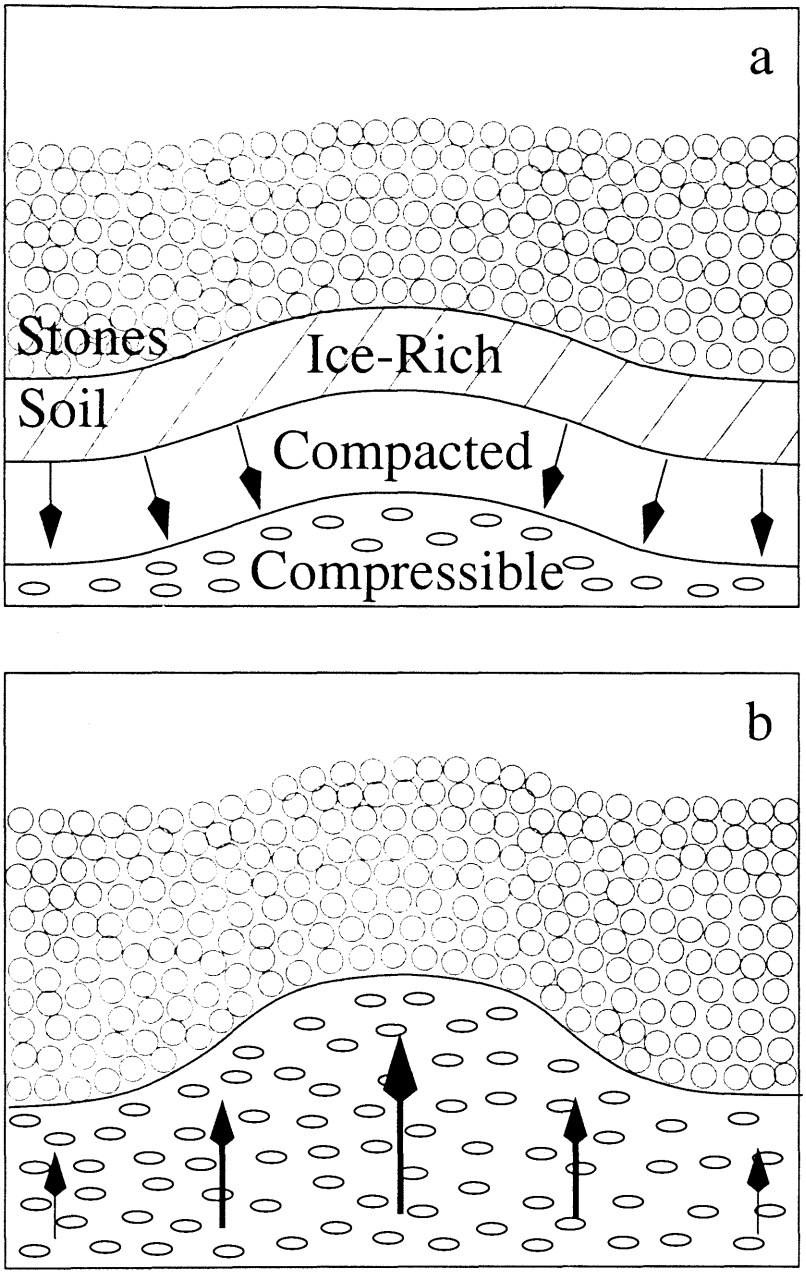

Figure 2.15: Instability of stone-soil interface in model (schematic cross sections). (a) Positive perturbations in the stone-soil interface. These are unstable because uniform frost heave near the stone-soil interface displaces soil laterally toward regions with taller soil columns, which have a greater number of void particles. (b) Cross section showing that during thaw, after ice-rich soil compacts, soil expands vertically by addition of void particles in proportion to the stone-soil interface height. The asymmetry between laterally biased frost-heave-induced displacements and unbiased vertical thaw compaction and soil expansion by addition of void particles results in net transport of soil toward regions where the interface height is greatest, further raising the interface.

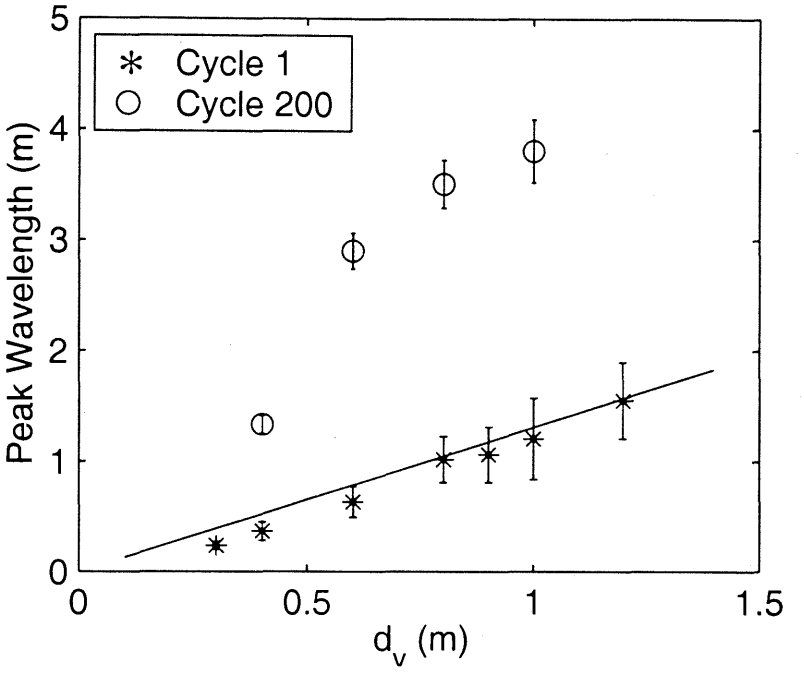

Figure 2.16: Peak wavelength of perturbations on the stone-soil interface after one freeze-thaw cycle and after 200 freeze-thaw cycles (when soil plugs have formed) versus d_v (peak from angle-averaged, radial power spectrum averaged over 20 independent simulations). Lines indicate the wavelength with maximum growth rate from a linear stability analysis ($\lambda = 2\pi/k_x$ from (4)). Dashed line assumes plane-wave perturbations ($k_y = 0$). Solid line assumes symmetric perturbations ($k_x = k_y$). Linear stability analysis prediction is consistent with the initial spacing, but soil plug spacing is decoupled from the initial spacing by nonlinearities.

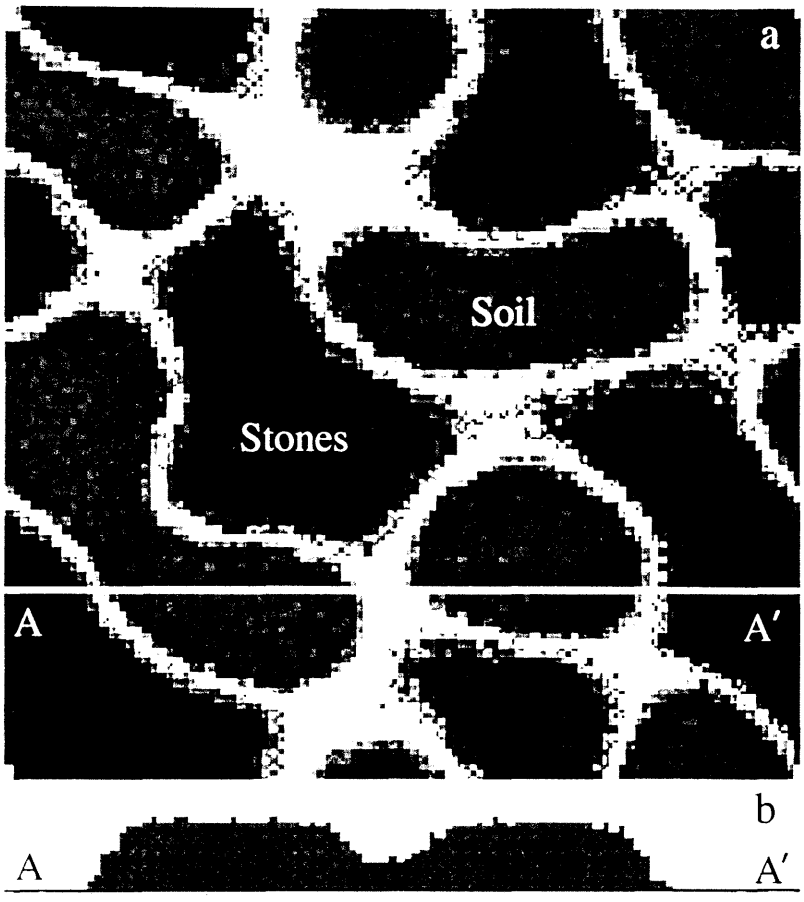

Figure 2.17: (a) Map of interface type for a 10 m × 10 m simulation with reference model parameters after 1300 freeze-thaw cycles: interface between soil domains and the ground surface (medium grey shading), interface between stone and soil domains (light grey or white shading), and interface between stone domains and the active layer base (solid black shading). (b) Cross-sectional view through A-A', showing soil only. Soil domains of neighboring sorted circles are connected at depth by soil conduits, which enable planform pattern changes through transfer of soil to, from, and through the conduits.

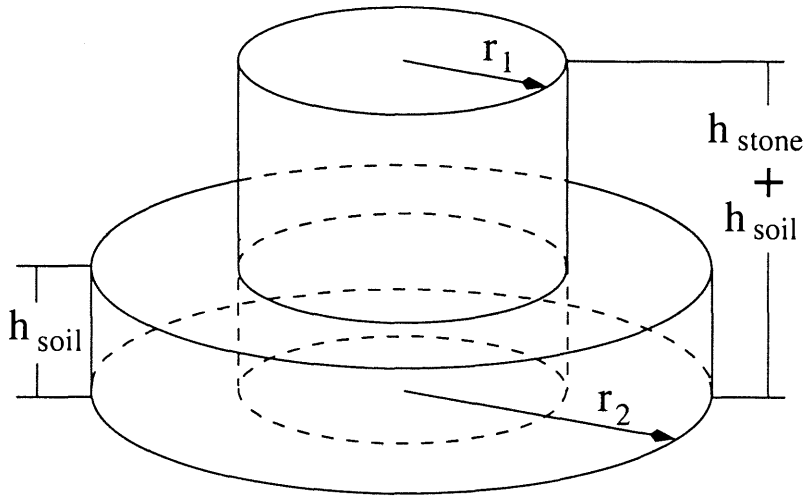

Figure 2.18: A simple model for soil domain radius and minimum sorted circle spacing. An inner soil cylinder, the height of the active layer, expands by depleting a disk-shaped region in the underlying soil layer. Assuming soil can be transported to the cylinder from a maximum distance of d_v, expansion continues until $r_2 - r_1 = d_v$. The final soil domain radius follows from the condition that $\pi {r_1}^2 (h_{\text{soil}} + h_{\text{stone}}) = \pi {r_2}^2 h_{\text{soil}}$. The minimum center-to-center spacing of noninteracting soil domains is then $2(r_1 + d_v)$.

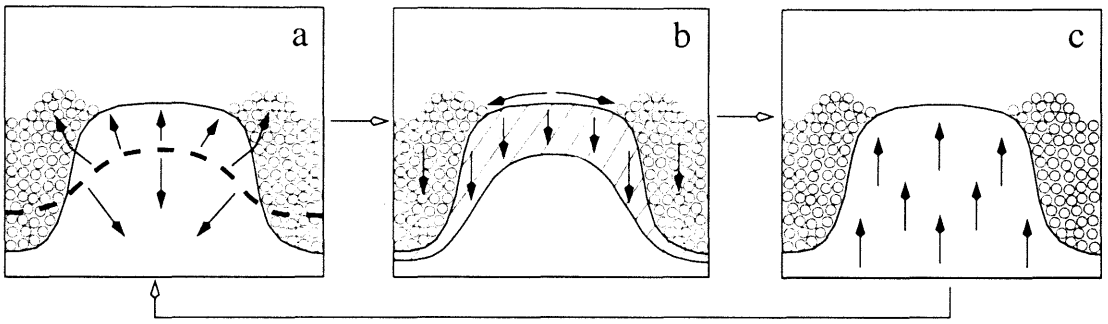

Figure 2.19: Maintenance of a fully developed sorted circle in the model (schematic cross sections). Solid arrows indicate transport direction during each stage of the freeze-thaw cycle. (a) Cross section showing that during freezing, frost heave displaces material away from the freezing front (dashed line): outward toward the ground surface and inward toward unfrozen soil. (b) Cross section showing that during thaw, ice-rich soil near the surface and stone-soil interface expels water and compacts vertically. Soil sifts downward through the pore space between stones (illuviation): soil on the surface creeps downslope. (c) During thaw, desiccated and compacted soil expands vertically by the addition of void particles.

Table 2.1: Reference Model Parameter Values

Parameter	Value
d_s, max. dist. heave to surface	0.6 m
d_v, max. dist. heave to void	0.6 m
h_{stone}, stone layer thickness	0.6 m
h_{soil}, soil layer thickness	0.4 m
w, vol. fraction water in soil	0.1
C, soil compressibility	0.05
T_b, active layer base temp.	0^oC
T_g, surface temp. before freezing	5^oC
T_a, air temp. during freezing	-5^oC
k_{heat}, heat diffusion const.	1×10^{-6} m^2/s
K_{surf}, height diffusion const.	5×10^{-3} m^2/yr

2.8 References

Anderson, S. P., The upfreezing process: Experiments with a single clast, *Geological Society of America Bulletin*, **100**, 609–621, 1988.

Combarnous, M. A. and S. A. Bories, Hydrothermal convection in saturated porous media, *Advances in Hydroscience*, **10**, 231–307, 1975.

Cook, F. A., Near surface soil temperature measurements at Resolute Bay, Nortwest Territories, *Arctic*, **8(1)**, 237–249, 1955.

Corte, A. E., The frost behavior of soils: Laboratory and field data for a new concept. Part I: Vertical sorting, *Tech. rep.*, U. S. Army Cold Regions and Engineering Laboratory, 1961.

Corte, A. E., Particle sorting by repeated freezing and thawing, *Biuletyn Peryglacjalny*, **15**, 175–240, 1966.

DuFort, E. C. and S. P. Frankel, Stability conditions in the numerical treatment of parabolic differential equations, *Mathematical Tables and Other Aids to Computation*, **7**, 135–152, 1953.

Elton, C., The nature and origin of soil polygons in Spitsbergen, *Geological Society of London Quarterly Journal*, **83**, 163–194, 1927.

Forman, S. L. and G. H. Miller, Time-dependent soil morphologies and pedogenic processes, *Arctic and Alpine Research*, **16(4)**, 381–394, 1984.

Gleason, K. J., W. B. Krantz, N. Caine, J. H. George, and R. D. Gunn, Geometrical aspects of sorted patterned ground in recurrently frozen soil, *Science*, **232**, 216–220, 1986.

Goldthwait, R. P., Frost sorted patterned ground: A review, *Quaternary Research*, **6**, 27–35, 1976.

Hallet, B., Measurement of soil motion in sorted circles, Western Spitsbergen, in *Proceedings of the Seventh International Conference on Permafrost*, edited by A. G. Lewkowicz, vol. 57, pp. 415–420, Centre d'Etudes Nordiques, Universite Laval, Quebec, PQ, 1998.

Hallet, B., S. P. Anderson, C. W. Stubbs, and E. C. Gregory, Surface soil displacements in sorted circles, Western Spitsbergen, in *Proceedings of the Fifth International Conference on Permafrost*, edited by K. Senneset, vol. 1, pp. 770–775, Tapir Publishers, Trondheim, Norway, 1988.

Hallet, B. and S. Prestrud, Dynamics of periglacial sorted circles in Western Spitsbergen, *Quaternary Research*, **26**, 81–99, 1986.

Hallet, B. and E. D. Waddington, Buoyancy forces induced by freeze-thaw in the active layer: Implications for diapirism and soil circulation, in *Periglacial Geomorphology*, vol. 22, pp. 251–279, 1992.

Jyotsna, R. and P. K. Haff, Microtopography as an indicator of modern hillslope diffusivity in arid terrain, *Geology*, **25(8)**, 695–698, 1997.

Krantz, W. B., Self-organization as patterned ground in recurrently frozen soils, *Earth-Science Reviews*, **29**, 117–130, 1990.

Lambe, T. W. and R. V. Whitman, *Soil Mechanics*, John Wiley & Sons, Inc., New York, New York, 1969.

Mackay, J. R., An equilibrium model for hummocks (nonsorted circles), Garry

Island, Northwest Territories, *Geological Survey of Canada Paper*, **79-1A**, 165–167, 1979.

Mackay, J. R., The origin of hummocks, Western Arctic coast, Canada, *Canadian Journal of Earth Sciences*, **17**, 996–1006, 1980.

Mortensen, H., Uber die physikalische moglichkeit der "brodel" -hypothese, *Centralblatt fur Mineralogie, Geologie und Palaontologie, Abt. B*, **1932**, 417–422, 1932.

Nicholson, F. H., Patterned ground formation and description as suggested by low Arctic and sub-Arctic examples, *Arctic and Alpine Research*, **8**, 329–34, 1976.

Nicolis, G. and I. Prigogine, *Self-Organization in Nonequilibrium Systems: From dissipative structures to order through fluctuations*, John Wiley & Sons, Inc., New York, New York, 1977.

Nogotov, E. F., *Applications of Numerical Heat Transfer*, United Nations Educational, Scientific, and Cultural Organization, Paris, France, 1978.

Pissart, A., Advances in periglacial geomorphology, *Ztschr. Geomorph.*, **79**, 119–131, 1990.

Prestrud, S., *The upfreezing process and its role in sorted circles*, Masters thesis, University of Washington, 1987.

Putkonen, J., Soil thermal properties and heat transfer processes near Ny-Alesund, Northwestern Spitsbergen, Svalbard, *Polar Research, Oslo: Norsk Polarinstitutt*, **17(2)**, 165–179, 1998.

Ray, R. J., W. B. Krantz, T. N. Caine, and R. D. Gunn, A model for sorted patterned-ground regularity, *Journal of Glaciology*, **29(102)**, 317–337, 1983.

Schmertmann, J. and R. S. Taylor, Quantitative data from a patterned ground site over permafrost, *Tech. rep.*, U.S. Army Cold Regions and Engineering Laboratory, 1965.

Taber, S., Frost heaving, *J. Geology*, **37**, 428–461, 1929.

Van Vliet-Lanoe, B., Differential frost heave, loadcasting and convection, converging mechanisms, a discussion of the origin of cryoturbations, *Permafrost and Periglacial Processes*, **2**, 123–139, 1991.

Washburn, A. L., Classification of patterned ground and review of suggested origins, *Geological Society of America Bulletin*, **67**, 823–865, 1956.

Washburn, A. L., Weathering, frost action, and patterned ground in the Mesters Vig District, Northeast Greenland, *Meddelelser om Gronland*, **176**, 1969.

Washburn, A. L., *Geocryology: A survey of periglacial processes and environments*, Halsted Press, New York, New York, 1980.

Washburn, A. L., *Plugs and Plug Circles: A Basic Form of Patterned Ground, Cornwallis Island, Arctic Canada-Origin and Implications*, The Geological Society of America, Inc., Boulder, Colorado, 1997, Memoir 190.

Werner, B. T., Eolian dunes; computer simulations and attractor interpretation, *Geology*, **23(12)**, 1107–1110, 1995.

Werner, B. T., Complexity in natural landform patterns, *Science*, **284**, 102–104, 1999.

Williams, P. J. and M. W. Smith, *The Frozen Earth: Fundamentals of Geocryology*, Cambridge University Press, New York, New York, 1989.

Chapter 3

A Two-Dimensional Model for Sorted Patterned Ground

3.1 Abstract

Circular, labyrinthine, polygonal and striped sorted patterns of stones and soil self-organize in polar and high alpine environments under cyclic freezing and thawing through an interplay between two positive feedback mechanisms. The first sorts stones and soil by displacing, via ice lens formation in freezing soils, soil toward soil-rich domains and the second transports stones along the axis of elongate stone domains, which are squeezed as surrounding soil freezes. In a numerical model implementing these feedbacks, the wide and broadly curving stone domains of circles form (transitioning to labyrinths and islands with decreasing volumetric fraction of stones) when sorting dominates; narrow, connected networks of stone domains enclosing polygonal soil domains form when stone domain squeezing

dominates. The passage from the first class of patterns to the second is effected by decreasing soil compressibility and increasing freezing rate in the stone domains.

3.2 Introduction

Patterns delineated by distinct stone and soil domains visible at the ground surface are formed by cyclic freezing and thawing of decimeter- to meter-thick soil layers in polar and high alpine environments. The observed range of sorted patterned ground includes sorted circles, labyrinthine stone and soil networks, stone islands, sorted polygons and sorted stripes on hillslopes (Figure 1). These quintessential forms constitute one of the most striking suites of geomorphic patterns. No comprehensive conceptual or quantitative model for their formation and development has been proposed, despite extensive study of underlying fundamental processes such as particle sorting (*1*), deformation of frozen soil (*2*), granular mechanics (*3*), freezing and thawing (*1,4,5*), and soil creep (*6*). We have developed a model within which these patterns self-organize, with transitions between patterns controlled by the relative magnitude of two competing transport processes.

The diversity of sorted patterned ground generally has been attributed to a multiplicity of processes (*7*): for example, desiccation fractures as a template for sorted polygon stone domains (*8,9*) and density- or frost-heave-induced ascent of soil plugs to the ground surface causing sorted circles (*7*). However, one model posits patterns of convecting water in the pore spaces of unfrozen soil as general mechanism for initiating sorted patterned ground (*10,11*), but it does not explicitly generate the observed range of patterns, does not treat sorting and relies on

a process that has not been documented in recurrently frozen soil layers.

Patterns in a broad range of environments have been hypothesized to form by self-organization (e.g. *12–17*), whereby nonlinear, dissipative interactions among the small- and fast-scale constituents of a system give rise to order at larger spatial and longer temporal scales. The operation of feedbacks to initiate and stabilize patterns and behaviors is central to self-organization (*18*). Within a single system, a change in controlling parameters can lead to an abrupt shift in the character of a self-organized pattern without a change in processes causing the pattern. Because transport in the active layer is highly nonlinear and dissipative, self-organization is a candidate for the general mechanism underlying sorted patterned ground (*12*). However, existing models (*19,20*) only treat specific patterns, have not addressed transitions between patterns, and have not generated the connected network of narrow stone domains characteristic of the most common pattern, sorted polygons (*7,21*). The promise of self-organization to model all forms of sorted pattern ground using a single set of transport processes has not been fulfilled.

To address these deficiencies, we have developed a numerical model that relies on varying the strength of two straightforward, robust feedback mechanisms (Figures 2, 3). The first feedback transports stones toward regions of high stone concentration, thereby inducing lateral sorting of stones and soil. Given a layer of stones overlying fine-grained soil, formed by depositional or vertical sorting processes, the freezing front (0^o isotherm) tends to follow the stone/soil interface, descending faster in dry stone regions than in wet soils (which must freeze as well as be cooled:*22–24*). This interface is unstable to perturbations because frost heave, soil expansion perpendicular to the freezing front owing to the growth of ice

lenses (*4*), near the stone/soil interface drives soil downward and toward soil-rich perturbations while pushing stones upward and outward, eventually giving rise to distinct stone and soil domains. This laterally isotropic lateral sorting mechanism favors broadly curved boundaries between wide stone and soil domains, because the correspondence between the freezing front and stone/soil interface, required for sorting, breaks down for small radius of curvature bends.

The second feedback results in transport of stones along the axis of elongate stone domains, once distinct stone/soil boundaries have formed. Laterally directed frost heave near the stone/soil interface applies compressive stresses that deform a stone domain, thereby elevating its surface. Greater lateral frost heave, either through enhanced ice lens formation or greater vertical stone domain thickness, results in greater uplift; gradients in uplift drive stone transport. Significant along-axis transport is possible only if stone motion is confined to stone domains, requiring that the surfaces of stone domains are flat or dip below the elevation of the stone-soil contact. This requirement is met when stone domains freeze rapidly so that frost heave and consequent soil removal from the stone/soil interface toward soil domains is uniform or increases with depth. Lateral squeezing can stabilize long, narrow stone domains to perturbations in vertical stone domain thickness because squeezing-induced uplift increases with thickness (stone/soil interface area), causing stones to ravel from regions of high to low thickness. Stabilization to perturbations in width occurs because wider sections are more easily deformed, experiencing greater uplift, than adjacent narrower sections. Lateral squeezing can cause elongate stone domains to thin and extend, because, as the thickness of a stone domain decreases near its free-standing ends, consequent lower uplift promotes raveling of stones toward and off the shallow ends.

Both feedbacks are consistent with the limited range of relevant field observations. Frost-susceptible soils overlain by surface stone layers often exhibit lateral sorting associated with soil plugs rising to the surface (*25*). A model for sorted circles including the first feedback is quantitatively consistent with field measurements (*20*). Observations within sorted polygons of upended stones, stones aligned parallel to the stone domain axis and mud folds parallel to the stone/soil contact are consistent with lateral squeezing of stone domains (*21,26*).

In our numerical model, particles representing stones undergo spatially continuous motion in two horizontal dimensions. Stones can overlap, representing stacking of stones, up to a limit corresponding to the maximum depth of freeze/thaw processes. Beginning with a random configuration of stones, abstractions of the two feedback mechanisms drive incremental stone displacements over repeated iterations, each of which represents an annual (or sometimes diurnal) freeze/thaw cycle. Additionally, during each iteration, surface stones are displaced downslope a distance proportional to the hillslope gradient (unless constrained by neighboring stones).

Lateral sorting is abstracted as stone displacement proportional to the gradient of a surface representing the stone/soil or air/soil interface: $\delta\vec{x_{ls}} = K_{ls}\vec{\nabla}H$, where K_{ls} is a diffusion constant (*29*) determining the rate of stone motion on the soil surface. The surface elevation H decreases linearly with local stone concentration, averaged over a radius D_{ls} and weighted by inverse distance. The length scale D_{ls} corresponds to the maximum lateral distance over which soil can be displaced by frost heave (*20*). Far from a stone domain, these displacements represent transport by surface creep; close to a stone domain, they represent the combined effects of surface creep and stone upfreezing perpendicular to freezing

fronts inclined to the stone/soil interface.

Stone motion within stone domains by lateral squeezing and confinement is abstracted as anisotropic diffusion of stones that is biased parallel to the axis of the stone domain: $\delta\vec{x_{sq}} = |K_{sq}\vec{\nabla}U|\hat{u}$, where U is the surface uplift owing to lateral squeezing of the stone domain (*30*) and K_{sq} is a diffusion constant (*29*) determining the rate of downslope stone transport. The direction of transport, $\hat{u}$, is the average of a unit vector pointing along the axis of the stone domain (determined over a distance D_{sq} and weighted by a constant factor C_{sq}) and a randomly oriented unit vector (weighted by the factor $1 - C_{sq}$). The length scale D_{sq} corresponds to the distance over which the direction of lateral frost heave varies, as determined by heat conduction and the thickness of the frozen layer. The weighting C_{sq} encapsulates the degree of confinement of stones to the stone domain; increasing C_{sq} increases the along-axis component of stone diffusion and decreases the radially symmetric component. Increasing K_{sq} represents increasing lateral squeezing and uplift, increasing the along-axis and radially symmetric stone diffusion. To change the along-axis component of stone diffusion independent of the radially symmetric component, K_{sq} and C_{sq} can be varied simultaneously, keeping $K_{sq}(1 - C_{sq})$ constant.

As the mean concentration of stones (volumetric fraction), the hillslope gradient and the degree of lateral confinement are varied, sorted circles, islands, labyrinths, stripes and polygons emerge (Figure 4). In the absence of lateral confinement, stone islands transition to labyrinths and then to sorted circles as stone concentration is increased (Figure 4a), because isolated stone domains coalesce when separated by a distance less than the length scale associated with subsurface soil motion by frost heave, D_{ls}. Increasing the hillslope gradient

results in gradient parallel stone stripes (Figure 4b), because, at a sufficiently high gradient, downslope transport away from a stone domain exceeds transport toward the stone domain by lateral sorting processes. Stone islands become more stable on higher slopes as lateral sorting into distinct stone and soil domains progresses. Stone islands transition to sorted polygons as the lateral confinement, C_{sq}, is increased (Figure 4c) or the along-axis transport is increased by increasing K_{sq}. For $C_{sq} > \sim 0.6$, the outward transport of stones owing to lateral squeezing exceeds the inward transport of stones by lateral sorting processes, therefore stone islands become unstable and are drawn out into the linear stone domains of sorted polygons. Decreased soil compressibility and rapid freezing in stone domains with large air cooled pores (large stones) underlie this transition. Less compressible soil reduces the lateral sorting mechanism and promotes the slow evolution of stone domain depth, relative to the diffusion of stones along stone domains, required for stability of narrow stone domains. Rapid freezing increases lateral frost heave at depth, which flattens stone domains and increases confinement. The emergence of sorted patterned ground from local feedbacks and the sharp transitions between patterns as parameters are varied are hallmarks of self-organization.

Sorted polygons (Figure 5) experience richer dynamics than other patterns because they result from an interplay between the two feedback mechanisms. Three-way intersections become equiangular because less uniform lateral frost heave in the soil domain bordered by the stone domains forming the smallest intersection angle results in less lateral squeezing and uplift. Therefore, stones preferentially ravel toward the smallest intersection angle, causing the intersection to migrate in this direction, thereby increasing the smallest intersection angle

at the expense of the other two. This mechanism also causes four-way intersections to be unstable. At the intersection, lateral squeezing from frost heave in the soil domains enclosed by the two (generally opposing) larger intersection angles is greater than that in the other two soil domains; therefore, stones are squeezed between the larger soil domains and consequently ravel toward the two soil domains enclosed by the smaller intersection angles. This divergent stone raveling from the intersection elongates the four-way intersection into a linear stone domain with a three-way intersection at each end.

The initial spacing of sorted polygons generally is two to three times the radius over which stone concentration is calculated, D_{ls}. The mean polygon size increases by elimination of polygons with fewer sides than surrounding polygons. The tendency of intersections to move in the direction of the smallest intersection angle causes polygons with fewer sides (and therefore smaller intersection angles) to shrink to 4-way or 5-way intersections that transition to 3-way intersections (Figure 5). Similar transitions in soap bubbles and magnetic fluid froths have been reported (*31,32*).

Large soil domains are dissected when random perturbations on the stone/soil interface develop into linear stone domains that extend across the soil domain, a process that is particularly active when lateral confinement is only moderate ($C_{sq} < \sim 0.8$, Figure 4c) or if stone diffusion by lateral squeezing is large compared to lateral sorting ($K_{sq} >> K_{ls}$). The polygon size stabilizes when the probabilities of dissection of a soil domain and elimination of a soil domain are equal; its value depends in a complicated manner on parameters, but usually lies in the range $\sim 3D_{ls}$ to $\sim 5D_{ls}$, above which the probability of soil domain elimination is negligible.

As a test of this model, distributions of intersection angles and normalized polygon areas predicted from the model (using parameters as in Figure 5) were compared with the corresponding distributions measured from sorted polygon networks within two desiccated pond basins in Interior Alaska (Figure 6, Table 1, *33*). Within the variability between the measured networks, modeled and measured polygons are consistent.

This new model produces all forms of sorted patterned ground via self-organization and it defines the properties that control transitions between different patterns (stone concentration, hillslope gradient, strength of sorting and degree of lateral squeezing and confinement). Sorted polygons develop when the previously unrecognized stone transport process of lateral squeezing and confinement dominates over lateral sorting mechanisms. Squeezing and lateral confinement are enhanced by rapid freezing in stone domains with large air cooled pores and low soil compressibility; lateral sorting increases with increasing soil compressibility. The conditions that we predict favor sorted polygons over other patterns are: low stone concentration, low overall slope, large stones and moderately compressible soil.

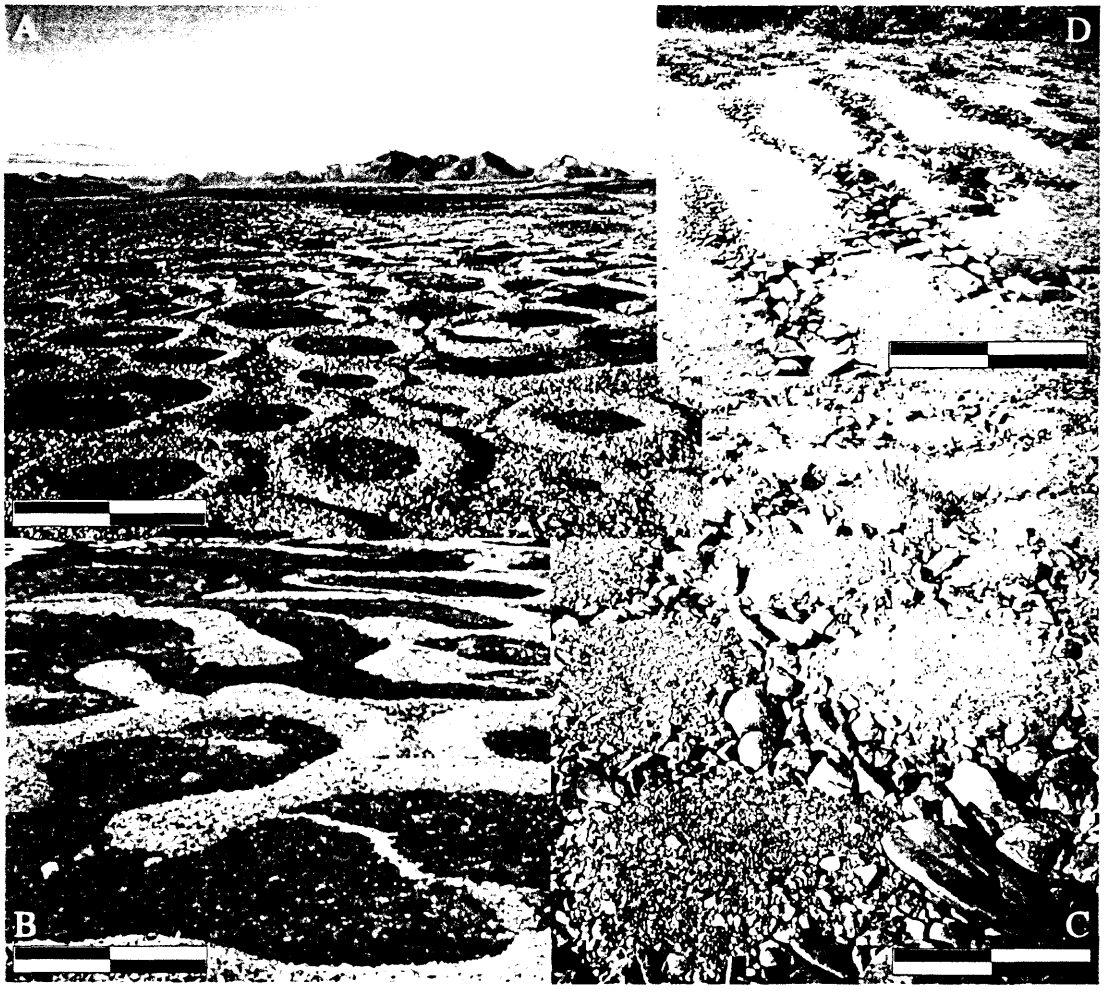

Figure 3.1: Forms of sorted patterned ground: (A) sorted circles (scalebar $\sim$2 m) and (B) sorted labyrinths (scalebar $\sim$1 m), Kvadehuksletta, Spitsbergen; (C) sorted polygons (scalebar $\sim$0.5 m), Denali Highway, Alaska; and (D) sorted stripes (scalebar $\sim$1 m), Tangle Lakes region, Alaska.

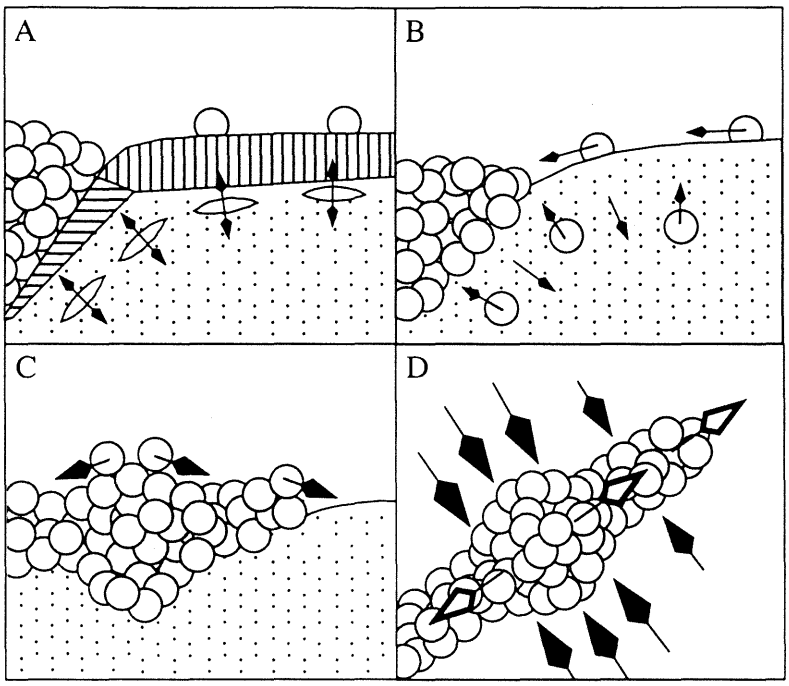

Figure 3.2: Feedback mechanisms for sorted patterned ground: lateral sorting (A-B) and lateral squeezing and confinement (A,C-D). (A) Frost heave expands soil perpendicular to the freezing front (cross-section). Horizontal lines indicate zone of lateral frost heave near the stone/soil interface; vertical lines indicate zone of vertical frost heave near the ground surface. (B) Surface stones creep toward stone domains, subsurface soil is driven toward the interior of the soil domain and stones are pushed toward stone domains by stone upfreezing (cross-section). (C) Stones ravel away from regions where stones domains are thicker, which experience greater uplift by lateral squeezing (section along the stone domain axis). (D) Regions where stone domains are wider experience greater lateral squeezing (planview); stone motion (open arrows) is away from wider areas and parallel to the stone domain axis.

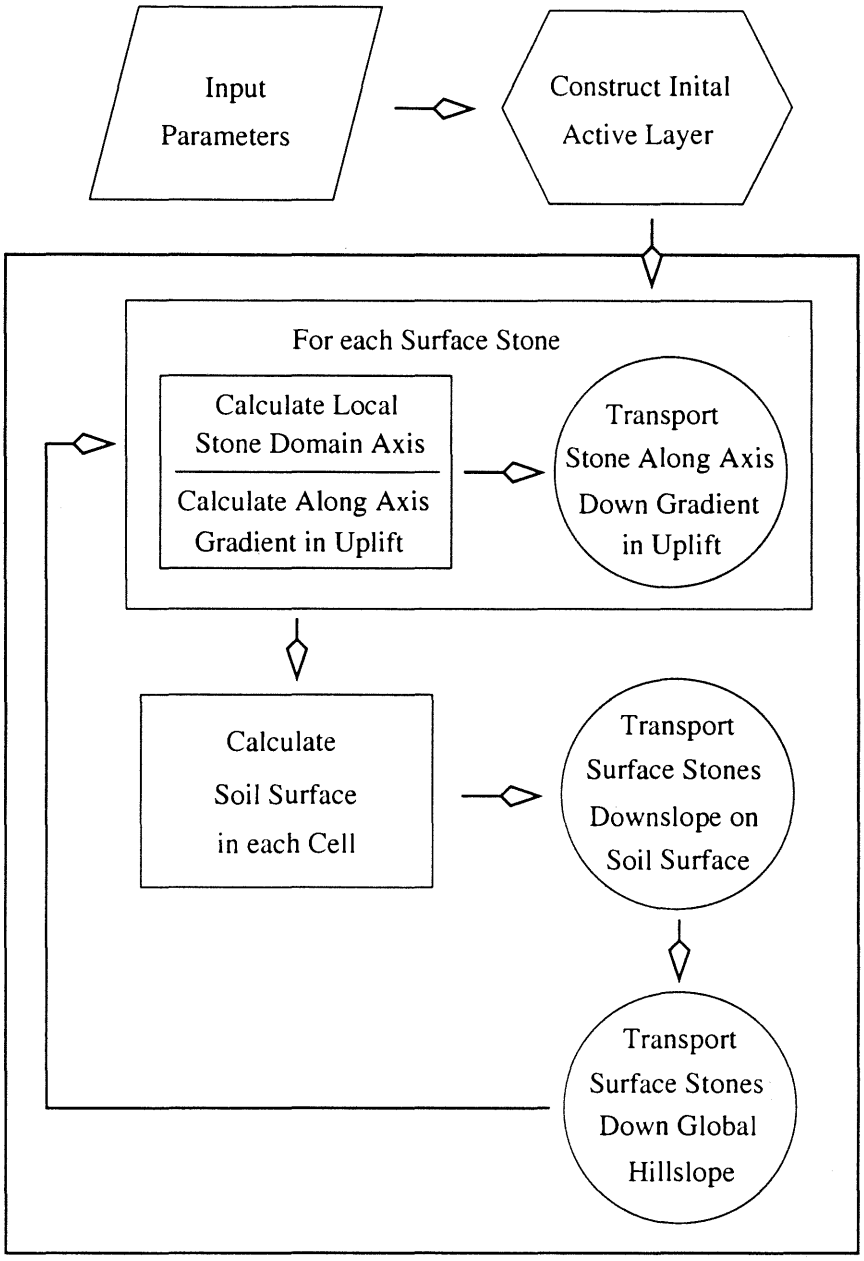

Figure 3.3: Numerical model algorithm. First, stones move along axis down gradients in surface uplift owing to lateral squeezing. Second, stones move downslope on a surface that dips toward stone domains. Third, stones move down the global hillslope.

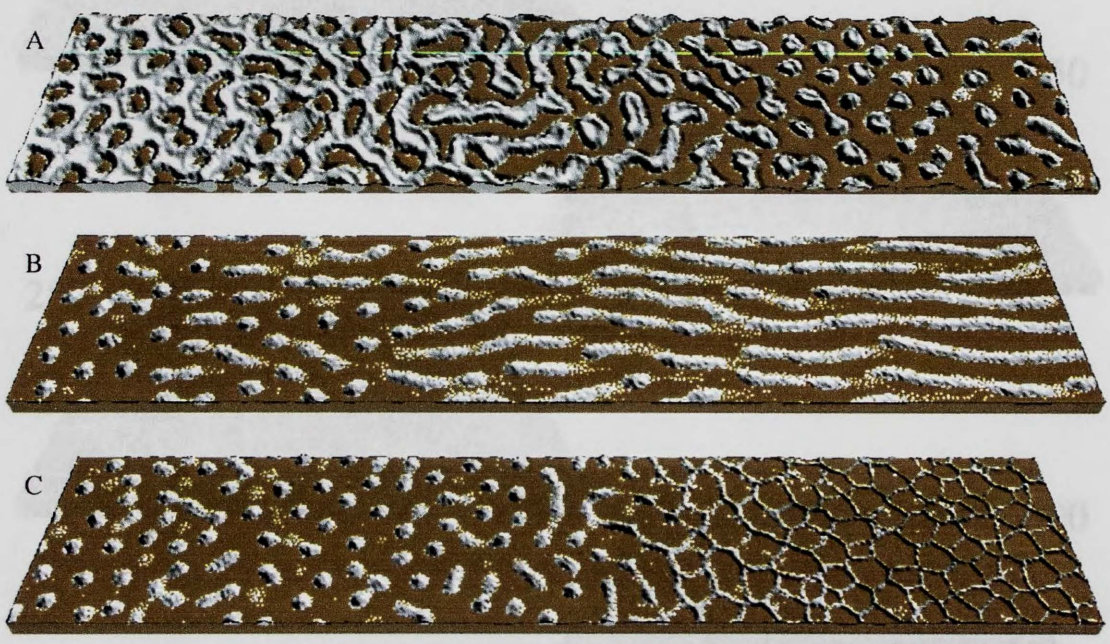

Figure 3.4: Sorted patterned ground model simulations showing pattern transitions with varying parameters (three-dimensional perspective view with gray stone domains and brown soil domains). (A) Stone concentration decreases left to right from 1400 to 100 $stones/m^2$, lateral confinement $C_{sq} = 0.0$. (B) Hillslope gradient increases left to right from 0^o to 30^o, $C_{sq} = 0.0$, 100 $stones/m^2$. (C) Lateral confinement, C_{sq}, increases left to right from 0.0 to 1.0, 100 $stones/m^2$. Simulation size = 50×10 m, lateral sorting length scale $D_{ls} = 0.5$ m, lateral sorting diffusion constant $K_{ls} = 0.005$ $m^2/cycle$, lateral squeezing lengthscale $D_{sq} = 0.2$ m, lateral squeezing diffusion constant $K_{sq} = 0.002$ $m^2/cycle$, maximum depth of stone domains $H_{max} = 20$, 500 iterations.

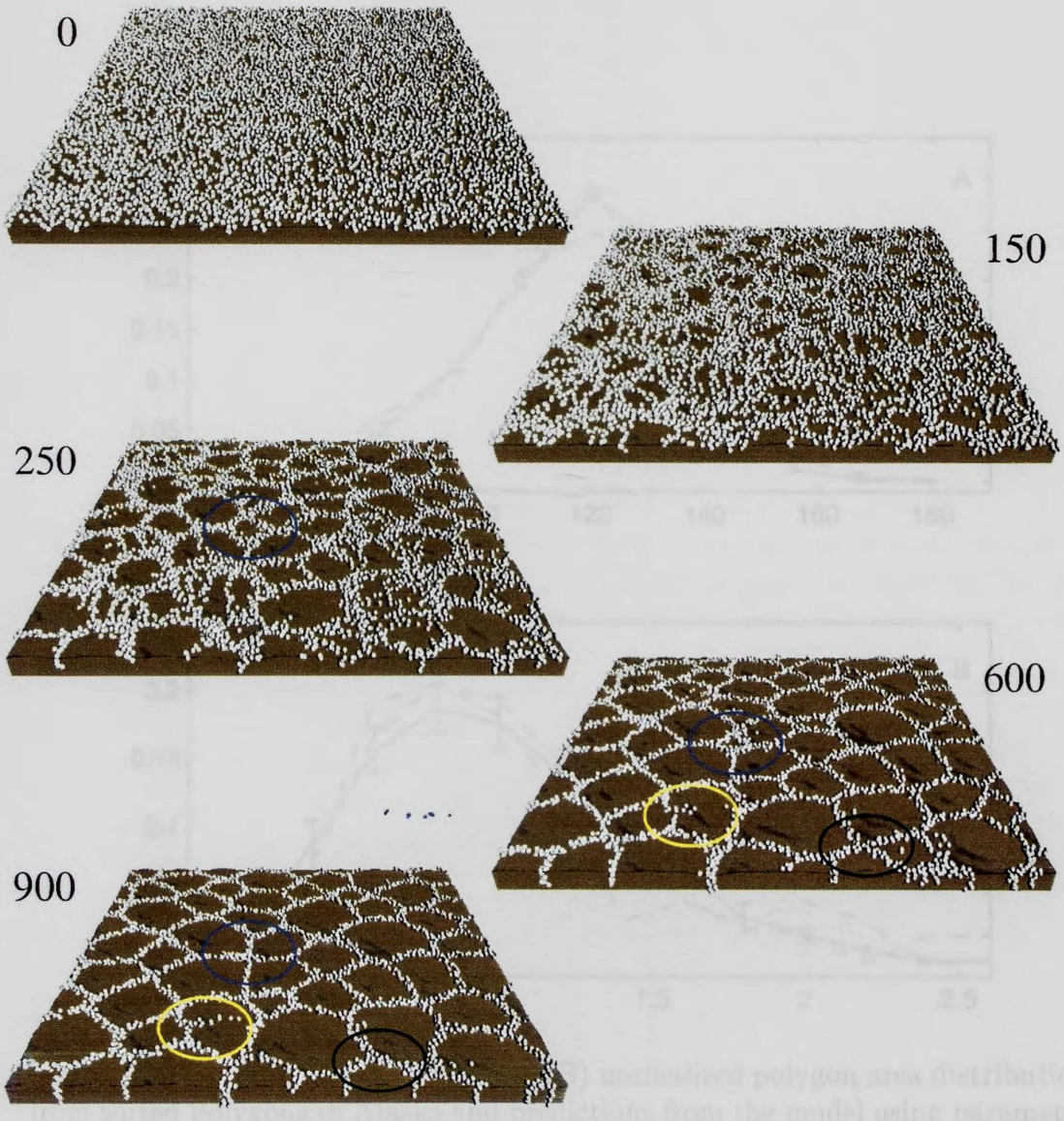

Figure 3.5: Development of sorted polygons from a random initial configuration. Blue ovals indicate a small polygon evolving to an intersection. Black ovals indicate a transition from a four-way to a three-way intersection through the shrinking of a neighboring soil domain. Yellow ovals indicate an unstable perturbation on a stone domain extending across a soil domain. Numbers indicate the iteration pictured. Simulation size = 10×10 m, $10,000$ stones, cell width = 0.1 m, $D_{ls} = 0.5$ m, $K_{ls} = 0.005$ $m^2/cycle$, $D_{sq} = 0.2$ m, $K_{sq} = 0.002$ $m^2/cycle$, $C_{sq} = 1.0$, maximum depth of stones, $H_{max} = 10$.

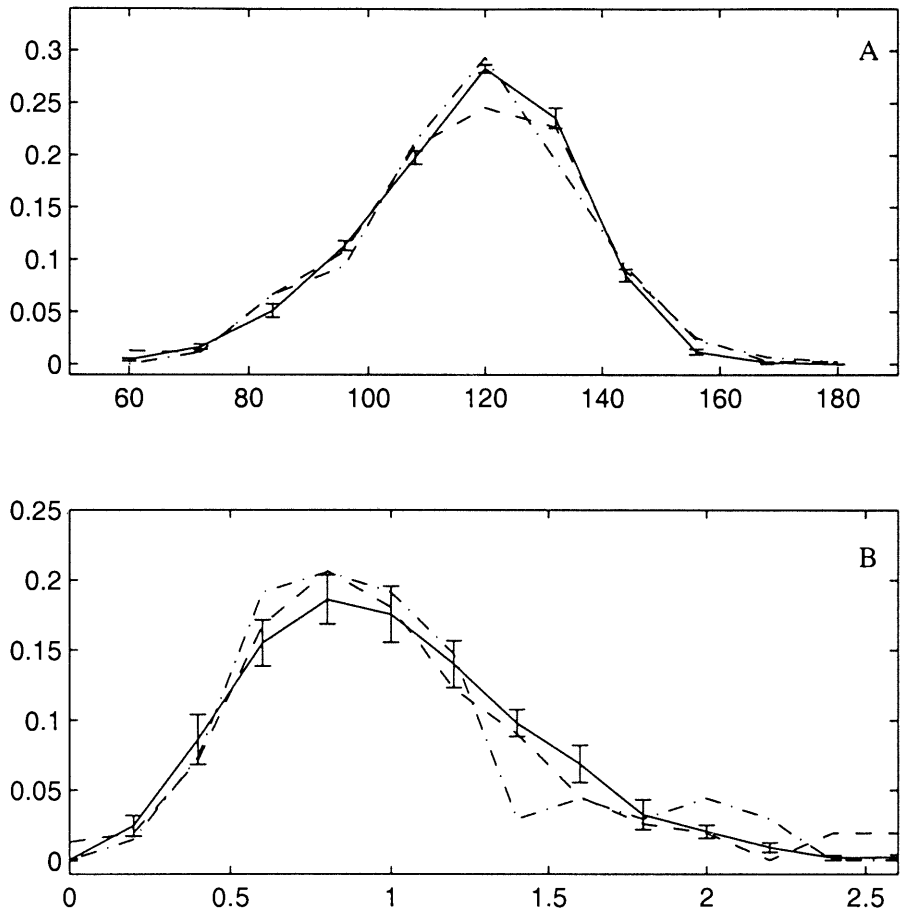

Figure 3.6: (A) Intersection angle and (B) normalized polygon area distributions from sorted polygons in Alaska and predictions from the model using parameters as in Figure 5, except simulation size of $30x30$ m. West pond dashed, east pond dash-dot, model solid. Error bars represent the standard deviation for 10 independent model runs. Model is consistent with measurements within their level of variability.

Table 3.1: Statistical comparisons of polygon area and angle distributions in Figure 6. Columns 2 and 3 give the probability of correctly rejecting the null hypothesis that the two distributions in column 1 do not share the same parent distribution, calculated using the Kolmogorov-Smirnov test.

Distributions	Angle	Area
model-model	0.7 ± 0.2	0.8 ± 0.2
East-model	0.6 ± 0.1	0.82 ± 0.05
West-model	0.5 ± 0.1	0.4 ± 0.2
East-West	0.67	0.91

3.3 References and Notes

1. A. E. Corte, *Biuletyn Peryglacjalny* **15**, 175 (1966).

2. N. Li, B. Chen, F. Chen, X. Xu, *Cold Regions Science and Technology* **31**, 199 (2000).

3. H. M. Jaeger, S. R. Nagel, R. P. Behringer, *Rev. Mod. Phys.* **68(4)**, 1259 (1996).

4. S. Taber, *J. Geology* **37**, 428 (1929).

5. A. C. Fowler, W. B. Krantz, *SIAM J. Appl. Math.* **54(6)**, 1650 (1994).

6. N. Matsuoka, *Earth-Science Reviews* **55**, 107 (2001).

7. A. L. Washburn, *Bull. Geo. Soc. America* **67**, 823 (1956).

8. P. A. Pissart, *Abhandlungen der Akademie der Wisenschaften in Gottingen, Mathematisch-Physikalische Klass* **31(3)**, 142 (1977).

9. C. K. Ballantyne, J. A. Mathews, *Arctic and Alpine Research* **15(3)**, 339 (1983).

10. R. J. Ray, W. B. Krantz, T. N. Caine, R. D. Gunn, *J. Glaciology* **20(102)**, 317 (1983).

11. K. J. Gleason, W. B. Krantz, N. Caine, J. H. George, R. D. Gunn, *Science* **232**, 216 (1986).

12. B. Hallet, *Earth-Science Reviews* **29**, 57 (1990).

13. B. T. Werner, T. M. Fink, *Science* **260**, 968 (1993).

14. A. B. Murray, C. Paola, *Nature* **371**, 54 (1994).

15. B. T. Werner, *Geology* **23(12)**, 1107 (1995).

16. H. H. Stolum, *Science* **271**, 1710 (1996).

17. P. Rohani, T. J. Lewis, D. Grunbaum, G. D. Ruxton, *TREE* **12(2)**, 70 (1997).

18. G. Nicolis, I. Prigogine, *Self-Organization in Nonequilibrium Systems: From Dissipative Structures to Order Through Fluctuations* (Wiley, New York, 1977).

19. B. T. Werner, B. Hallet, *Nature* **361**, 142 (1993).

20. M. A. Kessler, A. B. Murray, B. T. Werner, B. Hallet, *J. Geo. Res.* **106(B7)**, 13,287 (2001).

21. R. P. Goldthwait, *Quaternary Res.* **6**, 27 (1976).

22. J. H. Schmertmann, R. S. Taylor, *Quantitative Data from a Patterned Ground Site over Permafrost* (Tech. Rep. Cold Regions Research and Engineering Laboratory, Report 96, 1965).

23. F. H. Nicholson, *Arctic and Alpine Res.* **8(4)**, 329 (1976).

24. F. A. Cook, *Arctic* **8**, 237 (1955).

25. A. L. Washburn, *Plugs and Plug Circles* **190** (Geological Society of America, Boulder, CO, 1997).

26. J. S. Huxley, N. E. Odell, *Geographical J.* **63**, 201 (1924).

27. Unlike previous simulation models (*19,20,28*), stone position is not discretized, avoiding congestion effects that can cause trapping and jamming of stones on lattices. However, here a lattice with grid size corresponding to stone diameter is used to calculate the concentration of stones and to determine the depth to which they are stacked. This semi-continuous algorithm also allows for greater sensitivity to local biases because stones can move in any direction and over distances less then a cell width.

28. F. Ahnert, *Trans., Japanese Geomorphological Union* **2**, 301 (1981).

29. K_{ls} and K_{sq} are likened to diffusion constants because they quantify the ratio of stone flux to gradient.

30. Stone domain surface uplift, U, is calculated assuming stone domains are rectangular in cross-section and are squeezed from both sides by frost heave. Lateral squeezing is dependent on the width owing to increased resistance to deformation by narrower stone domains (relative to stone width); the increase in uplift with stone domain width is assumed to be linear.

31. D. Weaire, N. Rivier, *Contemp. Phys.* **25(1)**, 59 (1984).

32. F. Elias, C. Flament, J. C. Bacri, O. Cardoso, F. Graner, *Phys. Rev. E* **56(3)**, 3310 (1997).

33. Measured sorted polygons were located in the basins of two desiccated ponds 100 m north of Denali highway, approximately 115 km east from Cantwell, Alaska. Both ponds exhibit a gradation from high to low stone concentration moving outward from their centers. Well-formed polygons with narrow stone domains located midway in this gradation were digitized

from low-elevation aerial photographs that had been orthorectified using ground control points (*34*). East pond: 68 polygons, 436 angles. West pond: 155 polygons, 705 angles.

34. Y. I. Abdel-Aziz, H. M. Karara, in *Proceeding of ASP/UI Symposium on Close-Range Photogrametry*, 1, (1971).

35. We are grateful to A. B. Murray for many helpful discussions, B. Hallet for useful insights early in this research, and L. Clarke for assistance in image processing. Supported by the National Science Foundation, Arctic Natural Sciences Program [OPP-9530860], the Andrew W. Mellon Foundation and a National Defense Science and Engineering Graduate Fellowship.

Chapter 4

A Three-Dimensional Model for Sorted Patterned Ground

4.1 Abstract

The entire range of sorted patterned ground, including sorted circles, labyrinths, stone islands, sorted stripes and sorted polygons emerge in a three-dimensional cellular model that abstracts the active layer processes of frost heave, stone avalanching, soil creep, soil illuviation, soil expansion by water absorption, and lateral squeezing, deformation and uplift of stone domains during freezing. Circles, labyrinths and islands form through lateral sorting into distinct stone and soil domains driven by frost heave. Transitions between these three patterns are caused by variation of the volumetric fraction of soil in the active layer, V_s: circles transition to labyrinths at $V_s \sim 0.47$; labyrinths transition to islands at $V_s \sim 0.66$. Formation of polygons requires stabilization of narrow stone domains

to perturbations in depth and width. Squeezing of stone domains by lateral frost heave in adjacent soil domains provides stability because greater contraction of wide or deep sections causes greater uplift, leading to raveling and stable redistribution of stones along the stone domain axis. Increasing the compressibility of soil domains relative to the force required to squeeze and uplift stone domains results in a transition from polygons to labyrinths. Islands and polygons grade into sorted stripes on hillslopes steeper than $\sim 2^o$ and $\sim 4^o$ respectively.

4.2 Introduction

Sorted patterned ground, decimeter- to meter-scale patterns characterized by lateral sorting into distinct stone and soil domains, forms in active layers, which are surface ground layers experiencing cyclic freezing and thawing. The range of patterns includes: (i) stone islands within a continuous soil network, (ii) labyrinthine stone and soil domains, (iii) circular soil domains circumscribed by raised annuli of stones, (iv) polygonal soil domains demarcated by a connected network of stone domains, and (v) stripes of stones and soil on hillslopes. Active layers are dynamic environments in which cyclic freezing and thawing, wetting and drying, and gravity drive numerous transport processes. The diversity of patterned ground and active layer processes have lead to over twenty hypotheses regarding the formation and maintenance of sorted patterned ground (reviewed in [*Washburn*, 1956, 1997]). Most of these conceptual mechanisms are well grounded in field observations; however, few quantitative predictions have been made that can be used to distinguish between competing hypotheses.

Numerical simulation models for sorted patterned ground have been devel-

oped that address quantitatively some aspects of pattern development. Stone lines and clusters form in a two-dimensional model for patterning in granular media based solely on friction between grains of similar size [*Ahnert,* 1981]. This model is based on transport variations resulting from stones impeding the otherwise random motions of neighboring stones. Sorted stripes develop on a two-dimensional lattice corresponding to the ground surface via diurnal uplift of stones by columns of needle ice and their redistribution as the columns melt and topple [*Werner and Hallet,* 1993]. Toppling is biased downhill and toward stone domains, which lie lower than intervening soil domains elevated by frost heave.

A three-dimensional cellular model [*Kessler et al.,* 2001] has been employed to simulate the initiation, evolution and long-time-scale dynamics of sorted circles within a layer composed of stone and soil particles that are transported in response to cyclic freezing and thawing. The primary processes transporting stones and soil are differential frost heave, compaction during thaw, soil expansion by water absorption, soil illuviation, surface creep and stone avalanching. A descending freezing front follows the interface between a stone layer overlying a soil layer because it travels more rapidly through dry stones than through wet soil, where cooling is delayed by release of latent heat during freezing. Frost heave at the stone/soil interface lifts the overburden and compacts the underlying soil. Perturbations on the stone/soil interface are unstable, because frost heave transports soil uniformly from the stone/soil interface but preferentially toward existing soil-rich regions, which are more compressible. Soil plugs rise to the surface, pushing aside overlying stones, and form small sorted circles that expand radially by drawing soil from the underlying soil layer.

Initiation and pattern scale dynamics of all sorted patterned ground plan-

forms has been simulated using a more highly abstracted, two-dimensional model [Chapter 3]. Stones move on a surface that is determined by the local concentration of stones owing to two transport processes: (i) stones move downslope on this surface, which dips toward regions of higher stone concentration, abstracting the lateral sorting feedback of the three-dimensional model [*Kessler et al.*, 2001] and (ii) once lateral sorting has produced stone domains, stones move along the axis of elongate stone domains. The conceptual underpinning of this second mechanism is that stone domains are being squeezed by adjacent soil domains, which are expanding owing to lateral frost heave at inclined freezing fronts, causing stone domains to contract laterally and expand vertically. Increased surface uplift with increased stone domain width and depth causes perturbations in width and depth to diffuse and can stabilize narrow, elongate stone domains; a property that is critical to the formation of sorted polygons in the model. Because lateral frost heave increases with stone/soil interface area, uplift is proportional to stone domain depth; additionally, because wider stone domains are more easily deformed they experience greater lateral contraction. Stone islands transition to sorted polygons as the magnitude of stone motion along the axis of elongate stone domains increases relative to stone motion toward stone domains. The physical interpretation of this mechanism requires rapid freezing of stone domains and low soil compressibility to enable significant stone domain squeezing at depth.

The two-dimensional model employs significant abstractions of the physical processes causing sorted patterned ground. To investigate the physical basis and consistency of the abstractions, and in particular the correspondence between two- and three-dimensional patterns, I have modified the three-dimensional cellular model for sorted circles to include abstractions of the lateral squeezing and uplift

mechanisms. Additionally, with the aim of probing whether the two models are consistent, the transitions predicted by the two-dimensional model from islands to labyrinths to circles with increasing volumetric fraction of stones, from islands to polygons with increasing lateral squeezing and confinement, and from islands to stripes on hillslopes were compared with corresponding transitions in the modified model.

4.3 Existing Model for Sorted Circles

In a model for sorted circles [*Kessler et al.*, 2001], stones and soil move within the active layer driven by the annual descent of a freezing front and consequent expansion by frost heave in soil-rich regions (Figure 1). This model is described briefly here (see [*Kessler et al.*, 2001] for more detail).

The active layer is represented as a three-dimensional lattice of cells containing stone, soil, ice, or void particles. (Void particles are a discrete abstraction that allows for soil compression.) The lateral boundaries are periodic; the lower boundary is rigid and the upper boundary is a free surface. This simulated active layer experiences repeated freezing and thawing in which ice particles and void particles are created and destroyed by a set of rules that abstract physical processes, resulting in displacement of neighboring particles. The use of algorithmic rules to describe transport in the active layer, in preference to partial differential equations, permits modeling sorted patterned ground at long time-scales at which abstractions of short time-scale processes are spatially non-local. Over a single freeze/thaw cycle, five processes transport particles: frost heave, surface creep, compaction during thaw, soil illuviation and expansion of soil by

absorption of water. These processes are sensitive to the thermal, hydrological and rheological properties of stone and soil particles.

4.3.1 Freezing and frost heave

Active layers freeze, when air temperature dips below 0°C, by descent of a freezing front from the ground surface to the top of the underlying permafrost. In soil, water is drawn to the freezing front and freezes into thin layers of ice, ice lenses, desiccating and compacting the soil layer below and raising the overburden [*Taber,* 1929]. Because latent heat is released by freezing water, ice lens formation considerably slows the descent of the freezing front in moist soils.

In the model, the temperature profile before freezing is linear, ranging from $T_g = 5°C$ at the ground surface down to $T_b = 0°C$ at the base of the active layer. Void particles are introduced in proportion, V_v, to the local volumetric fraction of soil particles. The volumetric fraction of void particles, V_v, represents the total volume contraction that can occur given the compressive forces generated during freezing. The active layer is frozen by application of a constant air temperature of $T_a = -5°C$ in the cells above the ground surface. The temperature of each active layer cell is updated through time using a finite difference algorithm [*DuFort and Frankel,* 1953; Nogotov, 1978] to solve the three-dimensional temperature diffusion equation with a correction for the release of latent heat from soil cells at each time step. The freezing front starts at the ground surface and descends vertically as each cell is frozen.

After a soil cell freezes, a stochastic test for the creation of an ice particle within that cell, representing frost heave, is performed. An ice lens displaces

material toward a void particle or toward the ground surface, in either case driving particle displacement along a path that starts at the cell in which the ice particle formed and terminates at the cell containing the void particle or at the ground surface. The probability of displacement toward the surface, P_{surf}, and the probability of displacement toward the nearest void particle, P_{void}, are set to be proportional to the distances along these two paths, d_{surf} and d_{void}:

$$P_{\text{surf}} = \max(0, 1 - d_{\text{surf}}/d_s) \tag{4.1}$$

$$P_{\text{void}} = \max(0, 1 - d_{\text{void}}/d_v), \tag{4.2}$$

where d_s and d_v are constant distances at which the probabilities P_{surf} and P_{void} are zero. The probability of ice particle formation is given by the greater of the two probabilities. The forces generated by frost heave during freezing are abstracted, but not calculated, by this ice particle formation and transport algorithm.

4.3.2 Thawing and surface creep, compaction, illuviation and expansion

As soil domains thaw, surface morphology relaxes via surface creep. In the model, surface particles on the soil domain move downslope with a probability proportional to the surface slope. In the stone domain, stones avalanche if the dip exceeds the angle of repose.

As ice melts, thawed soil compacts vertically under the force of gravity by expelling water. In the model, ice particles are removed and particles in the

overlying cells are shifted downward.

Soil illuviates as water drains downward, carrying fines with it. In the model, stone and soil particles each occupy half the volume of a cell. In a stone cell, the remaining volume is empty; in a soil cell, the remaining volume is filled with a second soil particle or a stone particle. This arrangement provides a mechanism for soil particles to illuviate. After thawing, soil particles move downward to the lowest stone cell in the same column, thereby converting it to a soil cell; the cells vacated by soil particles become stone cells.

With the abundance of water from melting, soil that was compacted and desiccated during freezing absorbs water and expands vertically. In the model, void particles are added stochastically to the soil domain, with a probability proportional to the local volumetric fraction of soil, until a specified volumetric fraction of void particles, V_v, is achieved.

4.4 Modified Model

The three-dimensional numerical model for sorted circles has been modified to include the lateral squeezing mechanism of the two-dimensional model for sorted patterned ground described above [Chapter 3]. Implementing lateral squeezing in the three-dimensional model relies on changes to the spatial distribution of ice particle formation and consequent displacement paths. The key constraint on lateral squeezing that facilitates polygon formation is that narrow, elongate stone domains are stable to perturbations in width and depth. This requirement is met if: (i) stone domains are flat or have negative relief relative to

the stone/soil contact, thereby confining stones to stone domains and resulting in greater sensitivity to surface gradients along the axis of stone domains, (ii) stone domain uplift by lateral squeezing is proportional to vertical stone domain thickness, thereby causing diffusion of perturbations in depth, and (iii) stone domain uplift is proportional to stone domain width, thereby causing diffusion of perturbations in width. The manner in which these three constraints are implemented is discussed below.

The surface morphology of stone domains is determined by the volume of soil removed from beneath the stone/soil contact relative to removal from beneath the center of the stone domain; both occur as a result of frost heave displacing soil toward the soil domain. For a wedge-shaped stone domain, if frost heave decreases with depth, more soil is removed from beneath the stone/soil contact than from beneath the center of the stone domain, resulting in stone domains that are elevated above the stone/soil contact. In contrast, a uniform distribution of frost heave with depth, which results from rapid cooling in stone domains, reduces the surface relief of stone domains, thereby increasing the confinement of stones to stone domains. In the modified model, rapid cooling of stone domains is simulated by setting cells within the stone domain to the air temperature during freezing, $T_a = -5^o$C, and initiating the freezing front at the stone/soil interface rather than the air/stone interface. The primary effect of rapid stone domain freezing (Figures 2, 3) is an increase in the number of ice particles near the stone/soil interface at depth that displace soil particles toward void particles, which reduces stone domain surface relief and increases the surface slope of the soil domain. Both effects promote confinement of stone particles to stone domains.

The condition that stone domain squeezing and uplift are proportional to

stone domain thickness is equivalent to the probability of frost-heave-induced squeezing of the stone domain being independent of depth. In the modified model, the equations governing the probability of ice particle formation (eqns. 1, 2) were changed to enable simulation of this condition. First, if a displacement path toward the surface intersects a stone domain (squeezing), the probability of ice formation is given by P_{sqz}, which is not permitted to fall below a minimum value, P_s^{mn}. Second, coefficients P_s and P_v are added to the expression for P_{surf} and P_{void} to allow adjustment of the relative probability of displacement toward the surface and toward a void particle:

$$P_{\text{sqz}} = \max(P_s^{mn}, P_s(1 - d_{\text{surf}}/d_s)) \tag{4.3}$$

$$P_{\text{surf}} = \max(0, P_s(1 - d_{\text{surf}}/d_s)) \tag{4.4}$$

$$P_{\text{void}} = \max(0, P_v(1 - d_{\text{void}}/d_v)). \tag{4.5}$$

The condition that lateral squeezing of stone domains is approximately independent of stone domain depth is simulated by setting $P_s^{mn} = P_s$, thereby making P_{sqz} constant. With values $P_s^{mn} = P_s = 0.2$, the resulting distribution of ice particles that displace stone and soil particles toward the surface extends uniformly to the depth of the active layer near stone domains and is reduced near the free surface (Figures 2, 4).

The condition that stone domain uplift is proportional to stone domain width is crudely simulated in the modified model by application of a threshold stone domain width (W_{sd}, measured along the horizontal projection of the displacement path) below which probability P_{surf} is used and above which P_{sqz} is used. This minimum stone domain width inhibits displacements through narrow stone

domain sections, thereby focusing squeezing on wider stone domain sections (Figure 5) and simulating the greater ease with which wide stone domains can be deformed relative to narrow stone domains.

Squeezing and polygon formation are enhanced by less compressible soil domains, a condition that can be simulated by $P_s/P_v > 1$ or by $P_s^{mn} > 0$. The number of ice particles displacing toward void particles is reduced at the stone/soil interface, but extends to greater depth (Figures 2, 6). This method of reducing the relative compressibility of soil near the stone/soil interface, as opposed to reducing the volumetric fraction of void particles, is realistic in that: (i) as the lateral frozen layer thickens, compression of unfrozen soil is favored over deformation of both the stone domain and the frozen layer; and (ii) the activity of soil domains is not reduced.

Transport owing to a hillslope gradient was implemented with two modifications: (i) for relaxation of surface morphology, the surface slope is equal to the sum of the hillslope gradient and the local surface gradient (relative to a horizontal active layer base) and (ii) for consolidation during thaw, particles settle into empty cells downslope with probability equal to the hillslope gradient.

4.4.1 Reference model

Exploring the entire parameter space of this three-dimensional model is presently computationally infeasible. The dependence of model results on parameters is presented here in two ways: parameters are varied one at a time from a set of reference parameter values that represent best estimates of parameter values from a well-studied field site in western Spitsbergen (Table 1) [*Hallet and*

Prestrud, 1986; *Kessler et al.,* 2001], and parameter values are varied across the model domain.

4.5 Results

With the modifications to the model described above and otherwise using reference model parameters, features resembling sorted polygons develop over a temporal scale ($< 1000\ yr$) comparable to that governing development of sorted circles. All forms of sorted patterned ground result from changing the volumetric fraction of soil, the hillslope gradient, the freezing rate in stone domains and the relative probability of frost heave compression of underlying soil versus lateral squeezing uplifting stone domains. Unless otherwise noted, reference model parameters were used in all simulations.

4.5.1 Sorted Polygons

In the modified model with $P_s = P_s^{mn} = 0.2$ and $P_v = 0.2$, sorted polygons initiate within a hundred freeze/thaw cycles and then evolve over hundreds of subsequent cycles (Figure 7). Their evolution occurs in three stages. (i) Random perturbations in the stone/soil interface on short length scales are unstable, because frost heave at the stone/soil interface transports soil preferentially toward soil rich regions, causing perturbations on the soil layer to break through the stone layer (Figure 7: 0-100). (ii) Stone domains are sensitive to large initial fluctuations in stone domain depth and width: shallow stone domains are breached and soil domains then merge (Figure 7: 100-1000). (iii) Over long time scales,

elongate soil domains become more equidimensional through dissection by stone domains and migration of intersections within the context of existing connections (Figure 7: 1000-3000).

The patterns produced with the modified model can be classified as connected networks of stone domains, but they do not exhibit the narrow, straight stone domains of classic sorted polygons [*Schunke,* 1975] or of polygons produced with the two-dimensional model. Several straightforward modifications to this model result in connected networks with narrower stone domains (Figure 8): (i) increasing the transport rate of stones on the surface of soil domains by an order of magnitude, (ii) eliminating ice lenses that push to the surface without contacting stone domains ($P_{surf} = 0$), and (iii) reducing the active layer depth from 1.0 m to 0.55 m. The first increases the confinement of stones to stone domains by increasing the asymmetry in transport rates for stones on stone domains (angle of repose) and stones on soil domains (surface creep). This modification is reasonable near the stone/soil contact in that it abstracts the added confinement produced by the typical watchglass shape of soil domains (dipping sharply near the stone/soil contact) [*Sharp,* 1942], which is not resolved by the coarse cell size. The second change reduces the soil surface roughness resulting from discrete, stochastic transport, which can swamp surface gradients and prevent stone motion toward stone domains or off the ends of elongate stone domains. The third change reduces the depth of stone domains, thereby causing wedge-shaped stone domains to be narrower at the surface; this corresponds well with the field observation that the active layer depth (sometimes only the sorting depth has been measured) in sorted polygons is rarely over 0.5 m [*Huxley and Odell,* 1924; *Sharp,* 1942; *Washburn,* 1969], whereas the active layer depth in sorted

circles is ~1 m [*Schmertmann and Taylor,* 1965; *Hallet and Anderson,* 1986]. In addition to the features of the developmental sequence without these additional modifications, network evolution in this model includes collapse or shrinking of small soil domains by slow transfer of soil from small polygons into surrounding larger polygons.

4.5.2 Transitions between patterns

In the modified model with $P_s = P_s^{mn} = 0.2$ and $P_v = 0.2$, a transition from polygons to labyrinths is effected by increasing the probability of frost heave displacement toward a void particle, P_v (Figure 9). The transition occurs between P_v~0.3 and ~0.4. Qualitatively, this transition is consistent with increasing lateral confinement or increasing rate of stone diffusion along the axis of stone domains in the two-dimensional model [Chapter 3]; however, in the two-dimensional model, polygons transition to islands at this volumetric fraction of soil.

Varying only the volumetric fraction of soil cells, V_s, the model generates sorted circles ($V_s < 0.47$), labyrinths ($0.47 < V_s < 0.66$) and stone islands ($V_s > 0.66$) (Figure 10, Table 2). These transitions are consistent with those found with the two-dimensional model (Figure 11, Table 2; [Chapter 3]).

An increase in hillslope dip effects a transition from stone islands to sorted stripes between ~2^o and ~7^o (Figure 12). In the two-dimensional model, the transition between islands and stripes is more gradual, occurring between ~5^o and ~15^o (Figure 13) [Chapter 3]; islands are more stable on higher slopes for greater maximum stone depth. In both models, the transitional slope range is

dependent upon time; as stone and soil domains become more distinct, owing to lateral sorting, islands become more stable on higher slopes. In the modified model with rapid stone motion on soil domains, $P_s = 0$, $P_s^{mn} = 0.2$, $P_v = 0.2$, and $V_s \sim 0.7$, an increase in hillslope dip causes a transition between polygons and stripes at $\sim 4^o$ (Figure 14).

4.6 Discussion

A three-dimensional cellular model produces sorted circles, labyrinths, stone islands and sorted stripes. The principal processes operating in this model act to laterally sort stones and soil into distinct domains, which assume various shapes depending on the volumetric fraction of soil and hillslope gradient. These same processes act through all stages of initiation and development. In a modified model, in contrast to lateral sorting, the additional processes that permit formation of sorted polygons, namely squeezing, uplift and confinement of stone domains, are operative only after some sorting occurs; these processes increase in strength as the extent of sorting increases.

The critical requirement for the formation of connected networks versus isolated stone domains is the stability of narrow, elongate stone domains [Chapter 3]. In simulations that produce sorted polygons, small gaps (Figure 15) in otherwise uniform narrow, linear stone domains are bridged. In the model, this stability is related to spatial variation of ice lens formation near a gap. The concentration of ice particles that displace toward void particles in the soil domain exhibits only minor variation in and around the gap (Figure 16); however, the concentration of ice particles that displace toward the surface is markedly higher

in the gap than along the flanks of the stone domain (Figure 17), because displacements along the axis are more effective at deforming the stone domain (implemented in the model through the threshold stone domain width for squeezing, W_{sd}). The gap in the stone domain is bridged when soil particles from the gap are displaced into the stone domain, raising its surface and lowering the surface of the gap, causing stones to ravel into the gap (Figure 18). This mechanism differs from the physical interpretation given for the two-dimensional model [Chapter 3], in which reduced squeezing and surface uplift of a thinning stone domain near its terminus cause stones to ravel toward a gap. These two mechanisms possibly could be distinguished in the natural pattern using the along axis gradient in stone domain surface height near a gap.

Modifications to the three-dimensional model to produce connected networks of stone domains are based on emergent properties of stone and soil domains, properties that are not well defined until lateral sorting is pronounced. Highly porous stone domains cool more rapidly than predicted by heat conduction because convection of air through the pores between stones is more efficient than heat conduction. Frost-heave-induced displacements to the surface through stone domains are dependent on stone packing and compressibility of soil domains.

These properties of stone and soil domains depend on environmental conditions and variation in material properties. Rapid cooling of stone domains is enhanced for larger pore or stone size, implying that sorted polygons are favored in active layers with large stones. Convective cooling is inhibited by snow cover during freezing, implying that sorted polygons are favored where snowfall is late or where wind preferentially removes snow. The lower limit on the probability of displacement toward the surface by frost heave near the stone/soil interface

abstracts conditions where stone domain deformation is favored over soil domain compression. Low soil compressibility or high water mobility in soil domains, which must desiccate to be compressed, favors sorted polygon development.

The cellular framework used in the models described here, in which transport is both discrete and stochastic, is not well-suited for simulating continuous processes such as lateral squeezing of stone domains by frost heave in soil domains. In the natural system, lateral expansion of the soil domain is a continuous, distributed process for which the motions of adjacent soil particles are correlated; the stone/soil interface is shifted slowly and uniformly on a small scale. In contrast, ice lens formation in the model is a low probability, discrete event in which nearby particles are displaced independently. In many cases, subtle variations in surface height owing to gradients in squeezing induced uplift are swamped by surface roughness resulting from discrete transport events. This problem appears to be most pronounced for polygon formation, where stone domains are only a few cells wide. For wider stone domain forms, such as sorted circles, stochastic effects do not appear to inhibit stone domain stability. Improvements within the framework of the existing model could utilize multiple realizations of a freeze/thaw cycle to determine surface motions over a smoother surface.

In the model, the granular mechanics of stone deformation is highly abstracted. The deformation of a stone domain under lateral squeezing might proceed by localized deformation owing to non-uniform squeezing and incomplete relaxation following the previous freeze/thaw cycle. Numerical simulations, laboratory experiments and field measurements might contribute to better specification of these abstractions.

Sorted polygons often are formed in changing environments, such as ponds that are desiccating or near the terminus of receding glaciers [*Ballantyne and Mathews,* 1983]; conditions are changing (e.g. active layer depth, water availability and frost susceptibility of soil) from a regime in which the non-patterned state is stable to one in which it is not. Initiation and early development of patterns at the cusp of instability might affect properties of patterns as they emerge. The effect of changing environmental conditions on sorted patterned ground is unexplored.

The subset of active layer processes and properties in this model represent a hypothesis about sorted patterned ground that includes implicitly the assumption that other active layer processes and properties (e.g., non-horizontal thawing fronts, diapiric motion owing to inverted soil density gradients and non-uniform insulation by snow cover) do not play a role. The results of this model indicate that these neglected processes are not necessary for the formation of sorted patterned ground; however, the effect of these processes on sorted patterned ground has not yet been investigated.

4.7 Conclusions

A three-dimensional cellular model employing frost heave, stone avalanching, soil creep, soil illuviation, soil expansion by water absorption, rapid freezing of stone domains and stone domain squeezing and uplift produces all forms of patterned ground. Transitions from circles to labyrinths to islands result from increasing the volumetric fraction of stones. A transition from islands or polygons to stripes occurs as the hillslope gradient increases. Polygons transition to

labyrinthine patterns as the probability of soil compression increases relative to the probability of deforming and uplifting stone domains.

The model is in qualitative and sometimes quantitative agreement with a previous two-dimensional model for sorted patterned ground. The discrete, stochastic nature of the model renders simulation of sorted polygons, with narrow stone domains, highly sensitive to parameters and details of process implementation. This sensitivity contrasts with sorted patterned ground in nature, for which sorted polygons are the most common pattern. Future research will address whether alterations to the model to decrease stochastic, discrete effects can make modeled sorted polygon formation more robust.

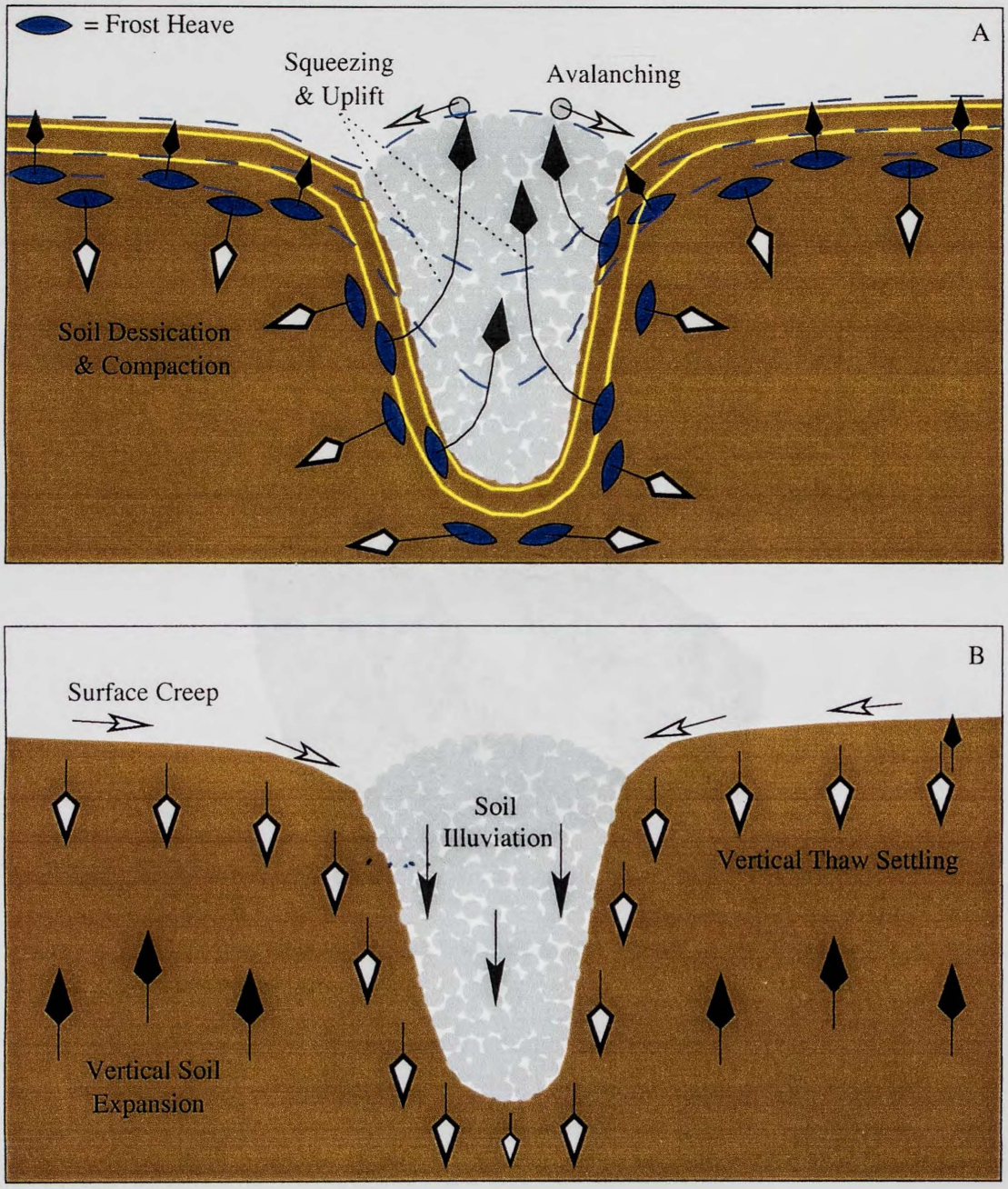

Figure 4.1: Schematic of processes in the three-dimensional model. (A) During freezing: (i) freezing front (dashed blue lines for unmodified model, yellow lines for modified model with rapid freezing in stone domain) descends from the surface, (ii) frost heave at the freezing front displaces particles upward toward the surface and downward toward void particles in the soil, and (iii) on the surface of stone domains, raised stone particles ravel down gradients exceeding the angle of repose. (B) During thawing: (i) downslope creep on the soil domain surface, (ii) ice particles are removed and soil settles vertically, (iii) soil in stone domains illuviates, and (iv) void particles are added, raising overlying particles.

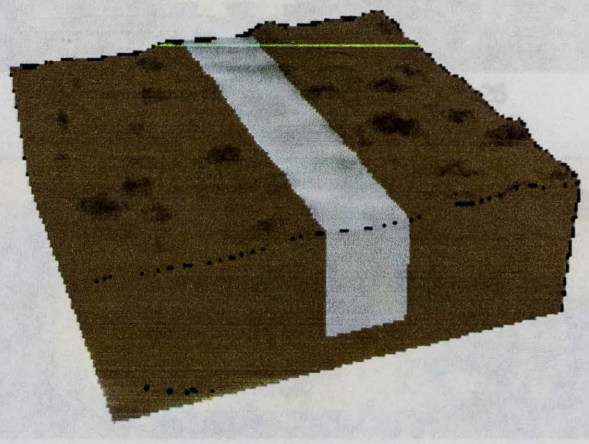

Figure 4.2: Oblique view of 3×3×1 m modeled active layer with a 0.5 m wide, 0.75 m deep stone domain.

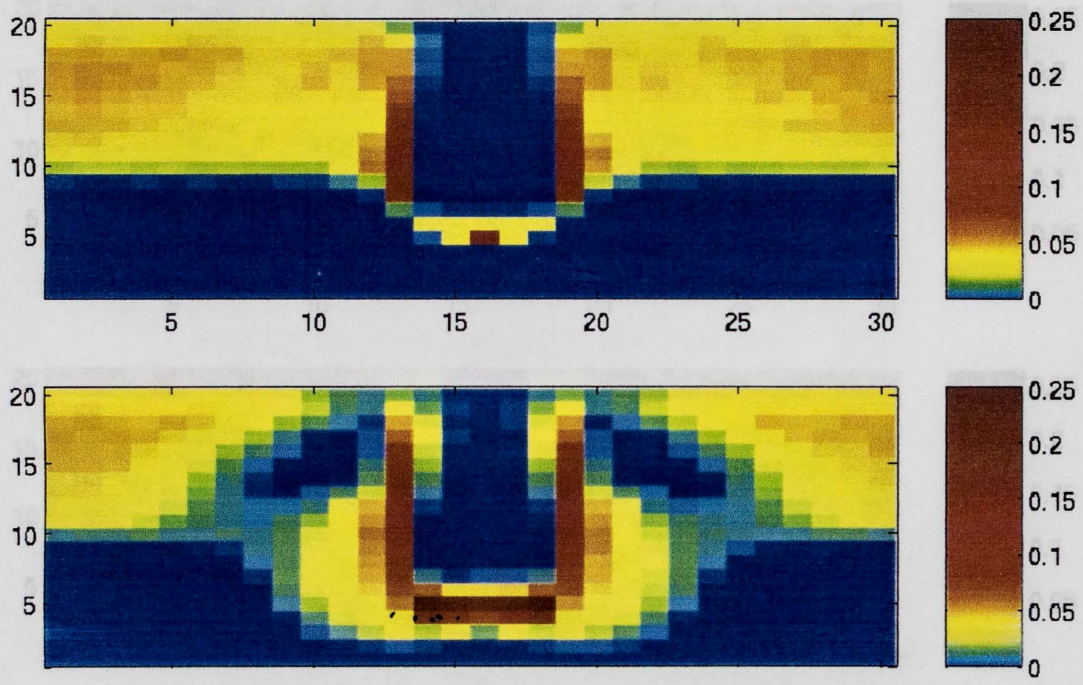

Figure 4.3: Vertical section normal to the stone domain axis in Figure 2, indicating the horizontally averaged number of ice lenses that displace soil toward void particles per cell per year in two models: (A) three-dimensional unmodified model with reference parameters, (B) three-dimensional model with reference parameters modified only for rapid freezing in stone domains. In (B), displacement toward void particles is enhanced and extends to greater depths near the stone/soil interface.

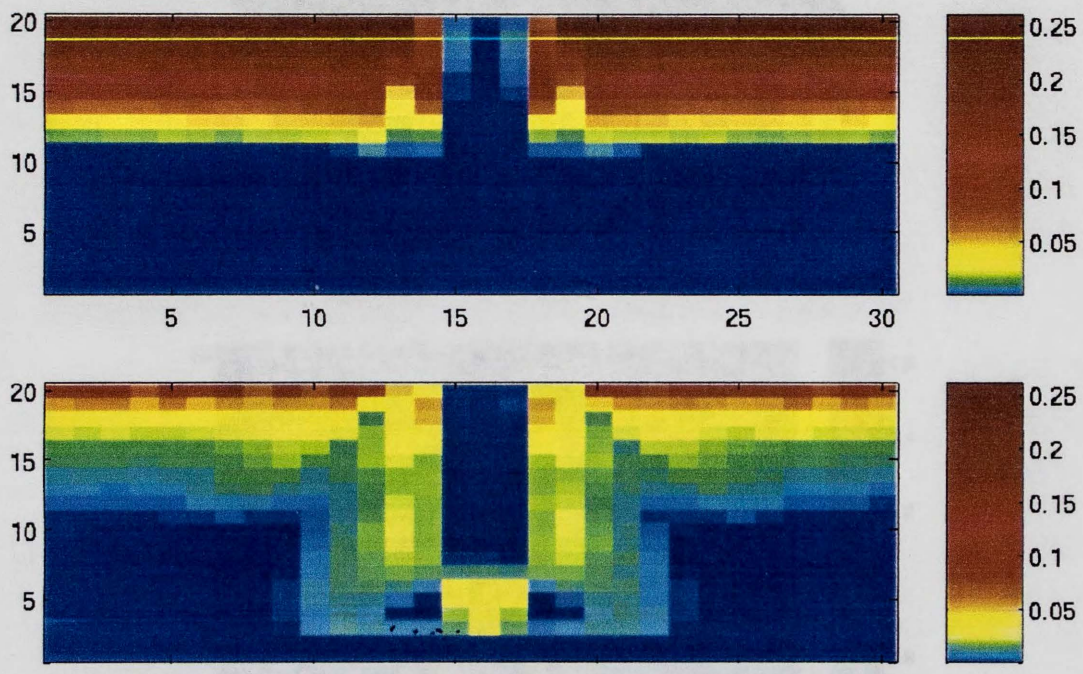

Figure 4.4: Vertical section normal to the stone domain axis in Figure 2, indicating the horizontally averaged number of ice lenses that displace soil toward the surface per cell per year in two models: (A) three-dimensional unmodified model with reference parameters, (B) three-dimensional modified model with $P_s = P_s^{mn} = 0.2$, $P_v = 0.2$, and $W_{sd} = 4$ *cells*. In (B), number of displacements toward the surface is generally reduced; however, it is increased near the stone/soil interface (squeezing) and uniform with depth owing to the threshold probability, $P_s^{mn} = 0.2$, for squeezing.

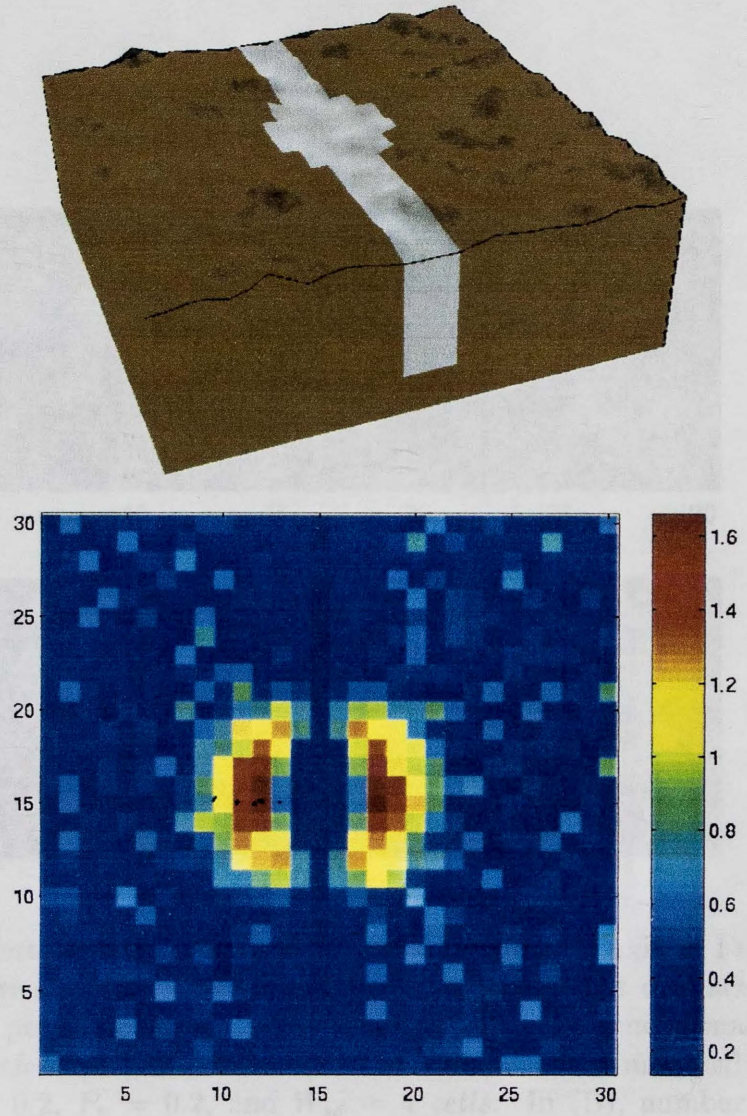

Figure 4.5: (A) Oblique view of 3×3×1 m modeled active layer with a 0.3 m wide 0.75 m deep stone domain with 0.7 m wide bulge. (B) Plan view indicating number of ice lenses that displace soil toward the surface per column per year in three-dimensional modified model with $P_s = P_s^{mn} = 0.2$, $P_v = 0.2$, and $W_{sd} = 4$ *cells*. Squeezing focused on wider section of the stone domain causes more uplift and diffusion of the perturbation.

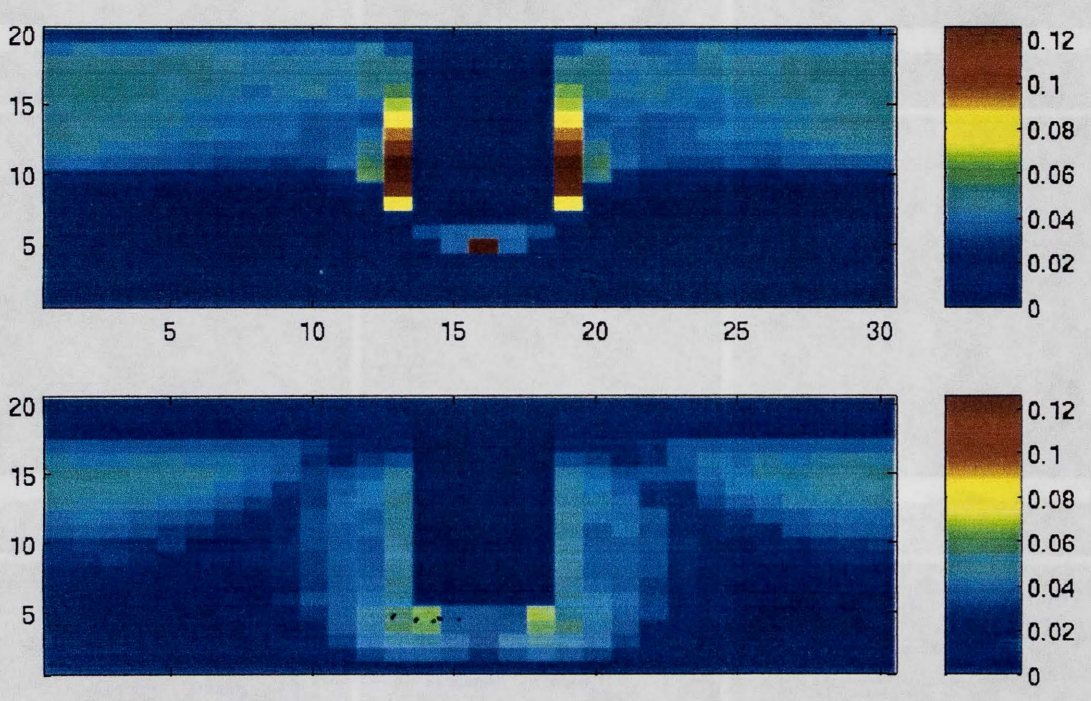

Figure 4.6: Vertical section normal to the stone domain axis in Figure 2, indicating the horizontally averaged number of ice lenses that displace soil toward void particles per cell per year in two models: (A) three-dimensional unmodified model with reference parameters, (B) three-dimensional modified model with $P_s = P_s^{mn} = 0.2$, $P_v = 0.2$, and $W_{sd} = 4$ *cells*. In (B), number of displacements toward void particles generally is reduced; near the stone/soil interface, it is roughly uniform with depth.

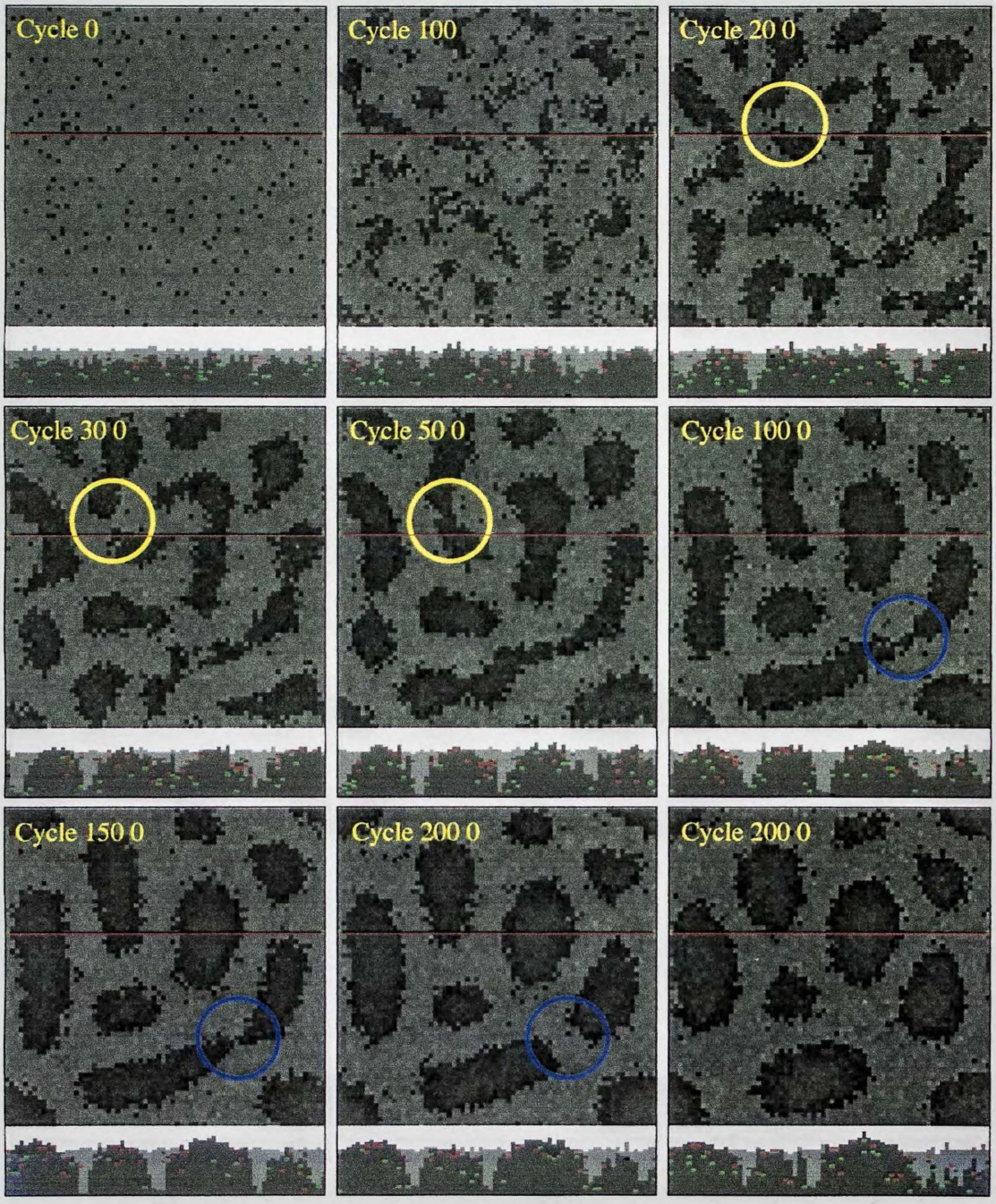

Figure 4.7: Plan view and cross sections of initiation and evolution of polygons from an initially non-patterned state in 7×7×1 m three-dimensional modified model with $P_s = P_s^{mn} = 0.2$, $P_v = 0.2$, $V_s \sim 0.75$, and $W_{sd} = 4$ *cells*. Red horizontal line indicates location of cross section (shown below plan view). Yellow circles highlight breach of a stone domain and consequent merging of two soil domains, blue circles highlight dissection of a soil domain. In cross sections, red dots indicate location of ice particles that displaced toward the surface, green dots indicate location of ice particles that displaced toward void particles. Dark gray is soil, light gray is stones, lighter shades indicate higher surface elevation.

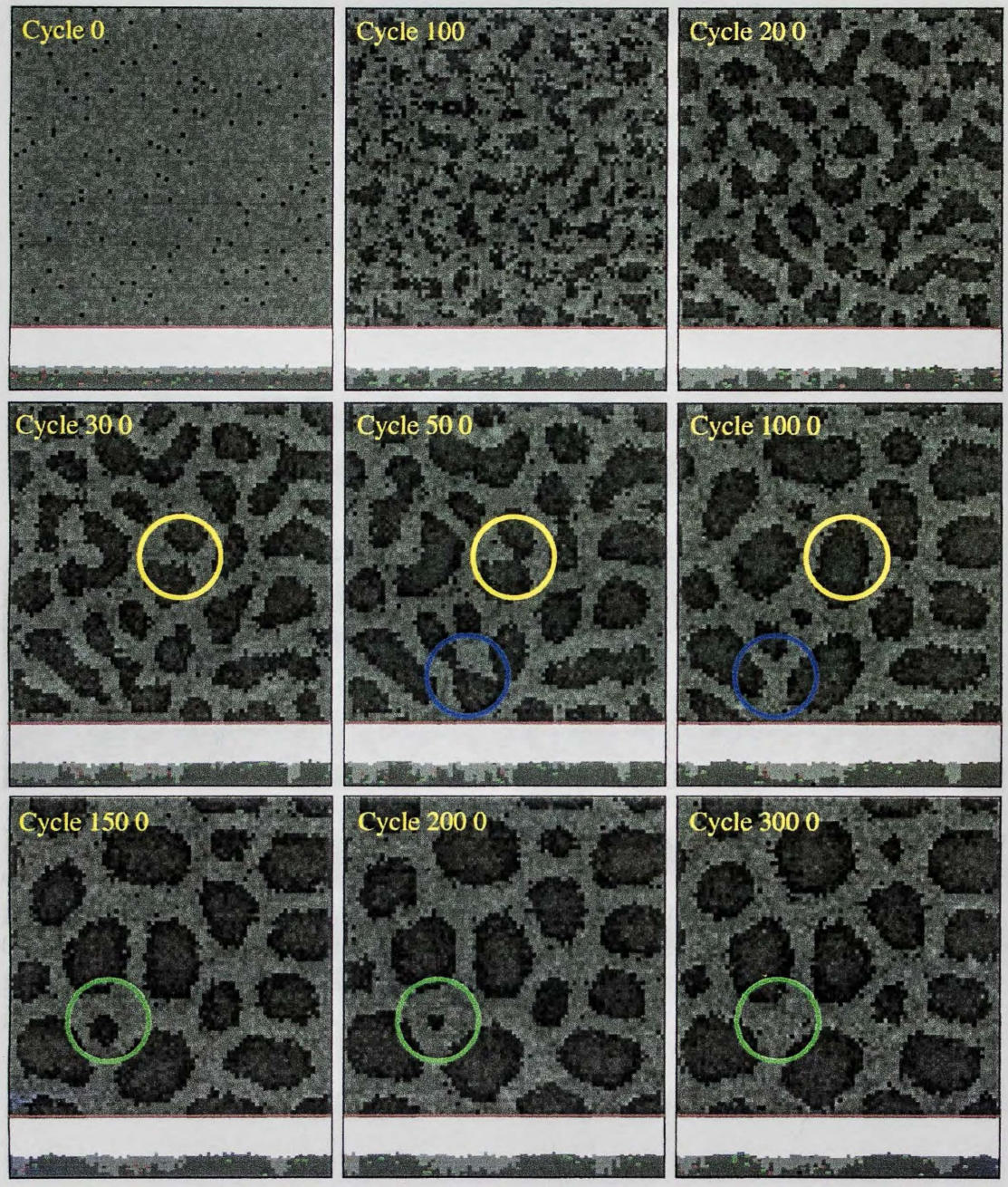

Figure 4.8: Plan views and cross sections of initiation and evolution of polygons from an initially non-patterned state in $8\times8\times0.55$ m three-dimensional modified model, also with rapid stone motion on soil domains, $P_s = 0$, $P_s^{mn} = 0.2$, $P_v = 0.2$, $V_s{\sim}0.7$, and $W_{sd} = 4$ $cells$. Red horizontal line indicates location of cross section shown below plan view. Yellow circles highlight breach of a stone domain and consequent merging of two soil domains, blue circles highlight dissection of a soil domain, and green circles highlight collapse of a soil domain. In cross sections, red dots indicate location of ice particles that displaced toward the surface, green dots indicate location of ice particles that displaced toward void particles. Dark gray is soil, light gray is stones, lighter shades indicate higher surface elevation.

Figure 4.9: Plan view of 7×30×1 m three-dimensional modified model after 500 cycles with $P_s = P_s^{mn} = 0.2$, $P_v = 0.2$, $V_s \sim 0.75$, and $W_{sd} = 4$ *cells*. The probability of displacement toward a void particle increases left to right from 0.1 to 0.8, with a consequent transition from connected networks to labyrinthine patterns ($P_v \sim 0.3 - 0.4$). Dark gray is soil, light gray is stones, lighter shades indicate higher surface elevation.

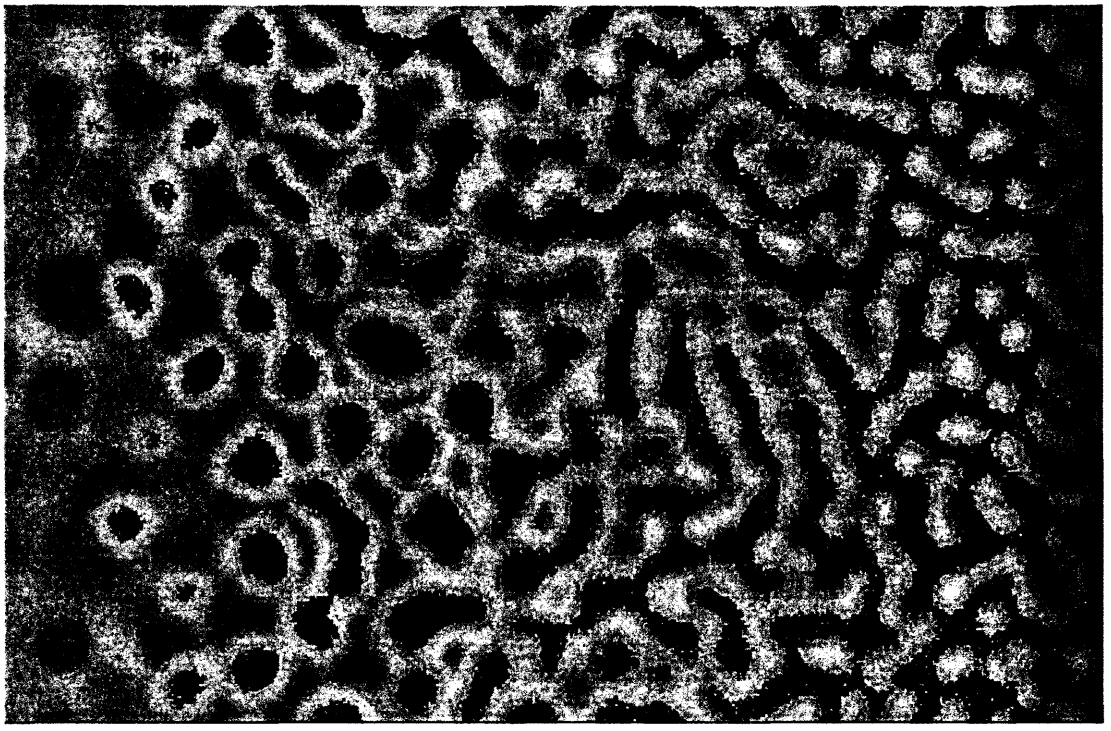

Figure 4.10: Plan view of $30 \times 50 \times 1$ m three-dimensional unmodified model with reference model parameters after 1200 cycles. The volumetric fraction of soil increases left to right from 0.25 to 0.75; sorted circle-labyrinth transition at $\sim$0.47, labyrinth-stone island transition at $\sim$0.66. Dark gray is soil, light gray is stones, lighter shades indicate higher surface elevation.

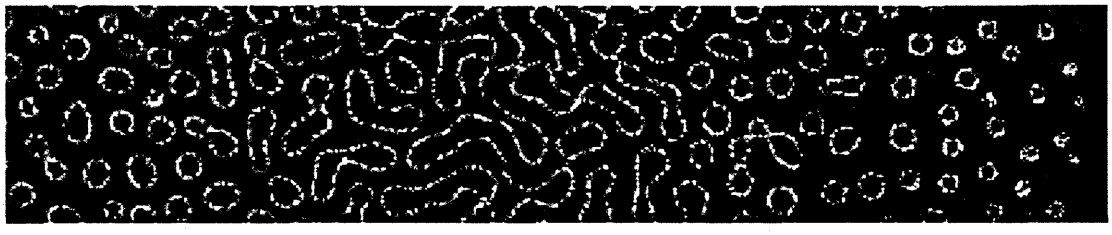

Figure 4.11: Plan view of 10×50 m two-dimensional model [Chapter 3] after 1200 cycles. The volumetric fraction of soil increases left to right from 0.25 to 0.75 (maximum depth of stones = 20); sorted circle-labyrinth transition at $\sim$0.45, labyrinth-stone island transition at $\sim$0.60. Dark gray is soil, light gray is stones, lighter shades indicate higher surface elevation.

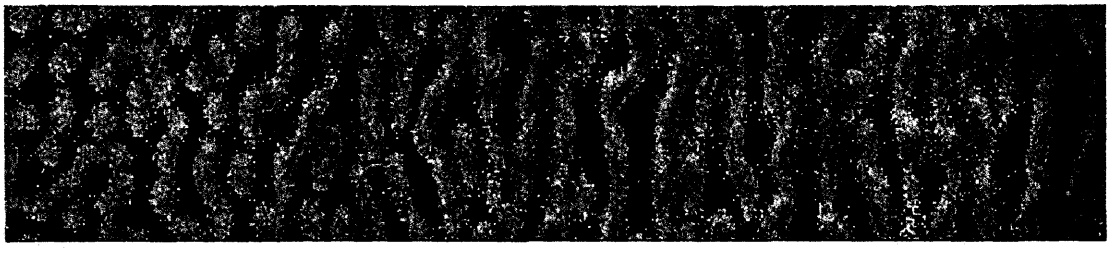

Figure 4.12: Plan view of $10 \times 50 \times 1$ m three-dimensional unmodified model with reference model parameters after 500 cycles, with volumetric fraction of soil $= 0.25$. The hillslope gradient (sloping downward toward page bottom) increases left to right from 0^o to 15^o: islands transition to stripes between $\sim 2^o$ and $\sim 7^o$. Dark gray is soil, light gray is stones, lighter shades indicate higher surface elevation.

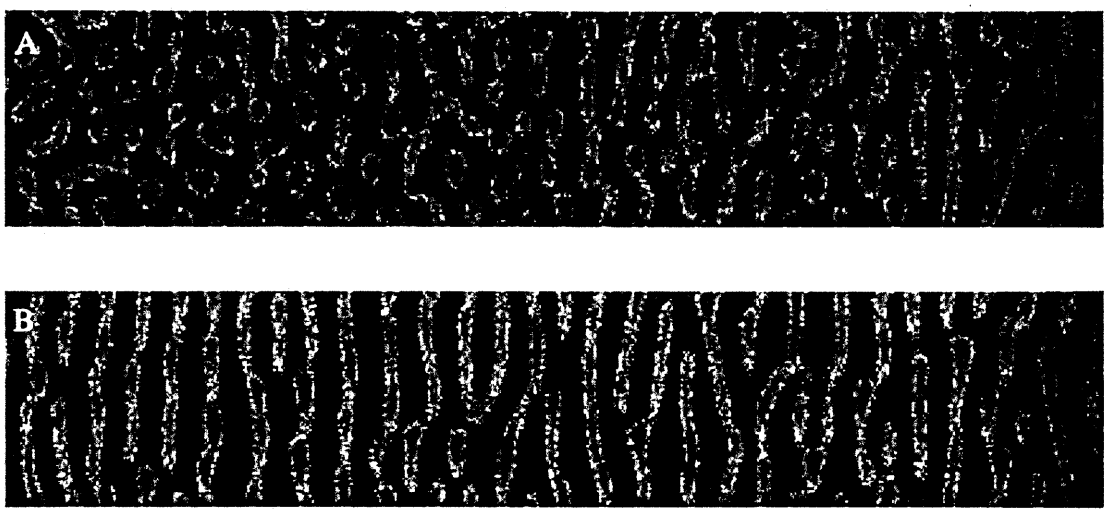

Figure 4.13: Plan view of two 10×50 m two-dimensional models [Chapter 3] after 500 cycles with volumetric fraction of soil = 0.25 (maximum depth of stones = 5). The hillslope gradient (sloping downward toward page bottom) increases left to right (A) from 0^o to 15^o and (B) from 15^o to 30^o. Islands transition to stripes between $\sim 5^o$ and $\sim 15^o$. Dark gray is soil, light gray is stones, lighter shades indicate higher surface elevation.

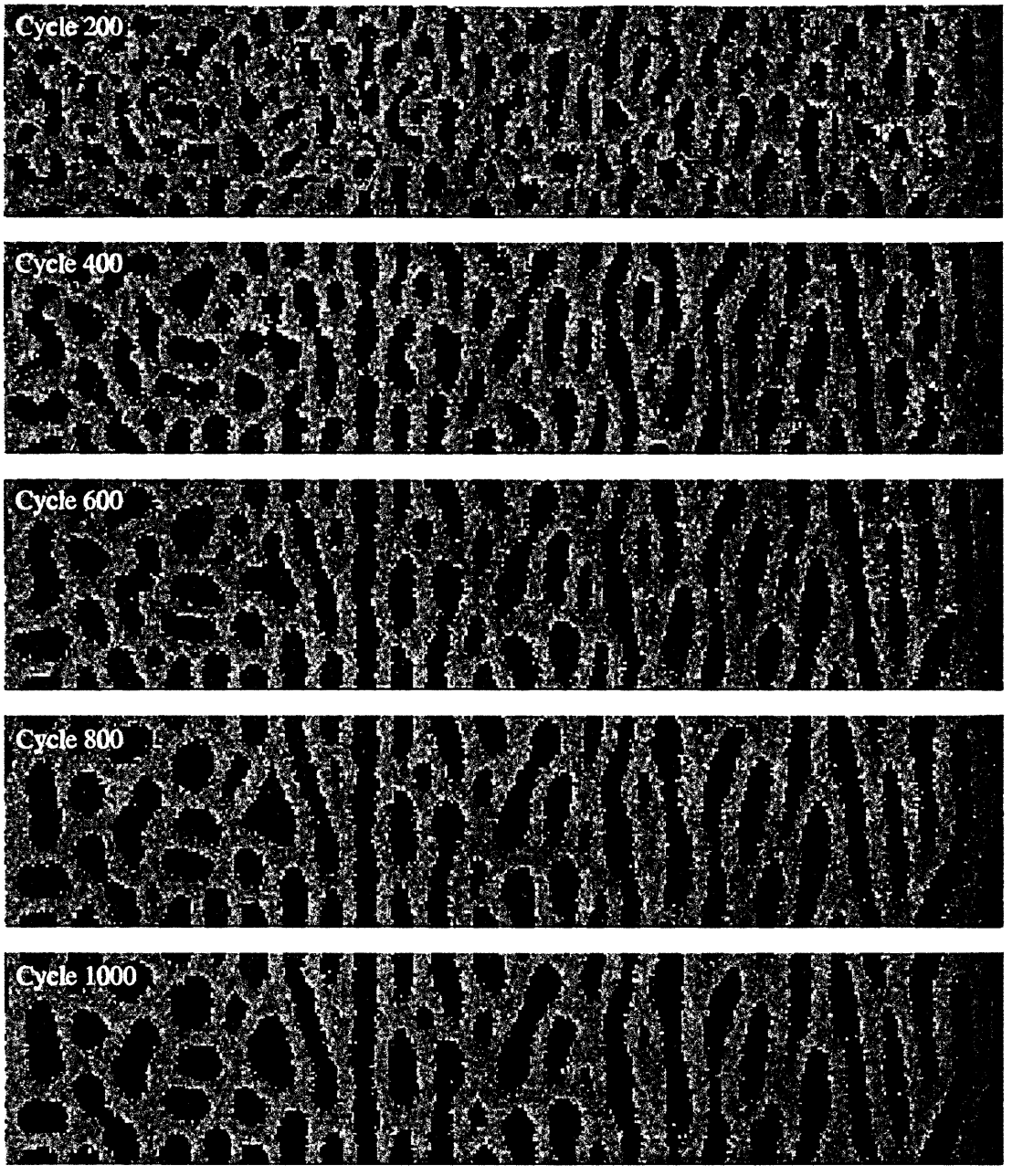

Figure 4.14: Plan view of $7 \times 35 \times 0.55$ m three-dimensional modified model after 500 cycles with rapid stone motion on soil domains. $P_s = 0$, $P_s^{min} = 0.2$, $P_v = 0.2$, $V_s \sim 0.7$, and $W_{sd} = 4$ $cells$. Hillslope gradient increases left to right from 0^o to 15^o. Polygons elongate downslope on gradients greater than $\sim 4^o$. The downslope continuity of stripes is much longer than the distance pattern features (such as junctions) have migrated. Dark gray is soil, light gray is stones, lighter shades indicate higher surface elevation.

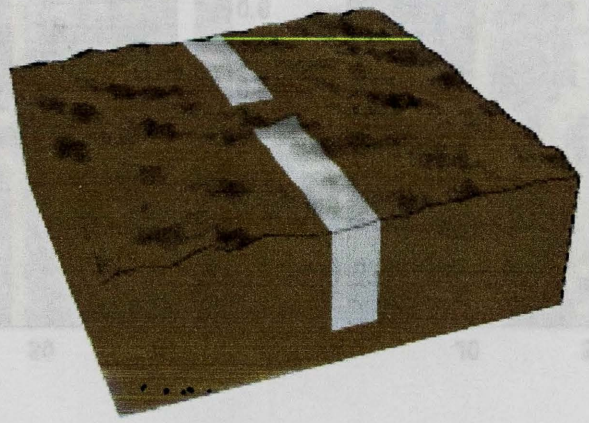

Figure 4.15: Oblique view of 3×3×1 m modeled active layer with a 0.3 m wide 0.75 m deep stone domain with a 0.3 m wide gap.

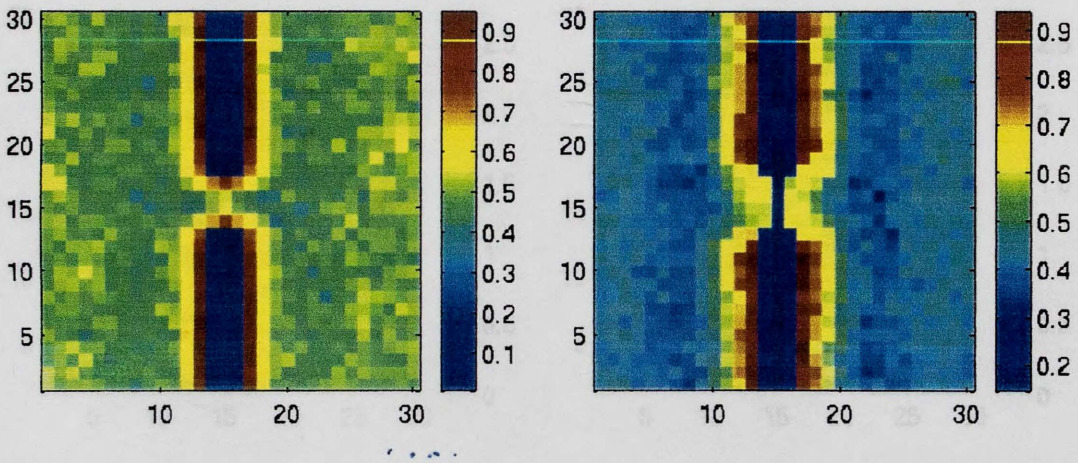

Figure 4.16: Plan view indicating number of ice lenses that displace soil toward void particles per column per year for linear stone domain with gap (Figure 15) in two models: (A) three-dimensional unmodified model with reference model parameters, (B) three-dimensional modified model with $P_s = P_s^{mn} = 0.2$, $P_v = 0.2$, and $W_{sd} = 4$ *cells*. In (B), ice particle formation is, on average, less frequent, but only minor differences between these models exists near the stone domain.

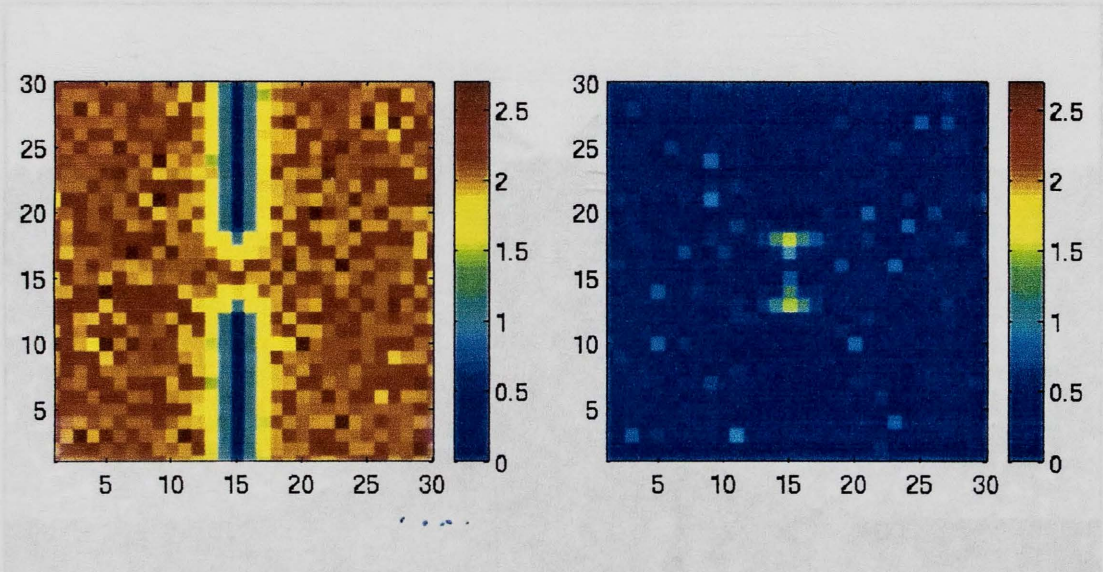

Figure 4.17: Plan view indicating number of ice lenses that displace soil toward the surface per column per year for linear stone domain with gap (Figure 15) in two models: (A) three-dimensional unmodified model with reference model parameters, (B) three-dimensional modified model with $P_s = P_s^{mn} = 0.2$, $P_v = 0.2$, and $W_{sd} = 4\ cells$. In (B), more displacements toward the surface in the gap raise the stone domain and lower the surface of the gap.

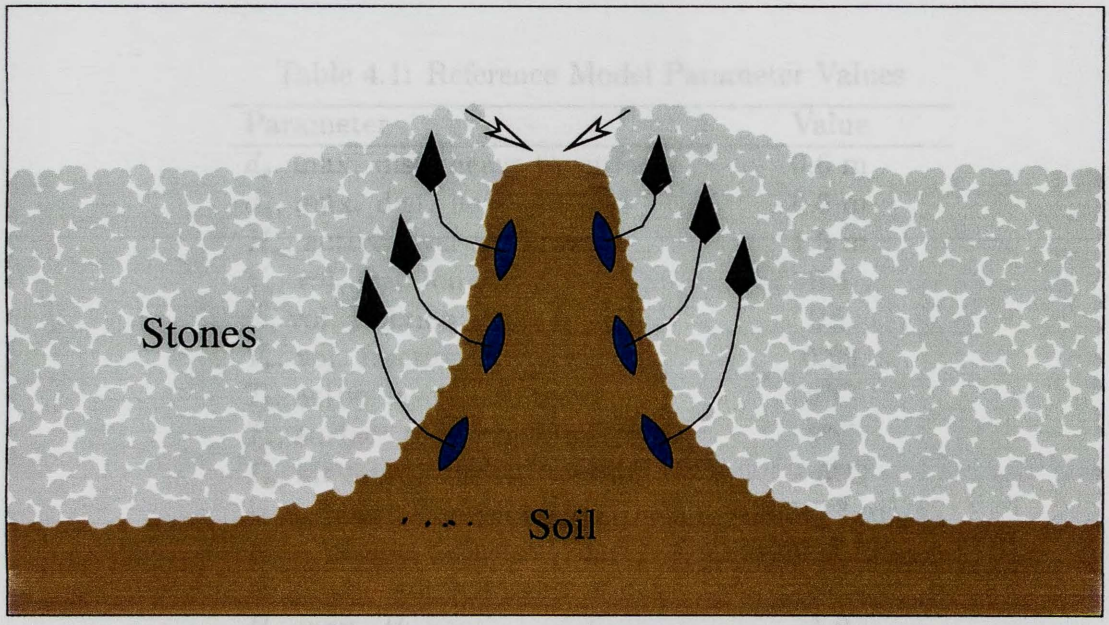

Figure 4.18: Schematic along-axis section through narrow stone domain with gap. Frost heave in gap displaces soil into stone domain, lowering surface in gap and raising surface in stone domain. Stones then ravel into gap owing to increased surface gradients.

Table 4.1: Reference Model Parameter Values

Parameter	Value
d_s, max. dist. heave to surface	0.6 m
d_v, max. dist. heave to void	0.6 m
H_a, active layer thickness	1.0 m
V_s, vol. fraction soil	0.4
w, vol. fraction water in soil	0.1
V_v, vol. fraction of voids	0.05
T_b, active layer base temp.	0°C
T_g, surface temp. before freezing	5°C
T_a, air temp. during freezing	−5°C
k_{heat}, heat diffusion const.	1×10^{-6} m^2/s
K_{surf}, height diffusion const.	5×10^{-3} m^2/yr
W_{sd}, min. stone domain width	$4 cells$
P_s, max. P_{surf}	1.0
P_v, max. P_{void}	1.0
P_s^{mn}, min. P_{sqz}	0.0
S, hillslope angle	0.0

Table 4.2: Pattern Transitions (* C measures degree of confinement, the direction of stone motion owing to lateral squeezing is given by $C\hat{u} + (1 - C)\hat{r}$ where $\hat{u}$ is a unit vector along the axis of the stone domain and $\hat{r}$ is a randomly chosen unit vector.)

Transition	2-D Model	3-D Model
Circle-Labyrinth	$V_s \sim 0.45$	$V_s \sim 0.47$
Labyrinth-Island	$V_s \sim 0.60$	$V_s \sim 0.66$
Island-Stripe	$S \sim 5^o - 15^o$	$S \sim 2^o - 7^o$
Polygon-Labyrinth		$P_v \sim 0.3 - 0.4$
Polygon-Island	$C = 0.56$*	
Polygon-Stripe		$S \sim 4^o$

4.8 References

Ahnert, F., Stone rings from random walks, *Transactions, Japanese Geomorphological Union*, **2**, 301–312, 1981.

Ballantyne, C. K. and J. A. Mathews, Desiccation cracking and sorted polygon development, Jotunheimen, Norway, *Arctic and Alpine Research*, **15(3)**, 339–349, 1983.

DuFort, E. C. and S. P. Frankel, Stability conditions in the numerical treatment of parabolic differential equations, *Mathematical Tables and Other Aids to Computation*, **7**, 135–152, 1953.

Hallet, B. and S. Prestrud, Dynamics of periglacial sorted circles in Western Spitsbergen, *Quaternary Research*, **26**, 81–99, 1986.

Huxley, J. S. and N. E. Odell, Notes on the surface markings in Spitsbergen, *Geographical Journal*, **63**, 207–229, 1924.

Kessler, M. A., A. B. Murray, B. T. Werner, and B. Hallet, A model for sorted circles as self-organized patterns, *Journal of Geophysical Research*, **106(B7)**, 13,287–13,306, 2001.

Nogotov, E. F., *Applications of Numerical Heat Transfer*, United Nations Educational, Scientific, and Cultural Organization, Paris, France, 1978.

Schmertmann, J. and R. S. Taylor, Quantitative data from a patterned ground site over permafrost, *Tech. rep.*, U.S. Army Cold Regions and Engineering Laboratory, 1965.

Schunke, E., Die periglazialerscheinungen islands in Abhangigkeit von klima und substrat, *Abhandlungen der Akademie der Wissenschaften in Gottingen, Mathematisch-Physikalische Klasse*, **30**, 1–273, 1975.

Sharp, R. P., Soil structures in the St. Elias Range, Yukon Territory, *Journal of Geomorphology*, **5**, 274–301, 1942.

Taber, S., Frost heaving, *J. Geology*, **37**, 428–461, 1929.

Washburn, A. L., Classification of patterned ground and review of suggested origins, *Geological Society of America Bulletin*, **67**, 823–865, 1956.

Washburn, A. L., Weathering, frost action, and patterned ground in the Mesters Vig District, Northeast Greenland, *Meddelelser om Gronland*, **176**, 1969.

Washburn, A. L., *Plugs and Plug Circles: A Basic Form of Patterned Ground, Cornwallis Island, Arctic Canada-Origin and Implications*, The Geological Society of America, Inc., Boulder, Colorado, 1997, Memoir 190.

Werner, B. T. and B. Hallet, Numerical simulation of self-organized stone stripes, *Nature*, **361**, 142–145, 1993.

4.9 Appendix 1: Program Flow Charts

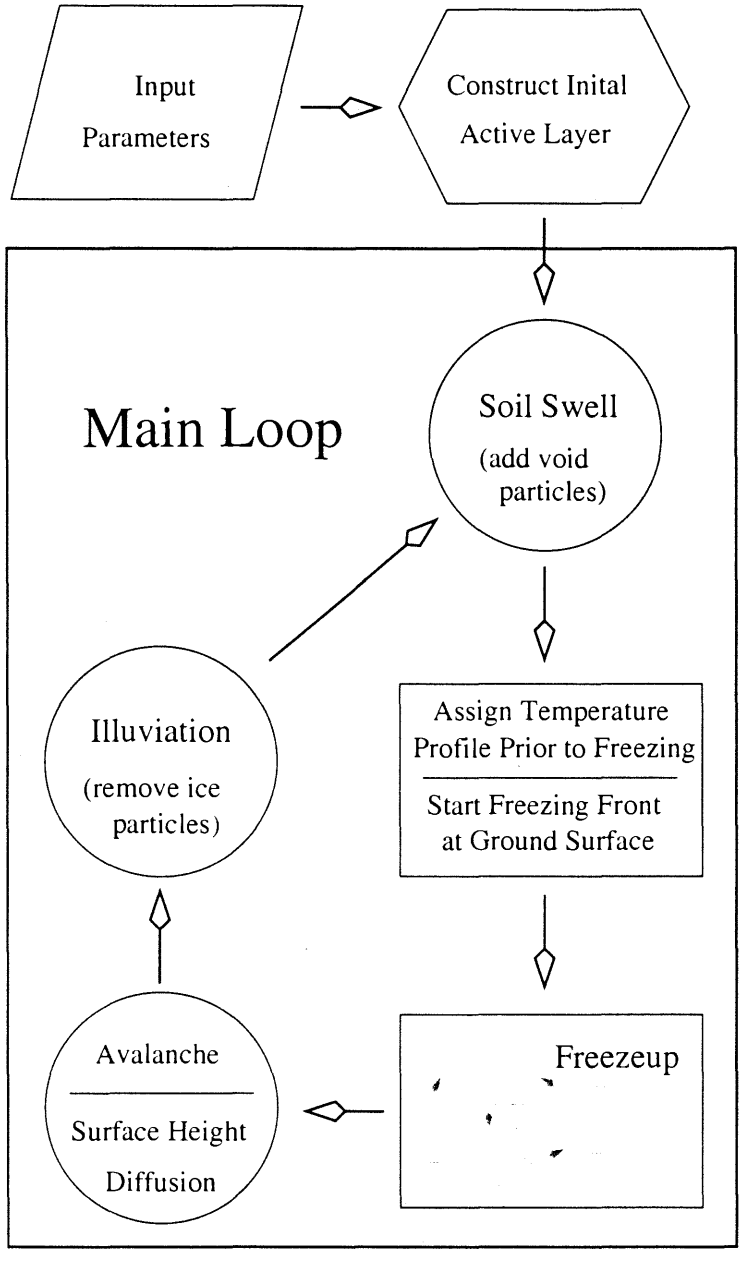

Figure 4.19: The main loop of the program representing a single freezing and thawing cycle.

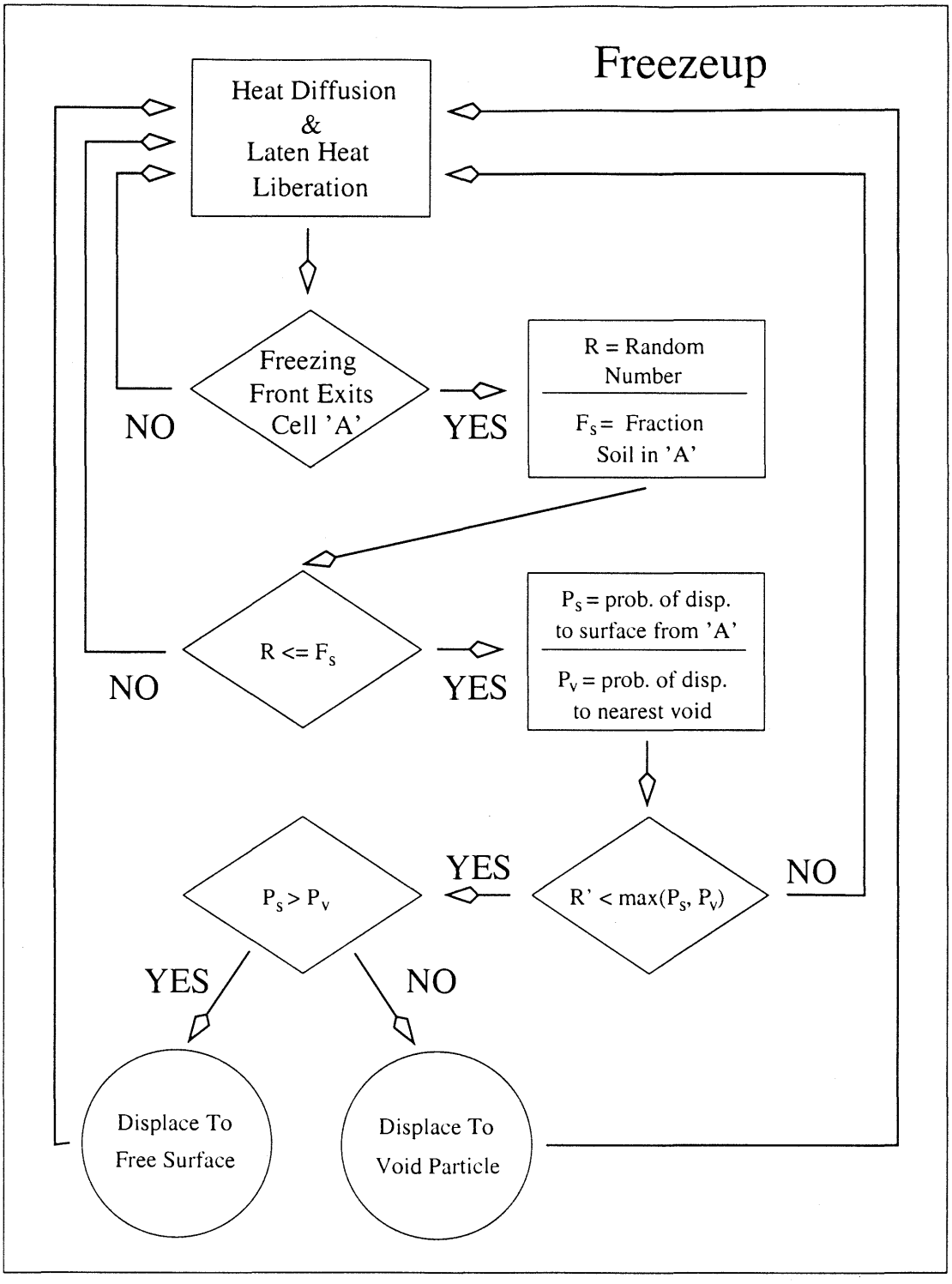

Figure 4.20: The loop that is iterated during freezing to lower the temperature, propagate the freezing front and create ice particles.

4.10 Appendix 2: Sample Source Code

This appendix includes several functions written in 'C' that show how ice particles are created in the sorted patterned ground model (Chapter 4) and the resulting displacements.

The function *lens_creation*(x, y, z) first determines the probability of an ice particle forming at (x,y,z) and pushing toward a void particle (abstracting frost heave compressing soil), then it determines the probability of an ice particle forming at (x,y,z) and pushing toward the free surface (abstracting frost heave uplifting the overburden). An ice particle is formed if a randomly chosen number (0-1] is less than the greater of these two probabilities. The functions *push_to_void*() and *push_to_surf*() displace particles along a path from (x,y,z) to a void and to the surface respectively.

```
int   lens_creation( int x, int y, int z )
{
   int      i, j, void_cell[3], cell[3], path[1000][3];

   float    surf_vect[3], ff_norm[3], p_surf_push, p_void_push;

   /* cell is a struct that acts as the basic spatial unit in this
   model; cells can contain two particles */
   struct   cell   displaced;


   cell[0] = x; cell[1] = y; cell[2] = z;

   /* void_search() puts the coordinates of the nearest void cell in
   void_cell[], and returns the probability of an ice lens pushing
   to that cell, given by:
      const * ( max_void_dist - depth ) / max_void_dist */
   p_void_push = void_search( cell, void_cell );

   /* get_ff_norm() puts the time averaged normal to the freezing
   front at cell[] in ff_norm[] */
   get_ff_norm( cell, ff_norm );
```

```
   /* find_surf_path() returns the probability of an ice lens
   pushing toward the free surface, and puts a path of cell
   displacements from cell[] to the free surface in path[][] */
   p_surf_push = find_surf_path( cell, ff_norm, path );

   if ( rand_num < more( p_surf_push, p_void_push ) )
   {
      if ( p_surf_push > p_void_push )
      {
         displaced = ice_lens_element;
         push_to_surface( displaced, path );
      } else {
         /* main_array is a 3d array of type struct cell
         that is the physical lattice of the model */
         displaced = main_array[x][y][z];
         main_array[x][y][z] = ice_lens_element;
         push_to_void( displaced, cell, void_cell);
      }
      return( YES );
   } else {
      return( NO );
   }
}


float   find_surf_path( int lens[3], float ff_norm[3], int path[100][3] )
{
   int      x, y, z, hit_target=NO, reached[3], moved=YES,
            stone_domain=0, path_length=-1, stone_contact=NO,
            displaced[3], type1, hit_surface;

   float    p_up, p_horz_x, p_horz_z,  tot_dist, t_t,
            d_t, total_path_length=0, surf_vect[3], traveled, depth,
            direct[3], dist, X_dir, Y_dir, Z_dir, XYZ_sum;


   x = lens[0]; y = lens[1]; z = lens[2];

   do
   {
      if ( moved == 1 )
      {
```

```
++path_length;
path[path_length][0] = x;
path[path_length][1] = y;
path[path_length][2] = z;

/* test_surf() returns YES if a neighboring cell in
an empty cell above the surface, and places its
coordinates in reached[] */
hit_surface = test_surf( path[path_length], reached );
if ( hit_surface == YES )
{
   ++path_length;
   path[0][0] = path_length;
   path[path_length][0] = reached[0];
   path[path_length][1] = reached[1];
   path[path_length][2] = reached[2];

   dist = find_distance(path[path_length], lens);

   /* p_surf_heave() return the probability of an ice lens
   pushing a distance "dist" to the surface, given by:
      const * ( max_surf_dist - dist ) / max_surf_dist */

  if ( stone_domain == YES )
      return ( more( min_surf_prob, p_surf_heave( dist ) ) );
  else
      return ( p_surf_heave( dist ) );
}

type1 = main_array[x][y][z].elems[1].type;
if ( (type1 == empty) && (stone_contact == NO) )
{
   stone_contact = YES;

   /* test_width() returns YES if there is a MINWIDTH span
   soil free cells from (x,y,z) in the direction ff_norm[] */
   stone_domain = test_width( x, y, z, ff_norm, MINWIDTH );
}

depth = find_depth( path[path_length], surf_vect );

/* find_distance() calculates the euclidean distance */
```

```
            traveled = find_distance( path[path_length], lens );
            tot_dist = depth + traveled;

            t_t = traveled/tot_dist;
            d_t = depth/tot_dist;
            direct[0] = t_t*surf_vect[0] + d_t*ff_norm[0];
            direct[1] = t_t*surf_vect[1] + d_t*ff_norm[1];
            direct[2] = t_t*surf_vect[2] + d_t*ff_norm[2];

            X_dir = fabs( direct[0] );
            Y_dir = (float)yresolution * fabs( direct[1] );
            Z_dir = fabs( direct[2]);

            XYZ_sum  =  sqrt( X_dir*X_dir + Y_dir*Y_dir + Z_dir*Z_dir ) ;
            p_up     =  Y_dir / XYZ_sum;
            p_horz_x =  X_dir / XYZ_sum;
            p_horz_z =  Z_dir / XYZ_sum;
         }

         moved = NO;
         if( rand_num < p_up )
         {
            ++y;
            moved = YES;
         }
         if( rand_num < p_horz_x )
         {
            x += sign_of( direct[0] );
            x = pos_calc( x, X_DIM );
            moved = YES;
         }
         if( rand_num < p_horz_z )
         {
            z += sign_of( direct[2] );
            z = pos_calc( z, Z_DIM );
            moved = YES;
         }
         reached[0]=x; reached[1]=y; reached[2]=z;

      } while ( hit_target == NO );
}
```

```
void   push_to_surface( struct cell displaced, int path[100][3] )
{
   int      x, y, z, p, path_length;
   struct   cell   temp;


   path_length = path[0][0];
   for ( p=1; p<=path_length; p++ )
   {
      x = path[p][0];
  y = path[p][1];
  z = path[p][2];
      temp = main_array[x][y][z];
      main_array[x][y][z] = displaced;
      displaced = temp;
   }
   ++surface[x][z];
}


void   push_to_void( struct cell displaced, int from[3], int target[3])
{
   int      x, y, z, X, Z, sign, del, cur, end, hit_target=NO,
            reached[3], del_x, del_y, del_z;

   float    m_x, m_y, m_z, star;

   struct cell   temp_element;


   x=from[0]; y=from[1]; z=from[2];

   del_x = target[0] - x;
   del_y = target[1] - y;
   del_z = target[2] - z;

   if( del_x > half_X_DIM )
   {
      del_x -= X_DIM;
      target[0] -= X_DIM;
   } else if ( del_x < -half_X_DIM ) {
```

```
   del_x += X_DIM;
   target[0] += X_DIM;
}

if( del_z > half_Z_DIM )
{
   del_z -= Z_DIM;
   target[2] -= Z_DIM;
} else if ( del_z < -half_Z_DIM ) {
   del_z += Z_DIM;
   target[2] += Z_DIM;
}

if ( (abs(del_x)>=abs(del_y)) && (abs(del_x)>=abs(del_z)) )
{
   sign = sign_of( del_x );
   del = del_x;
   cur = x;
   end = target[0];
} else if ( abs(del_y) >= abs(del_z) ) {
   sign = sign_of( del_y );
   del = del_y;
   cur = y;
   end = target[1];
} else {
   sign = sign_of( del_z );
   del = del_z;
   cur = z;
   end = target[2];
}

m_x = (float)del_x / (float)del;
m_y = (float)del_y / (float)del;
m_z = (float)del_z / (float)del;

/* test_target() returns YES if a cell neighboring from[]
is a void cell or an empty cell above the surface, and puts the
cells coordinates in reached[]  */
hit_target = test_target( from, reached );
while ( hit_target == NO )
{
   cur += sign;
```

```
        star = cur - end;

        X = round( (float)star*m_x ) + target[0];
        Z = round( (float)star*m_z ) + target[2];

        /* pos_calc() checks and implements periodic boundaries */
        from[0] = x = pos_calc( X, X_DIM );
        from[1] = y = round( (float)star*m_y ) + target[1];
        from[2] = z = pos_calc( Z, Z_DIM );

        temp_element = main_array[x][y][z];
        main_array[x][y][z] = displaced;
        displaced = temp_element;

        hit_target = test_target( from, reached );
    }

    x = reached[0]; y = reached[1]; z = reached[2];
    if( main_array[x][y][z].elems[0].type == air )
    {
        main_array[x][surface[x][z]+1][z] = displaced;
        ++surface[x][z];
    } else {
        main_array[x][y][z] = displaced;
    }
}
```